The development of efavirenz and praziquantel amorphous solid dispersions

A van Aswegen



orcid.org/ 0000-0000-1011-2834

Dissertation submitted in fulfilment of the requirements for the degree *Master of Science in Pharmaceutics* at the North West University

Supervisor: Prof N Stieger

Co-supervisor: Prof W Liebenberg

Graduation: May 2019

Student number: 24161217

Table of Contents

List of Figures vi

List of Tables x

Acknowledgements xi

Abstract xii

Chapter 1 1

1.1 Introduction 1

1.2 Polymorphism 1

1.3 Transformations 1

1.3.1 Solvent interactive transformations 2

1.3.2 Solid-solid transformations 2

1.3.3 Melt mediated transformations 2

1.4 Inclusion compounds 2

1.4.1 Solvates and hydrates 3

1.4.1.1 Stoichiometric 3

1.4.1.2 Non-stoichiometric 3

1.4.2 Desolvation / dehydration 3

1.4.3 Co-crystals 3

1.4.4 Clathrates 4

1.4.5 Salts 4

1.5 Amorphism 4

1.5.1 Amorphous solid dispersions (ASDs) 4

1.5.1.1 Preparation of amorphous solid dispersions 5

1.5.1.2 Glass transition temperature 5

1.6 Solubility and dissolution 5

1.7 pKa and Log P 7

1.7.1 pKa 7

1.7.2 Log P 7

1.8 Conclusion 7

References 8
Chapter 2 12
2.1 Introduction 12
2.2 Efavirenz 12
2.3 Praziquantel 13
2.4 Polymers 13
2.4.1 Hydroxypropyl methylcellulose (HPMC) 14
2.4.2 Hydroxypropyl methylcellulose acetate succinate (HPMCAS) 14
2.4.3 Polyvinylpyrrolidone (PVP) 15
2.4.4 Vinylpyrrolidone-vinyl acetate copolymer (PVP VA 64) 15
2.5 Surfactants 16
2.6 Screening process of polymers for amorphous drug stabilisation 16
2.6.1 Preparation methods 19
2.7 Characterisation methods 19
2.7.1 Simultaneous thermal analysis (STA) (TGA/DSC) 19
2.7.2 Hot-stage microscopy (HSM) 19
2.7.3 Scanning electron microscopy (SEM) 20
2.7.4 X-ray powder diffraction (XRPD) 20
2.7.5 High performance liquid chromatography (HPLC) 20
2.7.5.1 Efavirenz 21
2.7.5.2 Praziquantel 21
2.7.6 Stability testing 21
2.7.6.1 Temperature and humidity 21
2.7.7 Powder dissolution studies 22
References 23
Chapter 3 27
3.1 Primary screening to identify suitable efavirenz polymers 27
3.2 Physico-chemical properties of efavirenz (EFA) 30
3.2.1 Thermal analysis 30
3.2.1.1 Simultaneous thermal analysis (STA) of the EFA raw material 30

3.2.1.2 Scanning electron microscopy (SEM) 30
3.2.1.3 Hot-stage microscopy (HSM) 32
3.2.1.4 X-ray powder diffraction (XRPD) 34
3.2.1.5 Accelerated stability testing 35
3.2.1.6 Powder dissolution studies 37
3.2.1.6.1 Validation of HPLC assay method 37
3.2.1.6.2 Linearity 38
3.2.1.6.3 EFA glass 40
3.3 Physico-chemical properties of the prepared ASDs 41
3.3.1 EFA/PVP 25 41
3.3.1.1 Thermal analysis – screening for miscibility of EFA/PVP 25 41
3.3.1.2 Scanning electron microscopy (SEM) 42
3.3.1.3 Hot-stage microscopy (HSM) 44
3.3.1.4 X-ray powder diffraction (XRPD) 45
3.3.1.5 Stability testing 46
3.3.1.6 Powder dissolution studies 48
3.3.2 Efavirenz/PVP 30 49
3.3.2.1 Thermal analysis – screening for miscibility of EFA/PVP 30 49
3.3.2.2 Scanning electron microscopy (SEM) 51
3.3.2.3 Hot-stage microscopy (HSM) 52
3.3.2.4 X-ray powder diffraction (XRPD) 53
3.3.2.5 Stability testing 54
3.3.2.6 Powder dissolution studies 56
3.3.3 Efavirenz/PVP VA 64 57
3.3.3.1 Simultaneous thermal analysis (STA) (TGA/DSC) 57
3.3.3.2 Scanning electron microscopy (SEM) 58
3.3.4 Hot-stage microscopy (HSM) 59
3.3.5 X-ray powder diffraction (XRPD) 60
3.3.6 Stability testing 61
3.3.7 Powder dissolution studies 63

3.4 Conclusion 63
References 66
Chapter 4 68
4.1 Primary screening to identify suitable praziquantel polymers 68
4.2 Physico-chemical properties of praziquantel (PZQ) 68
4.2.1 Thermal analysis 68
4.2.1.1 Simultaneous thermal analysis (STA) of the PZQ raw material 68
4.2.1.2 Scanning electron microscopy (SEM) 70
4.2.2 Hot-stage microscopy (HSM) 71
4.2.3 X-ray powder diffraction (XRPD) 72
4.2.4 Powder dissolution studies 73
4.2.4.1 Validation of the HPLC method 73
4.2.4.2 Linearity of the method used 74
4.3 Unsuccessful praziquantel/polymer ASD candidates 75
4.3.1 Simultaneous thermal analysis (STA) (TGA/DSC) 75
4.4 ASD containing praziquantel/HPMCAS 78
4.4.1 Simultaneous thermal analysis (STA) (TGA/DSC) 78
4.4.2 Scanning electron microscopy (SEM) 78
4.4.3 Hot-stage microscopy (HSM) 79
4.4.4 X-ray powder diffraction (XRPD) 80
4.4.5 Stability testing 80
4.4.6 Dissolution studies 81
4.5 Conclusion 82
References 84
Chapter 5 85
Annexure 88

List of Figures

Figure 2.1: The molecular structure of efavirenz (Wiktionary, 2018). 12

Figure 2.2: The molecular structure of praziquantel (Wikipedia, 2018a). 13

Figure 2.3: The molecular structure of HPMC (Wikipedia, 2018b). 14

Figure 2.4: The molecular structure of HPMCAS (Pinto *et al.,* 2018). 15

Figure 2.5: The molecular structure of PVP (Sigma-Aldrich, 2018)..... 15

Figure 2.6: The molecular structure of PVP VA 64 (Aurora, 2018). 16

Figure 2.7: Modified screening of polymers for amorphous drug stabilization (SPADS) process (Stieger & Liebenberg, 2017)..... 18

Figure 3.1: Simultaneous thermal analysis (STA) thermogram of the EFA raw material. 30

Figure 3.2: SEM photo of the EFA raw material. 31

Figure 3.3: SEM photo of a physical mixture of EFA and 1.5% SLS. 31

Figure 3.4: HSM photos of the EFA raw material before and after melting. 32

Figure 3.5: HSM photos of the physical mixture of the EFA raw material and 1.5% SLS before and after melting..... 323

Figure 3.6: XRPD profile of the EFA raw material (bottom, blue) and a physical mixture of EFA and 1.5% SLS (top, red). 34

Figure 3.7: An overlay of the STA thermograms of a physical mixture of EFA and 1.5% SLS at initial (green), month 1 (purple), month 2 (blue) and month 3 (black) of stability testing. 35

Figure 3.8: XRPD overlay of a physical mixture of EFA and 1.5% SLS at initial (red), month 1 (blue), month 2 (green) and month 3 (grey) of stability testing. 36

Figure 3.9: Chromatogram of EFA at 260 nm. 37

Figure 3.10: Linear regression curve of EFA..... 38

Figure 3.11: Percentage of the EFA raw material with 1.5% SLS that had dissolved in distilled water at specific time intervals over a 3-hour period. 39

Figure 3.12: DSC thermogram overlay printed with permission from Stieger *et al*. (2013), illustrating the EFA glass (blue line) and the agitated glass (red line). 40

Figure 3.13: STA thermograms of an [EFA/PVP 25 (3:1) +1.5% SLS] physical mixture (top, purple), and a second run of the same sample (bottom, black)..... 41

Figure 3.14: STA thermogram of [EFA/PVP 25 (3:1) + 1.5% SLS] ASD, created by rotary evaporation. 42

Figure 3.15: SEM photo of a physical mixture of [EFA/PVP 25 (3:1) and 1.5% SLS]. 42

Figure 3.16: SEM photo of an ASD containing [EFA/PVP 25 (3:1) + 1.5% SLS]. 43

Figure 3.17: HSM photos of the physical mixture of [EFA/PVP 25 (1:3) + 1.5% SLS]. 44

Figure 3.18: XRPD profile of an ASD containing [EFA/PVP 25 (1:3) + 1.5% SLS] (top, red) and a physical mixture of [EFA/PVP 25 (1:3) + 1.5% SLS] (bottom, blue). 45

Figure 3.19: An overlay of the STA thermograms of an ASD containing [EFA/PVP 25 (1:3) + 1.5% SLS] at initial (green), month 1 (purple), month 2 (blue) and month 3 (black) of stability testing. 46

Figure 3.20: XRPD profile of an ASD containing [EFA/PVP 25 (3:1) + 1.5% SLS] at initial (red), month 1 (blue), month 2 (green) and month 3 (grey) of stability testing. 47

Figure 3.21: Dissolution profile of the ASD containing [EFA/PVP 25 (3:1) + 1.5% SLS]..... 48

Figure 3.22: STA thermograms of an [EFA/PVP 30 (3:1) +1.5% SLS] physical mixture (top, purple), and a second run of the same sample (bottom, black)..... 49

Figure 3.23: STA thermogram of the ASD containing [EFA/PVP 30 (3:1) + 1.5% SLS], created by rotary evaporation..... 50

Figure 3.24: SEM photo of a physical mixture of [EFA/PVP 30 (3:1) + 1.5% SLS]. 51

Figure 3.25: SEM photo of an ASD containing [EFA/PVP 30 (3:1) + 1.5% SLS]. 51

Figure 3.26: HSM photos of the physical mixture of [EFA/PVP 30 (3:1) + 1.5% SLS]. 52

Figure 3.27: XRPD profile of an ASD containing [EFA/PVP 30 (3:1) + 1.5% SLS] (top, red) and a physical mixture of [EFA/PVP 30 (3:1) + 1.5% SLS] (bottom, blue). 53

Figure 3.28: An overlay of the STA thermograms of an ASD containing [EFA/PVP 30 + 1.5% SLS] at initial (green), month 1 (purple), month 2 (blue) and month 3 (black) of stability testing. 54

Figure 3.29: XRPD profile of an ASD containing [EFA/PVP 30 (3:1) + 1.5% SLS] at initial (red), month 1 (blue), month 2 (green) and month 3 (grey) of stability testing. 55

Figure 3.30: Dissolution profile of the ASD containing [EFA/PVP 30 (3:1) + 1.5% SLS]..... 56

Figure 3.31: STA thermograms of an [EFA/PVP VA 64 (3:1) +1.5% SLS] physical mixture (top, purple), and a second run of the same sample (bottom, black)..... 57

Figure 3.32: STA thermogram of the ASD containing [EFA/PVP VA 64 (3:1) + 1.5% SLS], prepared by rotary evaporation..... 57

Figure 3.33: SEM photo of a physical mixture of [EFA/PVP VA 64 (3:1) + 1.5% SLS]. 58

Figure 3.34: SEM photo of an ASD containing [EFA/PVP VA 64 (3:1) + 1.5% SLS]. 58

Figure 3.35: HSM photos of the physical mixture of [EFA/PVP VA 64 (3:1) + 1.5% SLS]. ... 59

Figure 3.36: XRPD profile of an ASD containing [EFA/PVP VA 64 (3:1) + 1.5% SLS] (top, red) and a physical mixture of [EFA/PVP VA 64 (3:1) + 1.5% SLS] (bottom, blue)..... 60

Figure 3.37: An overlay of the STA thermograms of an ASD containing [EFA/PVP VA 64 + 1.5% SLS] at initial (green), month 1 (purple), month 2 (blue) and month 3 (black) of stability testing. 61

Figure 3.38: XRPD profile of an ASD containing [EFA/PVP VA 64 (3:1) + 1.5% SLS] at initial (red), month 1 (blue), month 2 (green) and month 3 (grey) of stability testing..... 62

Figure 3.39: Dissolution profile of the ASD containing [EFA/PVP VA 64 (3:1) + 1.5% SLS]. 63

Figure 3.40: Overlay of dissolution profiles of efavirenz and efavirenz ASDs..... 64

Figure 4.1: Simultaneous thermal analysis (STA) thermogram of the PZQ raw material with a melting point of 141.44°C. 70

Figure 4.2: SEM photos of the PZQ raw material. 70

Figure 4.3: HSM photos of the PQZ raw material before and after melting..... 71

Figure 4.4: XRPD profile of the PZQ raw material. 72

Figure 4.5: HPLC chromatogram of the PZQ raw material. 73

Figure 4.6: Linear regression curve of the PZQ raw material..... 74

Figure 4.7: Percentage of the PZQ raw material that had dissolved in distilled water at specific time intervals over a 3-hour period. 74

Figure 4.8: STA thermograms of the PZQ/HPMC (1:3) physical mixture (top, purple), and a second run of the same sample (bottom, black). 75

Figure 4.9: STA thermograms of the PZQ/PVP 25 (1:3) physical mixture (top, purple), and a second run of the same sample (bottom, black). 76

Figure 4.10: STA thermograms of the PZQ/PVP 30 (1:3) physical mixture (top, purple), and a second run of the same sample (bottom, black). 76

Figure 4.11: STA thermograms of the PZQ/PVP VA 64 (1:3) physical mixture (top, purple), and a second run of the same sample (bottom, black). 77

Figure 4.12: STA thermograms of the PZQ/HPMCAS (1:3) physical mixture (top, purple), and a second run of the same sample (bottom, black). 78

Figure 4.13: SEM photos of a physical mixture of PZQ and HPMCAS (1:3)..... 78

Figure 4.14: Images of the physical mixture of PZQ/HPMCAS (1:3) as observed under the microscope. 79

Figure 4.15: XRPD profile of the PZQ/HPMCAS (1:3) physical mixture. 80

Figure 4.16: The percentage of PZQ from the ASD containing PZQ/HPMCAS (1:3) having dissolved in distilled water at specific time intervals over a 24-hour period. 81

Figure 4.17: The percentage of PZQ from the ASD containing PZQ/HPMCAS (1:3) having dissolved in a buffer solution (pH 6.8) at specific time intervals over a 24-hour period..... 82

List of Tables

Table 1.1: Biopharmaceutics classification system (FDA, 2017) 6

Table 2.1: Physico-hemical properties of efavirenz 13

Table 2.2: Physico-chemical properties of praziquantel 13

Table 2.3: HPLC method for the analysis of efavirenz (Raju *et al*., 2008)..... 21

Table 2.4: HPLC method for the analysis of praziquantel (BP, 2017)..... 21

Table 3.1: Theoretical T_g values obtained for EFA (T_g = 33°C) and polymer combinations (blue shaded samples represent those that went through to the final test round.)..... 29

Table 3.2: Moisture content of the EFA raw material over the duration of the stability test period as measured by means of STA (TG analysis)..... 35

Table 3.3: HPLC assay results of the EFA raw material over the duration of the stability test period 36

Table 3.4: Moisture content of EFA/PVP 25 over the duration of the stability test period as measured by means of STA (TG analysis) 46

Table 3.5: HPLC assay results of EFA/PVP 25 over the duration of the stability test period. 47

Table 3.6: Moisture content of EFA/PVP 30 over the duration of the stability test period as measured by means of STA (TG analysis) 54

Table 3.7: HPLC assay results of EFA/PVP 30 over the duration of the stability test period. 55

Table 3.8: Moisture content of EFA/PVP 64 over the duration of the stability test period as measured by means of STA (TG analysis) 61

Table 3.9: HPLC assay results of EFA/PVP VA 64 over the duration of the stability test period 62

Table 4.1: Theoretical T_g values obtained for PZQ (TG = 38°C) and polymer combinations (blue shaded sample represents the one that went through to the final test round) 69

Acknowledgements

I would like to start by thanking the NWU for the best six years of my life, it was an honour to be a part of, in my opinion, the best university in the world. Thank you for making the financial burden lighter as well with all of the bursaries that was awarded to me.

I would like to thank the most wonderful supervisors, Prof. Wilna Liebenberg and Prof. Nicole Stieger. I cannot thank you enough for your unending patience, the wisdom that you shared, for being the best supervisors anyone could ask for and for the chance to do my master's degree, without you it would not have been possible.

Then I would like to thank Madelein for all of your help in the labs, I have learned so much from you and it was an honour working with you.

To my friends that I have known from the start or that I have met recently, I would like to thank you for your support and being there, in my times of need, and for the good times we've had. To Sarika and Niel, I want to thank you especially for being the best roommates and I would also like to say sorry for the times that I have made driven you mad, especially in the early morning hours, I love you guys!

To my parents Heidi and Waldo, I want to thank you for your love and support through everything. Thank you for being my pillars through life and thank you for the financial support that you have given for the last six years, I will make it up to you even if it is only by being successful and making you proud.

And last but by no means least I would like to thank God for this opportunity as without Him it would not have been possible.

May God bless everyone mentioned above as well as everyone that I had the opportunity meeting the last few years as you all have had great impact on my life.

Abstract

Many active pharmaceutical ingredients (API) that are highly permeable, have low aqueous solubility. Such APIs are classified as Biopharmaceutics classification system (BCS) class II drugs. Efavirenz and praziquantel both belong to this class. Efavirenz (EFA) is a non-nucleoside, reverse transcriptase inhibitor that is used in combination for the treatment of human immunodeficiency virus/acquired immunodeficiency syndrome (HIV/AIDS), whereas praziquantel (PZQ) is an anti-helminthic agent, used in the treatment of schistosomiasis (bilharzia). To increase the solubility of these drugs, amorphous forms can be created. The problem with amorphous forms is that they are unstable, whilst crystallisation is almost always a given. To increase the stability of these APIs, amorphous solid dispersions (ASD) are created by using polymers that increase the physical stability of the API and counter crystallisation.

Efavirenz ASDs were prepared by using polyvinylpyrrolidone (PVP) 25, PVP 30 and the PVP VA 64 copolymer. 1.5% of sodium laurel sulphate (SLS) was added as surfactant. The binary mixtures increased the physical stability of the API, whereas the amorphous form of efavirenz crystallised with agitation. The ASD containing [EFA/PVP 25 (3:1) + 1.5% SLS] was physically stable, since no crystallisation had occurred over the 3 months of accelerated stability testing at 40°C and 75% RH. It was, however, chemically unstable, as a total degradation of 66.7% had occurred. The dissolution of this ASD showed an increase in solubility with a total of 5.97% of the API having dissolved after 3 hours. The ASD containing [EFA/PVP 30 (3:1) + 1.5% SLS] was also physically stable, as no crystallisation took place over the 3 months of testing, but degradation of 79.4% was measured. The dissolution rate of this ASD after 3 hours was the best at 6.44%. The ASD containing [EFA/PVP VA 64 (3:1) + 1.5% SLS] was physically stable, as no crystallisation had occurred over the 3 months of testing, with degradation measured at 78.6%. Dissolution of the API from this ASD was 4.42% after 3 hours. It is also noteworthy that these ASDs remained amorphous after dissolution.

The preparation of praziquantel proved difficult and only one ASD was created that was rubbery and elastic, which made further testing difficult. This ASD contained praziquantel and HPMCAS in the ratio of 1:3. Because of the HPMCAS, which is used in modified release preparations, initial dissolution in water delivered unsatisfactory results. As a result of this, the dissolution studies were carried out in a buffered solution at pH 6.8 over 24 hours, resulting in 99.39% of the API having dissolved after 24 hours.

KEYWORDS: Efavirenz, praziquantel, polymer, amorphous solid dispersion, stability, dissolution, HPLC.

Chapter 1

Solid-state Properties of Drugs

1.1 Introduction

Most active pharmaceutical ingredients (APIs) are produced as solids in the form of crystalline powders. Various solid-state properties, such as polymorphic form, stability, solubility, dissolution rate, thermal behaviour, pharmacokinetics and surface activity determine which API form should be used to formulate a drug product that would deliver consistent quality and effectiveness. Since crystalline powders may not be ideally soluble, it may cause problems when formulating dosage forms, as they could have poor bioavailability when taken orally as tablets. As a result, the solid-state properties of a given API can be altered to enhance the solubility and bioavailability of a product (Byrn *et al*., 1999; Hilfiker *et al*., 2006).

1.2 Polymorphism

Polymorphism can be defined as a substance that consists of multiple crystal structures with different unit cells, while still having the exact same molecular formula (Brittain, 2009). Polymorphism results from differences in cooperative interactions of the crystal molecules (Brittain, 2009). Because of the differences in crystal structure, the physical properties of polymorphs can differ significantly. These differences are the result of differences in void volumes, capacity, crystal shapes, dimensions, and the symmetry of the unit cells within the crystal structures (Brittain, 2009). To obtain the most accurate information on the stability relationship of polymorphs, Gibbs' free energy difference ($\Delta \boldsymbol{G}$) is plotted against absolute temperature ($\boldsymbol{T}$), where the most stable polymorph has the lowest Gibbs free energy (Brittain *et al.,* 2001*).*

1.3 Transformations

A solid-state transformation can be defined as a transition from one solid-state form into another, which occurs because of changes in external factors, such as temperature, moisture and pressure (Sato, 1993). The three main types of transformations are solvent interactive, solid-solid, and melt mediated (Sato, 1993).

1.3.1 Solvent interactive transformations

This type of transformation of the solid-state is influenced in any way by the presence of a solvent in vapour, or in liquid form. Three types of solvent interactive transformations exist, i.e. solution-mediated, solvent mediated, and solvent catalysed transformation (Aucamp *et al*., 2015).

- Solution-mediated transformation: Occurs when the solid-state is transformed through a solid-solution-solid transformation.

  Examples: in dissolution where the metastable form transforms into the stable form; recrystallisation to obtain different polymorphic forms, hydrates or solvates.

- Solvent-mediated transformation: A solid-solid transformation during which no direct transformation occurs from the starting material to the final product. The undissolved starting material is mediated by a solvent.

  Examples: anhydrous form converts into a hydrate or solvate; amorphous form crystallises to form a solvate or a hydrate.

- Solvent catalysed transformation: Occurs when a solid-state is transformed by a solvent in vapour or in liquid state (a solid-solid transformation).

  Example: accelerated crystallisation of an amorphous form or glass into an anhydrous crystalline form (Aucamp *et al.,* 2015).

1.3.2 Solid-solid transformations

Solid-solid transformations occur as a result of the direct conversion from one solid-state form into another in the absence of any solution.

Example: Dehydration of the hydrate to the anhydrous crystalline form (Aucamp *et al*., 2015).

1.3.3 Melt mediated transformations

When a crystal is melted through heating above its melting point and successively cooled down, its original crystal form cannot be guaranteed, due to factors, such as impurities, cooling rate and excipients that may affect the recrystallisation course (Law *et al.,* 2004).

1.4 Inclusion compounds

According to Hollingsworth (1996), inclusion compounds can be viewed as a guest molecule that is captured within the crystal structure of the host. Inclusion compounds are used to alter the physico-chemical properties of pharmaceutical ingredients to make processing easier. Unlike a simple mixture, inclusion compounds may cause changes in the crystal structure, crystal properties, as well as growth behaviours (Gao *et al.,* 2017).

1.4.1 Solvates and hydrates

While processing crystals, solvents from the surrounding environment can be merged with the crystal structure to form solvates (Grant & Khankari, 1995). When water molecules are included as the solvate, a hydrate is formed. The water molecules are situated at definitive positions as a result of hydrogen bonding with the molecules within the crystal structure (Grant & Khankari, 1995).

These compounds are used to alter the properties of drugs to simplify manufacturing and formulation, as well as to improve drug stability in various storage environments (Datta & Grant, 2004).

Solvates can be divided into two main classifications, namely stoichiometric and non-stoichiometric solvates.

1.4.1.1 Stoichiometric

Stoichiometric solvates are solvates in which the number of solvent molecules that are present in the crystal structure are fixed at a given temperature and pressure (Baronsky, 2009).

1.4.1.2 Non-stoichiometric

Non-stoichiometric solvates are solvates in which the amount of solvent present within the crystal structure is dependent upon the solvent activity (Baronsky, 2009). According to Mimura *et al.* (2002), incomplete solvation of the crystal structure is what causes non-stoichiometric solvates to form.

1.4.2 Desolvation / dehydration

Desolvation or dehydration is the removal of any solvents that are present within crystals, typically through drying. The desolvation or dehydration rate can influence the final crystal form that is obtained (Hilfiker, 2006).

1.4.3 Co-crystals

Co-crystals are supra-molecular complexes that are formed between crystals of different molecular structures, mainly as a result of hydrogen bonding in the absence of hydrogen-ion transfer (Sekhon, 2009; Yadav *et al.,* 2009). Co-crystal structures are formed through inter-molecular interactions between molecular fragments of crystals, also called supra-molecular synthons (Yadav *et al.*, 2009). By selectively reorganising non-covalent interactions between solid-state molecules, the properties of these molecules can be changed (Yadav *et al*., 2009).

1.4.4 Clathrates

A clathrate is a compound which is entombed in the hollows within the crystal structure, without any bonding with the crystal molecules (Datta & Grant, 2004). Clathrates can be employed practically by adding functional properties to guest molecules, as well as being able to separate organic isomers (Kitamura & Fujimoto, 2003). According to Kitamura and Fujimoto (2003), crystal growth behaviour is essential in the formation of clathrates, as it dictates the final composition, as well as structure of the clathrate that forms. A pharmaceutical example of a clathrate is sodium warfarin, which is the host molecule in which iso-propanol and water act as guest molecules, in ratios varying from 8:4:0 to 8:2:2 (Hiskey & Melnitchenko, 1965).

1.4.5 Salts

Brittain (2013) states that salts are homogenous solids in which protons are shifted within the crystal structure. The physico-chemical properties that can be improved by salts include improved solubility, thermal properties, and enhanced organoleptic properties (Makary, 2014).

1.5 Amorphism

Compared to a crystal that has a long-range order of molecules, with the same order being repeated throughout the material, an amorphous solid lacks such long range order and has no clearly defined molecular structure (Yu, 2001).

Compared to crystals, amorphous solids possess much higher internal energies, which negatively impact their stability upon storage, during which they tend to recrystallise (Beyer *et al.,* 2016). The higher internal energies of amorphous substances result in an increase in vapour pressure, solubility and chemical reactivity, which enhance the bioavailability of drugs (Johari & Shanker, 2014).

1.5.1 Amorphous solid dispersions (ASDs)

To overcome the instability of amorphous forms, the manufacture of amorphous solid dispersions (ASDs) are becoming increasingly popular. Solid dispersions are a blend of two or more substances that are solids at ambient conditions (Lim *et al*., 2017), most likely a poorly water-soluble API and a suitable polymer. Solid dispersions are used to increase the stability of amorphous drugs by using polymers to prevent recrystallisation. They are prepared in the same manner as single amorphous substances, but with the addition of a polymer that acts as a stabiliser of the amorphous substance (Newman *et al*., 2011).

1.5.1.1 Preparation of amorphous solid dispersions

Amorphous solid dispersions can be prepared through several methods, including anti-solvent addition, hot melt, spray drying, solvent evaporation and freeze-drying methods (Benes *et al.*, 2017).

The hot melt method has many advantages, as it is environmentally friendly, it does not require any solvents, while scalable continuous processing can be utilised (Gao *et al*., 2017). These pharmaceuticals are melted by heating them above their glass transition temperatures (Gao *et al.,* 2017).

Spray drying entails creating a fine mist out of a super saturated solution, which is mixed with heated air that causes evaporation of the solvent, which in turn causes the solute to precipitate as drying occurs (Dobry *et al*., 2015).

Freeze drying can harm amorphous substances, as it includes moisture which in turn lowers the stability of the substance by lowering the glass transition temperature (Trnka *et al.,* 2015). Freeze drying entails freezing the substance at very low temperatures and drying it at ambient temperature (Trnka *et al.,* 2015).

The solvent evaporation method for preparing amorphous solid dispersions, for instance, involves rapid removal of the solvent in which the polymer and drug are dissolved, usually by employing rotary evaporation.

Anti-solvent addition is the addition of a substance to a super saturated solution, where the solubility of the substance is lowered in the presence of the anti-solvent, causing it to precipitate out of the solution (Nagy *et al*., 2008).

1.5.1.2 Glass transition temperature

The glass transition temperature is well below the substance's melting point, at which a continuous transformation between liquid and glass occurs (Korichi *et al*., 2016). At this temperature, changes occur in the physico-chemical properties of the substance, such as electric polarizability, compressibility and expansivity (Korichi *et al*., 2016).

1.6 Solubility and dissolution

Dissolution is the process by which molecules are transferred from a solid substance into solution (Aulton, 2013), whereas solubility is the amount of a solid substance that is able to dissolve in a specific amount of solute once equilibrium is attained, with all variables being equal (Shargel *et al.*, 2012).

Solubility is an important property of APIs, as it affects pharmacokinetics, such as release, degree of absorption and transport, drug efficacy, future development and formulation efforts (Sharapova *et al*., 2017). The solubility of a given API is affected by many factors, including temperature, pH, ionic strength, agitation, molecular structure of solutes, and the nature of the solutes (Yazdanshenas & Gharib, 2017).

Solubility directly influences the dissolution rate of APIs, thus when an API exhibits poor solubility the dissolution rate becomes limited, causing poor absorption and thus poor bioavailability (Kawabata *et al*., 2011).

The Biopharmaceutics classification system (BCS) categorises drugs into four classes (Table1.1) according to their solubility and permeability (Kawabata *et al*., 2011). BCS class II drugs typically are the most ideal candidates for applying any method of solubility improvement, as a minor increase in dissolution rate often results in a marked improvement in bioavailability (Kawabata *et al*., 2011).

Table 1.1: Biopharmaceutics classification system (FDA, 2017)

Class	Description
I	• High solubility • High permeability
II	• Low solubility • High permeability
III	• High solubility • Low permeability
IV	• Low solubility • Low permeability

The two drugs that were investigated during this study were both from the BCS class II drugs, which exhibit poor aqueous solubility. Most APIs are produced as crystalline powders. To establish the dosage form to be used, many physico-chemical properties are taken into consideration, such as the solid-state form, molecular structure, stability, solubility, dissolution rate, thermal behaviour, pharmacokinetics and surface activity (Byrn *et al*., 1999; Hilfiker *et al*., 2006). Such crystalline powders might not be ideally soluble, which causes problems when formulating dosage forms and also with regards to their bioavailability when taken orally (Hoffmeister *et al*., 2016; Cugovčan *et al.*, 2017). Methods that have been implemented to date to improve the solubility and dissolution of poorly soluble APIs include the preparation of pure amorphous forms, salts, co-crystals and more recently, the preparation of pharmaceutical amorphous solid dispersions (ASDs) (Brough & Williams, 2013).

1.7 pKa and Log P

1.7.1 pKa

According to Aulton (2013), pKa is the dissociation constant, which determines the ionisation profile of a substance, as well as its physico-chemical and pharmacokinetic properties. This is of importance, as the ionised fraction is more hydrophilic, whilst the unionised form is more lipophilic, making the unionised form easier absorbable by membranes, which increases its bioavailability.

1.7.2 Log P

The partition coefficient, log P, represents the lipophilicity of a substance and can be described as the ratio of solute present in the partition solvent that is immiscible in water, relative to the ratio of solute present in water (Aulton, 2013).

1.8 Conclusion

In conclusion, the physico-chemical properties of solid-state drugs, such as the stability, solubility and bioavailability differ from one form to another, which impact on the performance of an API as a useable drug. It can therefore be said that the correct solid-state form should be chosen for use in formulation for a maximum therapeutic effect of the final product, since the incorrect form would have a negative impact on its bioavailability.

References

Aucamp, M.E., Liebenberg, W. & Stieger, N. 2015. Solvent-interactive transformations of pharmaceutical compounds. (*In* Mastai, Y., *ed.* Advanced topics in crystallisation. InTech, DOI: 10.5772/59586. [Web:] http://www.intechopen.com/books/advanced-topics-in-crystallization/solvent-interactive-transformations-of-pharmaceutical-compounds) [Date of access: 2018-07-24].

Aulton, M.E. 2013. Dissolution and solubility. (*In* Aulton, M.E., *ed*. Pharmaceutics: the design and manufacture of medicines. New York: Churchill Livingstone. p. 20-37).

Baronsky, J. 2009. Solid form analysis with special consideration of perfusion calorimetry. PhD thesis. Universität, Düsseldorf. 150p.

Benes, M., Pekarek, T., Beranek, J., Havlicek, J., Krejcik, L., Simek, M., Tkadlecova, M. & Dolezal, P. 2017. Methods for the preparation of amorphous solid dispersions: a comparative study. *Journal of drug delivery science and technology*, 38:125-134.

Beyer, A., Grohganz, H., Löbman, K., Rades, T. & Leopold, C.S. 2016. Influence of the cooling rate and the blend ratio on the physical stability of co-amorphous naproxen/ indomethacin. *European journal of pharmaceutics and biopharmaceutics*, 109:140-148.

Brittain, H.G., Grant, D.J.W. & Vippagunta, S.R. 2001. Crystalline solids. *Advanced drug delivery reviews*, 48:3-26.

Brittain, H.G. 2009. Theory and principles of polymorphic systems. (*In* Brittain, H.G., *ed*. Polymorphism in pharmaceutical solids. New York: Informa Healthcare. p. 1-23).

Brittain, H.G. 2013. Pharmaceutical co-crystyals: the coming wave of new drug substances. *Journal of pharmaceutical sciences*, 102:311-317.

Brough, C. & Williams, R.O. 2013. Amorphous solid dispersions and nano-crystal technologies for poorly water-soluble drug delivery. *International journal of pharmaceutics*, 453:157-166.

Byrn, S.R., Pfeiffer, R.R. & Stowell, J.G. 1999. Solid-state chemistry of drugs. 2nd ed. West Lafayette, Ind.: SSCI. 574p.

Cugovčan, M., Jablan, J., Lovrić, J., Cinčić, D. & Galić, N. 2017. Biopharmaceutical characterization of praziquantel cocrystals and cyclodextrin complexes prepared by grinding. *Journal of pharmaceutical and biomedical analysis*, 137:42-53.

Datta, S. & Grant, D.J.W. 2004. Crystal structures of drugs: advances in determination, prediction and engineering. *Nature reviews, 3:42-57.*

Dobry, D.E., Settell, D.M. & Baumann, J.M. 2015. Spray drying and scale-up (*In* Newmann, A., *ed*. Pharmaceutical amorphous solid dispersions. John Wiley & Sons. p. 488).

FDA see United States Food and Drug Administration.

Gao, N., Gou, M., Fu, Q. & He, Z. 2017. Application of hot melt extrusion to enhance the dissolution and oral bioavailability of oleanolic acid. *Asian journal of pharmaceutical sciences,* 12(1): 66-72.

Grant, D.J.W. & Khankari, R.K. 1995. Pharmaceutical hydrates. *Thermochimica acta*, 248:61-79.

Hilfiker, R., Blatter, F. & Van Raumer, M. 2006. Relevance of solid-state properties for pharmaceutical products. (*In* Hilfiker, R., *ed.* Polymorphism in the pharmaceutical industry. Weinheim: Wiley-VCH. p. 1-15; 333-360).

Hiskey, C.F. & Melnitchenko, V. 1965. Clathrates of sodium warfarin. *Journal of pharmaceutical sciences*, 54(9):1298-1302.

Hoffmeister, C.R.D., Fandaruff, C., Da Costa, M.A., Cabral, L.M., Pitta, L.R., Bilatto, S.E.R., Prado, L.D., Corrêa, D.S., Tasso, L., Silva, M.A.S. & Rocha, H.V.A. 2016. Efavirenz dissolution enhancement III: colloid milling, pharmacokinetics and electronic tongue evaluation. *European journal of pharmaceutical sciences*, 99:310-317.

Hollingsworth, M.D. 1996. Inclusion compounds. *Current opinion in solid state and material science,* 1:514-521.

Johari, G.P. & Shanker, R.M. 2014. On the solubility advantage of a pharmaceutical's glassy state over the crystal state, and of its crystal polymorphs. *Thermochimica acta*, 598:16-27.

Kawabata, Y., Wada, K., Nakatani, M., Yamada, S. & Onoue, S. 2011. Formulation design for poorly water-soluble drugs based on biopharmaceutics classification system: basic approaches and practical applications. *International journal of pharmaceutics*, 420:1-10.

Korichi, M., Mokadem, K. & Thumba, K. 2016. An enhanced group-interaction contribution method for the prediction of glass transition temperature of ionic liquids. *Fluid phase equilibria*, 425:259-268.

Kitamura, M. & Fujimoto, M. 2003. Release control of industrial biocide (CMI) using clathrate crystal with TEP. *Journal of crystal growth*, 256:393-400.

Law, D., Qui, Y., Schmitt, E.A. & Zhang, G.G.Z. 2004. Phase transformation consideration during process development and manufacture of solid oral dosage forms. *Advanced drug delivery reviews,* 56:371-390.

Lim, R.T.Y., Ong, C.K., Cheng, S. & Ng, W.K. 2017. Amorphization of crystalline active pharmaceutical ingredients *via* formulation technologies. *Powder technology*, 311:175-184.

Makary, P. 2014. Principles of salt formation. *UK journal of pharmaceutical and biosciences*, 2(4):01-04.

Mimura, H., Kitamura, S., Kitagawa, T. & Kohda, S. 2002. Characterization of the non-stoichiometric and isomorphic hydration and solvation in FK041 clathrate. *Colloids and surfaces B: biointerfaces*, 26(4):397-406.

Nagy, Z.K., Fujiwara, M. & Braatz, R.D. 2008. Modelling and control of combined cooling and antisolvent crystallization process. *Journal of process control*, 18(9):856-864.

Newman, A., Knipp, G. & Zografi, G. 2011. Assessing the performance of amorphous solid dispersions. *Journal of pharmaceutical sciences*, 101(4):1355-1377.

Sato, K. 1993. Polymorphic transformations in crystal growth. *Journal of physics D: applied physics,* 26:B77-B84.

Sekhon, B.S. 2009. Pharmaceutical co-crystals: a review. *ARS pharmaceutica,* 50(3):99-117.

Sharapova, A., Ol'khovich, M., Blokhina, S. & Perlovich, G. 2017. Physico-chemical characterization of antituberculosis thioacetazone: vapor pressure, solubility and lipophilicity. *Journal of chemical thermodynamics*, 108:18-25.

Shargel, L., WU-Pong, S. & Yu, A.B.C. 2012. Applied biopharmaceutics and pharmacokinetics. 6th ed. New York: McGraw Hill, 811 p.

Trnka, H., Rantanen, J. & Grohganz, H. 2015. Well-plate freeze drying: a high throughput platform for screening of physical properties of freeze-dried formulations. *Pharmaceutical development and technology*, 20(1):65-73.

United States Food and Drug Administration. 2017. Waiver of *in vivo* bioavailability and bioequivalence studies for immediate-release solid oral dosage forms based on a biopharmaceutics classification system guidance for industry. [Web:] https://www.fda.gov/downloads/Drugs/GuidanceComplianceRegulatoryInformation/Guidances/UCM070246 [Date of access: 20 April 2018].

Yadav, A.V., Shete, A.S., Dabke, A.P., Kulkarni, P.V. & Sakhare, S.S. 2009. Co-crystals: a novel approach to modify physicochemical properties of active pharmaceutical ingredients. *Indian journal of pharmaceutical sciences*, 71(4):359-370.

Yazdanshenas, R. & Gharib, F. 2017. Solubility and thermodynamic functions measurement of morin hydrate in different alcohols. *Journal of molecular liquids,* 233:9-14.

Yu, L. 2001. Amorphous pharmaceutical solids: preparation, characterization and stabilization. *Advanced drug delivery reviews*, 48:27-42.

Chapter 2

Materials and Methods

2.1 Introduction

The research problem is the inadequate solubility, dissolution rate and subsequently poor bioavailability of both efavirenz and praziquantel when administered orally in crystalline form, as well as the instability of their pure amorphous forms, as demonstrated by Stieger *et al*. (2013).

2.2 Efavirenz

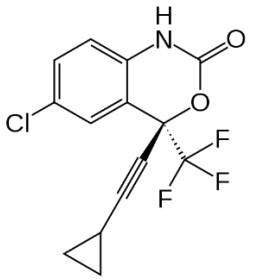


Figure 2.1: The molecular structure of efavirenz (Wiktionary, 2018).

Efavirenz (Fig. 2.1) is a synthetic, purine derived, non-nucleoside, reverse transcriptase inhibitor (NNRTI) used in combination treatments of human immunodeficiency virus/acquired immunodeficiency syndrome (HIV/AIDS) (Ravikumar & Sridhar, 2009). Efavirenz is a BCS class II drug, having poor aqueous solubility and high permeability, whereas its absorption rate is dependent upon its dissolution rate (Pawar *et al*., 2016). The oral bioavailability of efavirenz is between 40 - 50%, with high inter-subject variability. Efavirenz is marketed as a 600 mg tablet. By improving the solubility of efavirenz, its bioavailability would likely improve as well. To date, no salt form has been published or marketed, which may be indicative thereof that it could be difficult to produce. The physico-chemical properties of efavirenz are illustrated in Table 2.1.

Table 2.1: Physico-chemical properties of efavirenz

Colour	Fine white crystalline powder
Solubility	0.093 µg/ml in water at 25°C (Pubchem, 2018a)
Dissociation constant	12.52 (Drugbank, 2018a)
Melting point	138.53°C as determined in-house

2.3 Praziquantel

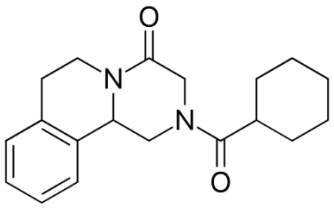


Figure 2.2: The molecular structure of praziquantel (Wikipedia, 2018a).

Praziquantel (Fig. 2.2) is an anti-helminthic and the primary drug of choice for the treatment of schistosomiasis, better known as bilharzia (Trastullo *et al*., 2015). Praziquantel is also a BCS class II drug with poor solubility and high permeability (Lindenberg *et al*., 2004). Praziquantel is marketed as a 600 mg tablet. It is not possible to prepare a salt from praziquantel, as it does not contain any salt forming groups in its chemical structure (Cugovčan *et al.*, 2017). The physico-chemical properties of praziquantel are illustrated in Table 2.2.

Table 2.2: Physico-chemical properties of praziquantel

Colour	Fine white crystalline powder
Solubility	400 µg/ml in water at an unspecified temperature (Pubchem, 2018b)
Dissociation constant	19.38 (Drugbank, 2018b)
Melting point	141.44°C as determined in-house

2.4 Polymers

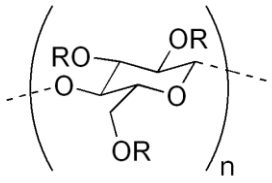
Synthetic polymers were used during this study. Soluble polymers with moderate molecular weights, such as hydroxypropyl methylcellulose (HPMC) and polyethylene glycol (PEG) were used. The other group of polymers consisted of the hydrogels, such as polyvinylpyrrolidone (PVP), which, although it has the capability to swell, it does not dissolve when in contact with water. These polymers were chosen, because of their wide use in pharmaceutical, cosmeceutical and food applications and therefore because of their proven safety records (Narayan *et al*., 2015). Polymers that were available for use in this study included:

- Hydroxypropyl methylcellulose (HPMC), having a status of being 'generally recognised as safe' (GRAS) (Teja *et al*., 2013);
- Hydroxypropyl methylcellulose acetate succinate (HPMCAS), maximum oral potency 560 mg per day (FDA, 2017a);
- Polyvinylpyrrolidone (PVP 25), GRAS status (Teja *et al*., 2013);
- Polyvinylpyrrolidone (PVP 30), GRAS status (Teja *et al*., 2013);
- Polyvinylpyrrolidone (PVP 90), maximum oral potency 78 mg per day (FDA, 2017b);
- Vinylpyrrolidone-vinyl acetate copolymer (PVP VA 64) copolymer, GRAS status (Teja *et al*., 2013); and

Inactive ingredients (including polymers and surfactants) that are used in pharmaceuticals are not usually evaluated independently by the FDA, but rather as part of a complete new product application. The above maximum oral potency values are therefore representative of the highest amounts having been approved in oral products to date, as part of existing drug products and they do not necessarily indicate the maximum safe daily intake amounts. Exceptions are made for inactive ingredients when used in food products, where the developer of such an ingredient opts to apply for the GRAS status. Such status is granted if toxicological studies have indicated that the consumption of relatively large quantities over a prolonged period of time have not resulted in any adverse, carcinogenic, or teratogenic effects (Davis, 2006).

2.4.1 Hydroxypropyl methylcellulose (HPMC)

HPMC (Fig. 2.3) is an excipient that is used in various applications in pharmaceutical manufacturing, for example as a hydrophilic matrix in extended release tablet forms, as a binder, as well as to prevent precipitation and to maintain super saturation (Guo *et al.,* 1998).



R = H or CH_3 or $CH_2CH(OH)CH_3$

Figure 2.3: The molecular structure of HPMC (Wikipedia, 2018b).

2.4.2 Hydroxypropyl methylcellulose acetate succinate (HPMCAS)

HPMCAS is a mixture of acetic and mono-succinic acid esters of HPMC, which is present at diverse grades, because of differences in succinyl and acetyl group substitution (Grasman, 2012).

HPMCAS is widely used in the manufacturing of solid dispersions (Dong & Choi, 2008). The molecular structure of HPMCAS is shown in Figure 2.4.

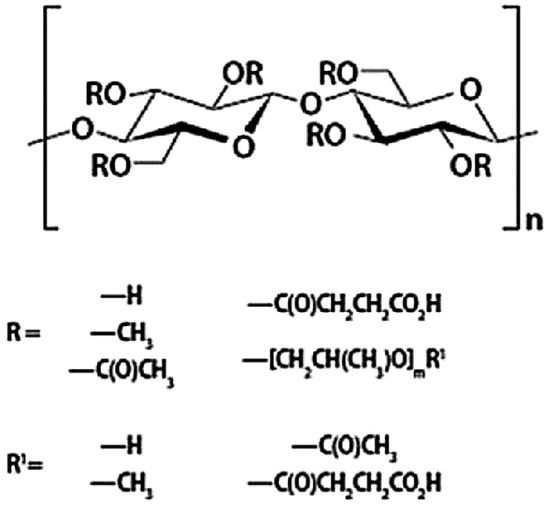


Figure 2.4: The molecular structure of HPMCAS (Pinto *et al.,* 2018).

2.4.3 Polyvinylpyrrolidone (PVP)

Polyvinylpyrrolidone is the polymerised form of vinylpyrrolidone, with molecular weights between 2 500 - 3 000 000 (Leuner & Dressman, 2000). PVP is mainly used as binder and disintegrant in tablets and is it one of the most common and popular polymers used in the pharmaceutical industry (Anon, 2018a). The molecular weight of PVP 25 is between 28 000 – 34 000, and that of PVP 30, between 44 000 – 54 000 (Anon, 2018b). The molecular structure of PVP is shown in Figure 2.5.

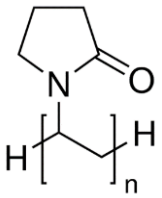


Figure 2.5: The molecular structure of PVP (Sigma-Aldrich, 2018).

2.4.4 Vinylpyrrolidone-vinyl acetate copolymer (PVP VA 64)

PVP VA 64 is a copolymer consisting of 1-vinyl-2-pyrrolidone and vinyl acetate in a ratio of 6:4 by mass (Song *et al.,* 2013). PVP VA 64 is used in granulation, as dry binder in tabletting, and also as a solubilizer in hot-melt extrusion processes (Anon, 2018c). The molecular structure of PVP VA 64 is illustrated in Figure 2.6.

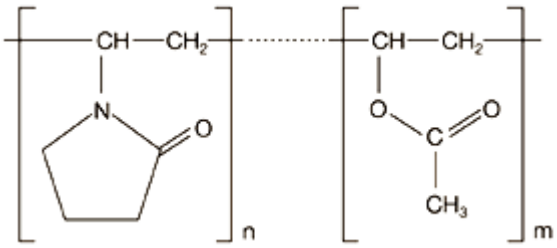


Figure 2.6: The molecular structure of PVP VA 64 (Aurora, 2018).

2.5 Surfactants

The addition of a small amount (determined experimentally during this study) of surfactant, as third component to an amorphous solid dispersion (ASD), has in many cases demonstrated an improved solubility, dissolution and to prolong the period of solubility advantage. Again, the surfactants being used in this study were chosen because of their wide use in pharmaceutical, cosmeceutical and food applications hence their proven safety records (Narayan *et al*., 2015). The amount of each surfactant being used was dependent upon the glass transition temperature (T_g), experimental results during this study, as well as safety considerations. The surfactants that were available (in-house) for investigation included:

- Polysorbate 80, maximum oral potency 418.37 mg (FDA, 2017d);
- Sodium lauryl sulphate (SLS), maximum oral potency 96 mg (FDA, 2017e);
- Phosphatidylcholine, maximum oral potency 325 mg (FDA, 2017f); and
- Lauryl macrogol-32 glycerides, maximum oral potency 218 mg (FDA, 2017g).

2.6 Screening process of polymers for amorphous drug stabilisation

The aim of this study was to improve the solubility and dissolution rates of efavirenz and praziquantel, by creating stable amorphous solid dispersions (ASDs), using a labour efficient modified process, i.e. ‘Screening of polymers for amorphous drug stabilisation’ (SPADS) (Fig. 2.7).

A modified SPADS method (Fig. 2.7) has been used to derive the most optimal mixture and ratio of API:polymer:surfactant, with minimum labour input. The unsuccessful and less successful combinations were abandoned, and only the successful combinations were tested, until the ASD with the best physico-chemical properties had been identified.

The steps taken to identify the ASD with the best physico-chemical properties is summarised below.

- Eliminate polymers and drug:polymer ratios that would potentially result in ASDs having theoretically combined T_g values too low for stability or production processes;
- Determine the miscibility of the remaining drugs and polymers at the chosen ratios to eliminate any ratios or polymers that would not result in ASDs being dispersed at molecular level (thermal analysis, X-ray powder diffractometry, Fourier-transform infrared spectroscopy, hot-stage microscopy, and variable temperature X-ray diffractometry where needed);
- Prepare ASDs for testing using the hot-melt method, rapid solvent evaporation, rapid precipitation, or grinding (with or without solvents);
- Perform *in vitro* solubility and dissolution tests on the most [#]promising ASDs, eliminating all but those with the best dissolution profiles;
- During production, add a third component to the [#]best ASDs in the form of surfactants that are commonly used in the pharmaceutical industry;
- The three-component ASDs must be prepared and tested similarly as the two-component ASDs;
- Only some of the very best performing ASDs would go through to the next round of testing, which would involve accelerated stability testing.
- From all these steps it should be possible to select an ASD with improved solubility and good stability for product development.

[#] Most promising or best ASD would be the ASD with the best physico-chemical properties, such as solubility, stability and dissolution profile. If multiple ASDs show improved properties, those improvements should be quantified and only the best few candidates should proceed to the next round of testing (refer to Fig. 2.7). The practicality of production must also be taken into account.

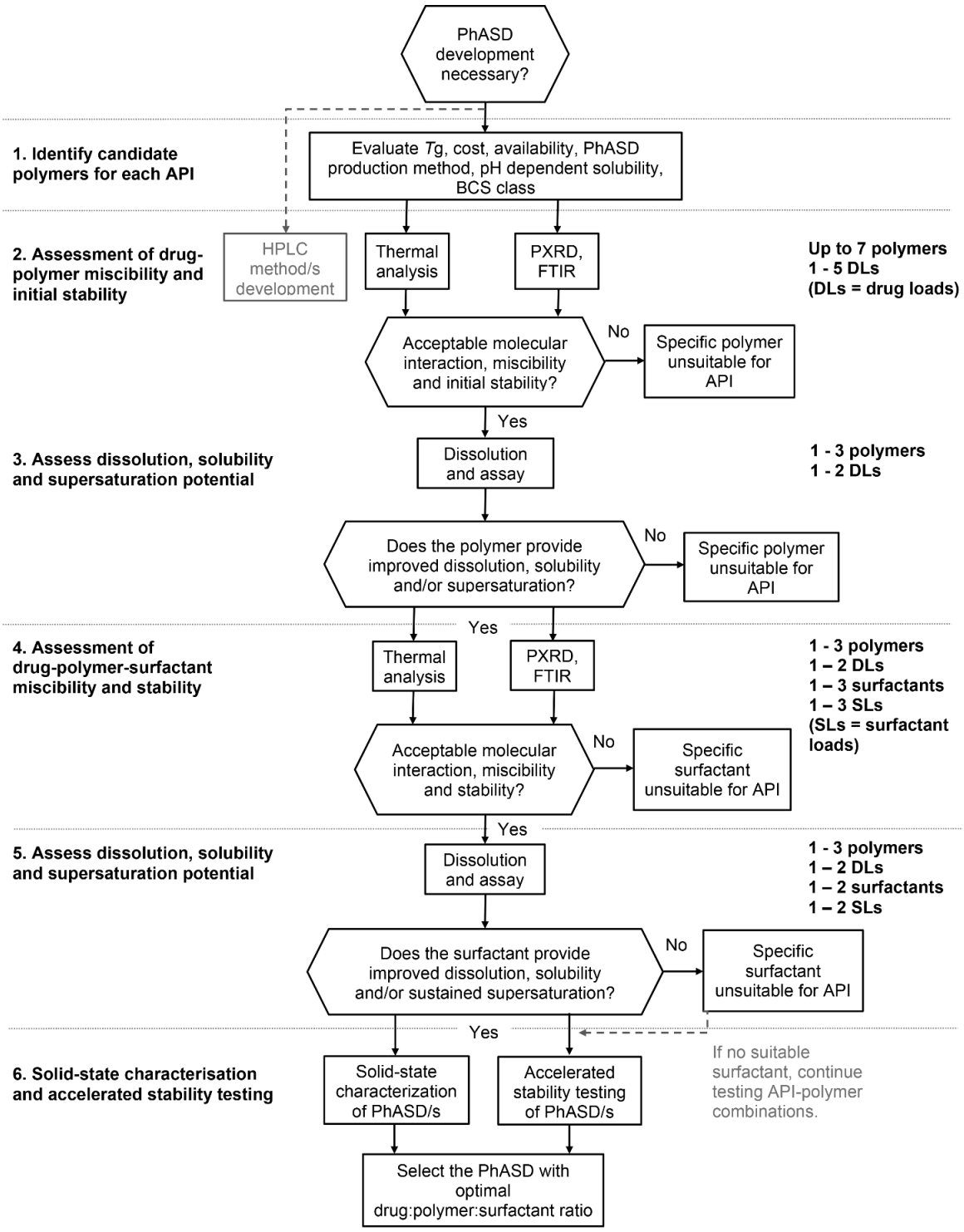


Figure 2.7: Modified screening of polymers for amorphous drug stabilization (SPADS) process (Stieger & Liebenberg, 2017).

2.6.1 Preparation methods

Various methods for the preparation of laboratory scale amorphous solid dispersions (ASDs) have been reported in literature. All methods report on the challenge of mixing the correct matrix and drug in the correct ratio. The first ever published ASD for pharmaceutical applications was prepared by the fusion method. This method, however, has limitations, such as the possible occurrence of degradation of the drug, while the two compounds must also be compatible with each other.

The solvent evaporation method involves the rapid removal of the solvent in which both the polymer and drug are dissolved, usually by employing rotary evaporation.

Other methods include physical grinding, with or without a small amount of solvent, and rapid precipitation by adding an anti-solvent (Dhirenda *et al*., 2009).

2.7 Characterisation methods

2.7.1 Simultaneous thermal analysis (STA) (TGA/DSC)

A simultaneous thermal analysis procedure simultaneously measures the mass loss (TGA) and heat flow (DSC) of a test sample during the heating process. With this combined technique, information about the mass loss, melting point, glass transition, solid-state transformation(s), loss of solvents and degradation of a sample can be obtained (Brown, 2001).

A Mettler DTG 3^+ (Mettler Toledo, Greifensee, Switzerland) was used to record the DSC and TGA thermograms. Powder samples, weighing approximately 3 - 5 mg, were placed in aluminium crimp cells, each open or sealed (100 µl) and heated to an end temperature, dependent upon the melting point of the API and/or polymer, at a heating rate of 10°C/min and a nitrogen gas flow of 35 ml/min. The samples were then allowed to cool down, after which they were once more subjected to the same thermal program. The test results aimed at showing whether a glass had formed, if a T_g could be observed and whether crystallisation has occurred during heating.

2.7.2 Hot-stage microscopy (HSM)

Hot-stage microscopy is used to visually examine a sample during heating (Brown, 2001). HSM enables the study and physical characterisation of materials as a function of temperature and time, due to the combination of microscopy and thermal analysis (Stieger *et al.,* 2012). With this technique, the diversity or homogeneity of a crystal sample can be observed, melting points can be compared, polymorphic transformations can be observed and solvates can be detected (Bernstein, 2002). Hot-stage microscopy provides qualitative information on the behaviour of

different solid-state forms of a drug. When this technique is combined with quantitative DSC data, more meaningful information can be obtained (Brown, 2001).

The hot-stage microscope used in this study was a Nikon Eclipse 50i microscope (Tokyo, Japan) fitted with a Nikon DS-Fi1 camera and a Linkam THMS600 heating stage (Surrey, UK), equipped with a T95 LinkPad temperature controller.

2.7.3 Scanning electron microscopy (SEM)

Scanning electron microscopy (SEM) scans a sample by means of a focused beam of electrons to produce an image of that sample. It is used to examine the morphology, crystal habit and surface topography of a sample (Bernstein, 2002).

An FEI Quanta 200 FEG SEM with an X-Max 20 EDS system (FEI, USA) was used to obtain micrographs of the various crystal and amorphous forms. In preparation, samples were adhered to a small piece of carbon tape, mounted onto a metal stub and coated with a gold-palladium film (Eiko Engineering Ion Coater IB-2, Japan).

2.7.4 X-ray powder diffraction (XRPD)

X-ray powder diffraction (XRPD) is a useful technique for the crystallographic characterization of an API. It can be used to differentiate between and identify different solid-state forms of the same API (Bhattacharya *et al*., 2009).

X-ray powder diffraction patterns were obtained using a PANalytical Empyrean diffractometer (PANalytical, Almelo, Netherlands). The measurement conditions were: target, Cu; voltage, 40 kV; current, 30 mA; divergence slit, 2 mm; anti-scatter slit, 0.6 mm; detector slit, 0.2 mm; monochromator; scanning speed, 2°/min (step size, 0.025°; step time, 1.0 sec).

2.7.5 High performance liquid chromatography (HPLC)

High performance liquid chromatography (HPLC) is a technique that is used to quantify and identify individual components present in a sample (Hassan, 2012). In HPLC, a pump produces an elevated pressure that causes the mobile phase to move through a column. The column, packed with very small porous particles, is the stationary phase (Moldoveanu & David, 2013).

For HPLC analysis, a Shimadzu (Kyoto, Japan) UFLC chromatographic system was used. The system consisted of a SIL-20AC auto-sampler, fitted with a sample temperature controller, a UV/VIS photodiode array detector (SPD-M20A) and an LC-20AD solvent delivery module. The mobile phase was degassed and filtered prior to use. The mobile phase and column were

dependent upon the active being analysed. Official monograph methods were followed, where available. The methods used were validated in-house for this study.

2.7.5.1 Efavirenz

Table 2.3: HPLC method for the analysis of efavirenz (Raju *et al*., 2008)

Solvent	60:40 Acetonitrile: deionised water
Mobile phase	60:40 Acetonitrile:0.03 M KH_2PO_4 in deionised water (adjusted to pH 3.2 with orthophosphoric acid)
Flow rate	1 mL/min
Run time	15 min
Wavelength	260 nm
Injection volume	20 µL
Column	Phenomenex, C-18 (250 x 4.6 mm)

2.7.5.2 Praziquantel

Table 2.4: HPLC method for the analysis of praziquantel (BP, 2017)

Solvent	55:45 Acetonitrile: deionised water
Mobile phase	55:45 Acetonitrile: deionised water
Flow rate	1 mL/min
Run time	15 min
Wavelength	210 nm
Injection volume	20 µL
Column	Phenomenex, C-18 (250 x 4.6 mm)

2.7.6 Stability testing

2.7.6.1 Temperature and humidity

The effects of increased temperature and humidity were determined by storing approximately 500 mg of each selected ASD in a Petri dish each. The samples were distributed evenly on the surface of the Petri dishes and were 3 samples prepared for every storage condition. The samples were stored at controlled conditions in a climatic chamber (Binder, Germany) at 40°C / 75% relative

humidity (RH) for a period of 3 months. A sufficient amount of each sample was taken at 0, 1, 2 and 3-month intervals. The samples were assayed to determine their purity and signs of possible degradation by means of HPLC analysis. STA and XRPD analyses were also done to determine whether any solid-state changes had occurred during storage of the samples.

2.7.7 Powder dissolution studies

The dissolution rate of a drug has an important impact on its bioavailability and bioequivalence (Byrn *et al*., 1999). Amorphous drugs, or multi-component drug systems exhibit an initial apparent solubility that is much higher than that of the crystalline drug. However, the concentration decreases over time, as the amorphous form crystallises into the stable and less soluble form. Dissolution studies yield information pertaining to the apparent solubility being acquired in a particular medium at a certain temperature, and also shows how long the solubility advantage can be maintained (Stieger *et al.,* 2017).

A VanKel700 (Varian, Palo Alto, USA) dissolution bath was used for dissolution testing. USP apparatus 2 (paddle) had been set up at 37°C ± 2°C at a rotational speed of 75 rpm, and 900 mL of the dissolution medium (distilled water) was added to each dissolution vessel. A *powder mass, which had been determined experimentally from the preceding solubility studies was weighed into 10 mL test tubes each, to which glass beads with half the mass of the API, ≤ 106 µm (Sigma-Aldrich, South Africa), were added. 5 mL of dissolution medium, maintained at 37°C ± 2°C, was added to each test tube. The mixtures were agitated for a period of 60 seconds, using a vortex mixer. The resulting mixtures were then each transferred into a dissolution vessel. 5 mL samples were withdrawn from each dissolution vessel at predetermined time intervals.

*Powder mass used for efavirenz = 600 mg.

*Powder mass used for praziquantel = 500 mg.

The dissolution medium was not replaced after each sampling interval, since a super saturated solution was required to observe any solution-mediated transformations. After withdrawal, each sample was filtered through a 0.45 µm PVDF filter into an HPLC vial each. The filtered solutions were subsequently analysed on HPLC.

References

Anon. 2018a. PVP BASF technical data. [Web:] https://pharmaceutical.basf.com/en/PVP-Polyvinyl-pyrrolidone.html [Date of access: 2018-08-23].

Anon. 2018b. Soluble Kollidon grades: technical information. [Web:] http://www2.pharm.u-szeged.hu/phtech/tananyagok/tablettazo/Soluble_Kollidon.PDF [Date of access: 2018-09-30].

Anon. 2018c. Excipients for drug formulation: Kollidon VA64. [Web:] https://pharmaceutical.basf.com/en/Drug-Formulation/Kollidon-VA64.html [Date of access: 2018-10-12].

Aurora. 2018. *Kollidon® VA 64*. [WEB] Available at: http://www.aurora-pharma.com/en/products_catalogue/excipients/binders/1507.htm [Date of access: 2018-11-11].

Bernstein, J. 2002. Polymorphism in molecular crystals. Oxford: Clarendon Press. 410p.

Bhattacharya, S., Brittain, H.G. & Suryanarayanan, R. 2009. Thermoanalytical and crystallographic methods. (*In* Brittain, H.G., *ed*. Polymorphism in pharmaceutical solids. New York: Informa healthcare. p. 318-346).

BP see British Pharmacopoeia.

British Pharmacopoeia. 2017. Praziquantel. [Web:] https://www-pharmacopoeia-com.nwulib.nwu.ac.za/bp-2017/monographs/praziquantel.html?published-date=2016-08-23&text=praziquantel [Date of access: 2017-07-02].

Brown, M.E. 2001. Introduction to thermal analysis. Netherlands: Kluwer Academic Publishers. 264p.

Byrn, S.R., Pfeiffer, R.R. & Stowell, J.G. 1999. Solid-state chemistry of drugs. 2nd ed. West Lafayette, Ind.: SSCI. 574p.

Cugovčan, M., Jablan, J., Lovrić, J., Cinčić, D. & Galić, N. 2017. Biopharmaceutical characterization of praziquantel cocrystals and cyclodextrin complexes prepared by grinding. *Journal of pharmaceutical and biomedical analysis*, 137:42-53.

Davis, H. 2006. Food and Drug Administration perspective on regulation of pharmaceutical excipients. (*In* Katdare, A. & Chaubal, M.V., *eds*. Excipient development for pharmaceutical, biotechnology and drug delivery systems. New York: Informa Healthcare. p. 3-13).

Dhirenda, K.S., Lewis, S., Udupa, N. & Atin, K. 2009. Solid dispersions: a review. *Pakistan journal of pharmaceutical science*, 22(2):234-246.

Dong, Z. & Choi, D.S. 2008. Hydroxypropyl methylcellulose acetate succinate: potential drug-excipient incompatibility. *AAPS PharmSciTech*, 9(3):991-997.

Drugbank. 2018a. Efavirenz-Drugbank. [Web:] https://www.drugbank.ca/drugs/DB00625 [Date of access: 2018-10-25].

Drugbank. 2018b. Praziquantel-Drugbank. [Web:] https://www.drugbank.ca/drugs/DB01058 [Date of access: 2018-10-25].

FDA see United States Food and Drug Administration.

Grasman, N. 2012. Effect of acetate and succinate substitution levels on spray dried dispersions of hypromellose acetate succinate: a quality by design approach. Conference proceedings as published in 2012 AIChE Annual meeting, Pittsburg, PA, USA.

Guo, J.W., Skinner, G.W., Harcum, W.W. & Barnum, P.E. 1998. Pharmaceutical applications of naturally occurring water-soluble polymers. *Pharmaceutical science and technology today,* 1(6):254-261.

Hassan, B.A.R. 2012. HPLC uses and importance in the pharmaceutical analysis an industrial field. *Pharmaceutica analytica acta*, 3(9):1.

Leuner, C. & Dressman, J. 2000. Improving drug solubility for oral delivery using solid dispersions. *European journal of pharmaceutics and biopharmaceutics*, 50:47-60.

Lindenberg, M., Kopp, S. & Dressman, J.B. 2004. Classification of orally administered drugs on the World Health Organization Model list of Essential Medicines according to the biopharmaceutics classification system. *European journal of pharmaceutics and biopharmaceutics*, 58:265-278.

Moldoveanu, S.C. & David, V. 2013. Essentials in modern HPLC separations. [Web:] http://www.sciencedirect.com.nwulib.nwu.ac.za/science/article/pii/B9780123850133020012 [Date of access: 2017-10-27].

Narayan, P., Porter, W.W. III, Brackhagen, M. & Tucker, C. 2015. Polymers and surfactants. (*In* Newman, A. *ed*. Pharmaceutical amorphous solid dispersions. Hoboken: John Wiley & Sons Inc. p. 42-84).

Pawar, J., Tayade, A., Gangurde, A., Moravkar, K. & Amin, P. 2016. Solubility and dissolution enhancement of efavirenz hot melt extruded amorphous solid dispersions using combination of polymeric blends: A QbD approach. *European journal of pharmaceutical sciences*, 88:37-49.

Pinto, J.M.O., Leao, A.F., Riekes, M.K., Franca, M.T. & Stulzer, H.K. 2018. HPMCAS as an effective precipitation inhibitor in amorphous solid dispersions of the poorly soluble drug candesartan cilexetil. *Carbohydrate polymers,* 184:199-206.

Pubchem. 2018a. *Efavirenz | C14H9ClF3NO2 - PubChem*. [Web:] https://pubchem.ncbi.nlm.nih.gov/compound/efavirenz [Date of access: 2018-11-12].

Pubchem. 2018b. *Praziquantel | C19H24N2O2 - PubChem*. [Web:] https://pubchem.ncbi.nlm.nih.gov/compound/4891 [Date of access: 2018-11-12].

Raju, N.A., Rao, J.V., Prakesh, K.V., Mukkanti, K. & Srinivasu, K. 2008. Simultaneous estimation of tenofovir disoproxil, emtricitabine and efavirenz in tablet dosage form by RP-HPLC. *Oriental journal of chemistry,* 24(2):645-650.

Ravikumar, K. & Sridhar, B. 2009. Molecular and crystal structure of efavirenz: a potent and specific inhibitor of HIV-1 reverse transcriptase and its monohydrate. *Molecular crystals and liquid crystals*, 515:190-198.

Rodrigues-Spong, B., Price, C.P., Jayasankar, A., Matzger, A.J. & Rodriguez-Hornedo, N. 2004. General principles of pharmaceutical solid polymorphism: a supramolecular perspective. *Advanced drug delivery reviews*, 56(3):241-274.

Sigma-Aldrich. 2018. Polyvinylpyrrolidone average mol wt 40,000 | Sigma-Aldrich. [Web:] https://www.sigmaaldrich.com/catalog/product/sial/pvp40?lang=en®ion=ZA [Date of access: 2018-11-11].

Song, Y., Wang, L., Yang, P., Wenslow, R.M., Tan, B., Zhang, H. & Deng, Z. 2013. Physicochemical characterization of Felodipine-Kollidon VA64 amorphous solid dispersions prepared by hot-melt extrusion. *Journal of pharmaceutical sciences,* 102(6):1915-1923.

Stieger, N. & Liebenberg, W. 2017. Developing a SPADS process for academic research. Ongoing NRF / NWU research project. NRF grant # 112078.

Stieger, N., Aucamp, M. & Liebenberg, W. 2013. Relative stability of efavirenz glass: agitated *vs*. non-agitated. Poster presented at the AAPS Annual Meeting and Exposition, San Antonio, Texas, USA.

Stieger, N., Aucamp, M., Zhang, S.W. & De Villiers, M.M. 2012. Hot-stage optical microscopy as an analytical tool to understand solid-state changes in pharmaceutical materials. *American pharmaceutical review*, 15(2).

Stieger, N., Joubert, A. & Liebenberg, W. 2017. Solution-mediated crystallization of amorphous azithromycin. Pharmazie, 72:447-448.

Teja, S.B., Patil, S.P., Shete, G., Patel, S. & Bansal, A.K. 2013. Drug-excipient behavior in polymeric amorphous solid dispersions. *Journal of excipients and food chemistry*, 4(3):70-94.

Trastullo, R., Dolci, L.S., Passerini, N. & Albertini, B. 2015. Development of flexible and dispersible oral formulations containing praziquantel for potential schistosomiasis treatment of pre-school age children. *International journal of pharmaceutics*, 495:536-550.

United States Food and Drug Administration. 2017a. Inactive ingredient approved drug products: Hypromellose acetate succinate. [Web:] https://www.accessdata.fda.gov/scripts/cder/iig/getiigWEB.cfm [Date of access: 2017-05-22].

United States Food and Drug Administration. 2017b. Inactive ingredient approved drug products: Copovidone K90. [Web:] https://www.accessdata.fda.gov/scripts/cder/iig/getiigWEB.cfm [Date of access: 2017-05-22].

United States Food and Drug Administration. 2017d. Inactive ingredient approved drug products: Polysorbate 80. [Web:] https://www.accessdata.fda.gov/scripts/cder/iig/getiigWEB.cfm [Date of access: 2017-05-22].

United States Food and Drug Administration. 2017e. Inactive ingredient approved drug products: Sodium lauryl sulfate. [Web:] https://www.accessdata.fda.gov/scripts/cder/iig/getiigWEB.cfm [Date of access: 2017-05-22].

United States Food and Drug Administration. 2017f. Inactive ingredient approved drug products: Lecithin. [Web:] https://www.accessdata.fda.gov/scripts/cder/iig/getiigWEB.cfm [Date of access: 2017-05-22].

United States Food and Drug Administration. 2017g. Inactive ingredient approved drug products: Lauroyl polyoxylglycerides. [Web:] https://www.accessdata.fda.gov/scripts/cder/iig/getiigWEB.cfm [Date of access: 2017-05-22].

Wikipedia. 2018a. Praziquantel. [Web:] https://en.wikipedia.org/wiki/Praziquantel [Date of access: 2018-10-28].

Wikipedia. 2018b. Hypromellose. [Web:] https://en.wikipedia.org/wiki/Hypromellose [Date of access: 2018-10-28].

Wiktionary. 2018. Efavirenz. [Web:] https://en.wiktionary.org/wiki/efavirenz [Date of access: 2018-10-28].

Chapter 3

Preparation of Efavirenz Amorphous Solid Dispersions

3.1 Primary screening to identify suitable efavirenz polymers

An API/polymer combined glass transition temperature (T_g) of approximately 80°C or higher is ideal so as to ensure the stability of the product at room temperature, bar exposure to moisture (Newman & Munson, 2012). The higher the storage temperature, or the temperature to which the amorphous solid dispersion (ASD) will be exposed during processing, the higher the required T_g. The general rule of thumb is that the combined T_g should exceed the temperature to which the ASD will be exposed by at least 50°C (Narayan *et al*., 2015). Polymers were added in theoretically feasible ratios during this study in an attempt to create ASDs with an ideal glass transition temperature.

The feasibility of drug:polymer ratios depends on factors, such as the required T_g and the size of the solid dosage forms that would result. Drug:polymer ratios that were considered during this study were 4:1 and up to 1:4, depending on the resulting T_g and the maximum oral potency of the polymers, as reported by the United States Food and Drug Administration (FDA, 2017a-g).

During the primary screening, the miscibility of the drugs and polymers were determined at the chosen ratios, in order to eliminate any ratios or polymers that would not result in ASDs being dispersed at molecular level (thermal analysis).

The preparation of the physical mixture differed from that of an ASD in that the API and polymer were ground by pestle in a mortar for 2 minutes, to achieve thorough mixing of the two components. In some cases, it was possible to prepare an amorphous solid dispersion simply through physical mixing. In this study, the primary screening was done on the physical mixtures, from where the ASD was prepared through solvent evaporation.

Table 3.1 was compiled after calculating the resulting theoretical glass transition temperature of each API and polymer combination (Formula 3.1) in mass ratios ranging from 4:1 to 1:4, assuming that each mixture would produce an ASD. The ratio units x and y in Formula 3.1 may have any practical unit of mass, as long as it is the same for both the API and polymer. The mass ratio of 1:4 API:polymer was not exceeded, as doing so would result in impractically large numbers of tablets or capsules.

Formula 3.1

$$\text{Resulting theoretical } T_g = \frac{(xT_g(API)+yT_g(polymer))}{(x+y)}$$

Where:

x = Ratio/mass of API in the mixture

y = Ratio/mass of polymer in the mixture

T_g(API) = Glass transition temperature of the API

T_g(polymer) = Glass transition temperature of the polymer

Previous studies showed that efavirenz had formed a rubbery like glass, which was extremely unstable (Stieger *et al.,* 2013). Although an ideal T_g should have been above 80°C, the mixtures being used (as highlighted in Table 3.1) appeared to be miscible at an even lower T_g. It was decided to continue to investigate those mixtures, to establish whether a small ratio of polymer would indeed inhibit recrystallisation and produce a stable ASD. Low melting point pharmaceutical substances also exhibit better solubility properties (Chu & Yalkowsky, 2009), while a small ratio of polymer (and thus more API), hence a smaller dosage form, should be more desirable as a dosage form.

The acronym of **EFA** is used for **efavirenz** from hereafter.

Table 3.1: Theoretical T_g values obtained for EFA (T_g = 33°C) and polymer combinations (blue shaded samples represent those that went through to the final test round.)

Efavirenz and Polymer	Ratio	Theoretical T_g (°C)
EFA:HPMC	1:1	74
	1:2	88
	1:3	95
	1:4	99
	2:1	60
	3:1	54
EFA:HPMCAS	1:1	79
	1:2	94
	1:3	102
	1:4	107
	2:1	64
	3:1	56
EFA:PVP 25	1:1	92
	1:2	112
	1:3	122
	1:4	128
	2:1	73
	3:1	63
EFA:PVP 30	1:1	91
	1:2	110
	1:3	120
	1:4	126
	2:1	72
	3:1	62
EFA:PVP VA 64	1:1	67
	1:2	78
	1:3	84
	1:4	87
	2:1	56
	3:1	50

3.2 Physico-chemical properties of efavirenz (EFA)

3.2.1 Thermal analysis

3.2.1.1 Simultaneous thermal analysis (STA) of the EFA raw material

STA analysis was performed according to the method described in Section 2.7.1.

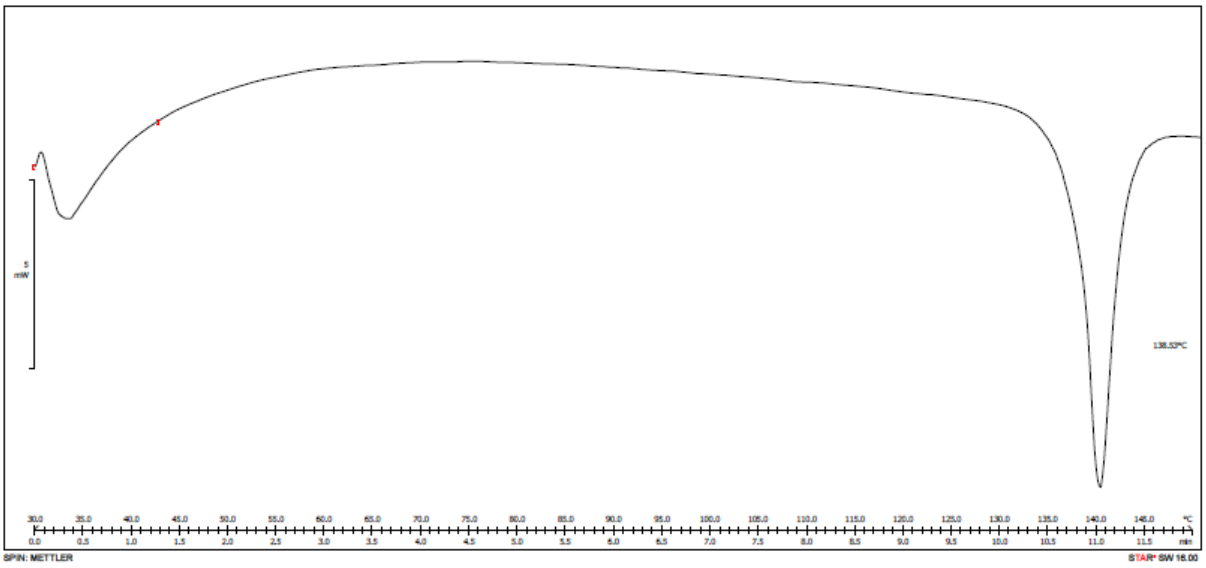


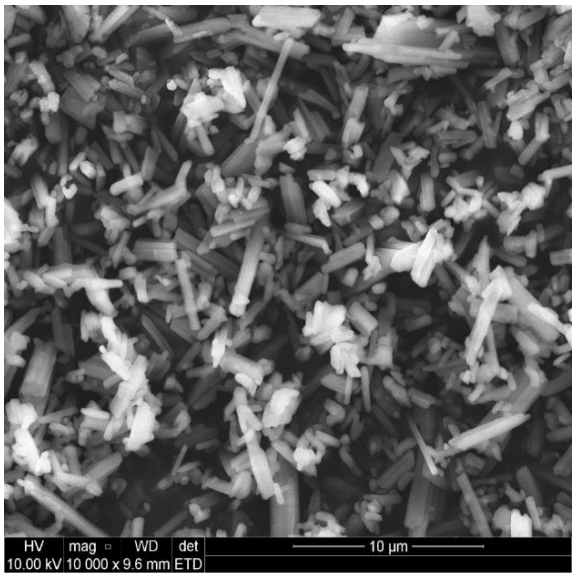
Figure 3.1: Simultaneous thermal analysis (STA) thermogram of the EFA raw material.

The STA thermogram of the EFA raw material indicated a melting point of 138.53°C (Fig. 3.1).

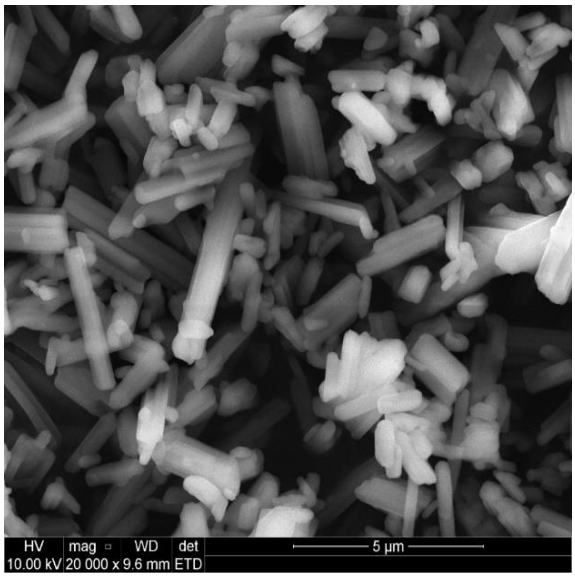
3.2.1.2 Scanning electron microscopy (SEM)

The scanning electron microscopy images were recorded in accordance with the method being described in Section 2.7.3.

It was clear from the SEM images of the EFA raw material, as well as the physical mixture of EFA and 1.5% sodium lauryl sulphate (SLS) (Figures 3.2 and 3.3**)** that those powders were crystalline. The crystals were rod shaped, with the crystals of the raw material being longer than those of the physical mixture, as a result of the grinding during mixing of the components that had reduced their lengths.

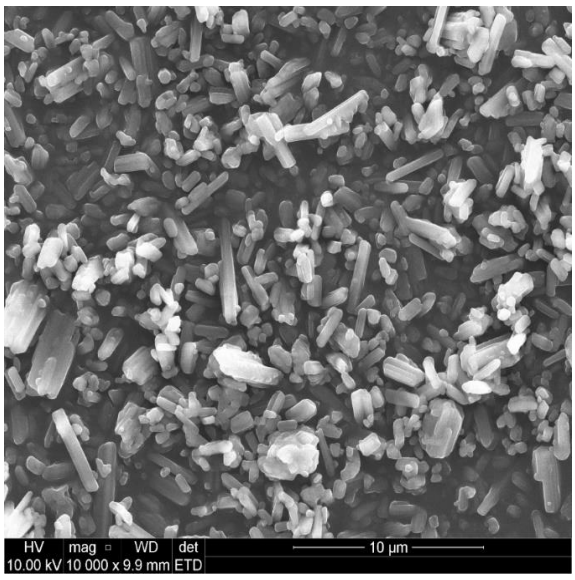


A 10 000x magnification

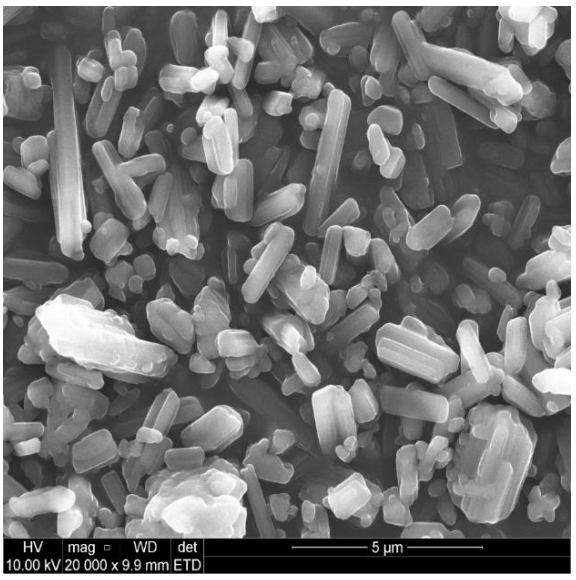


B 20 000x magnification

Figure 3.2: SEM photos of the EFA raw material.



A 10 000x magnification

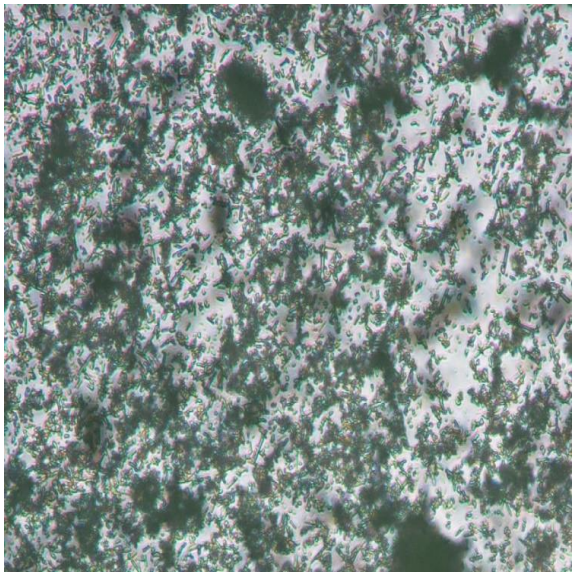


B 20 000x magnification

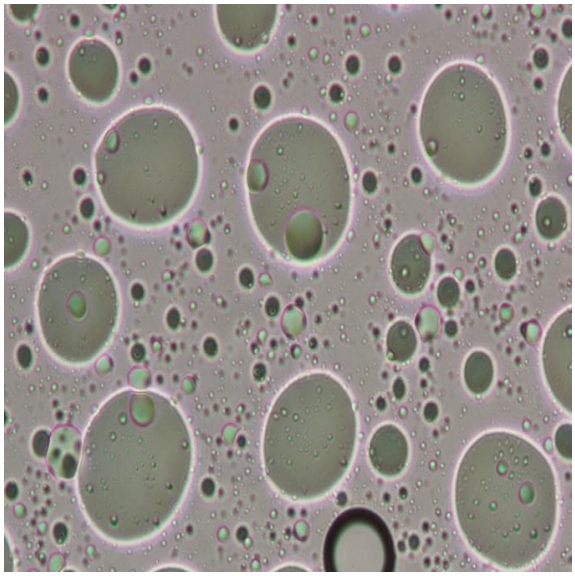
Figure 3.3: SEM photos of a physical mixture of EFA and 1.5% SLS.

3.2.1.3 Hot-stage microscopy (HSM)

The HSM photos were taken according to the method as described in Section 2.7.2.

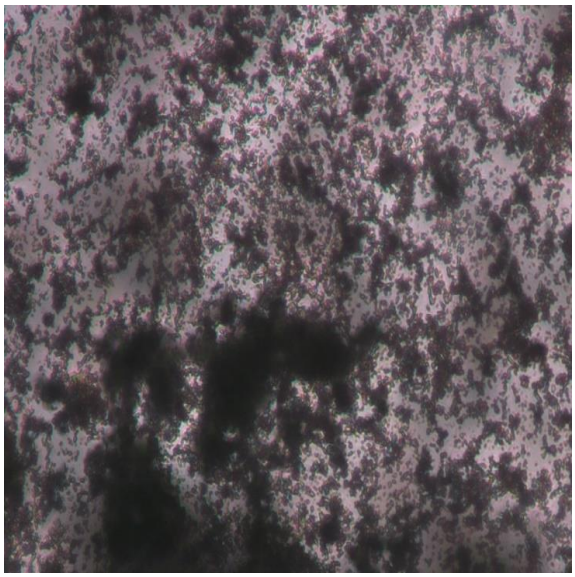


A Before melting

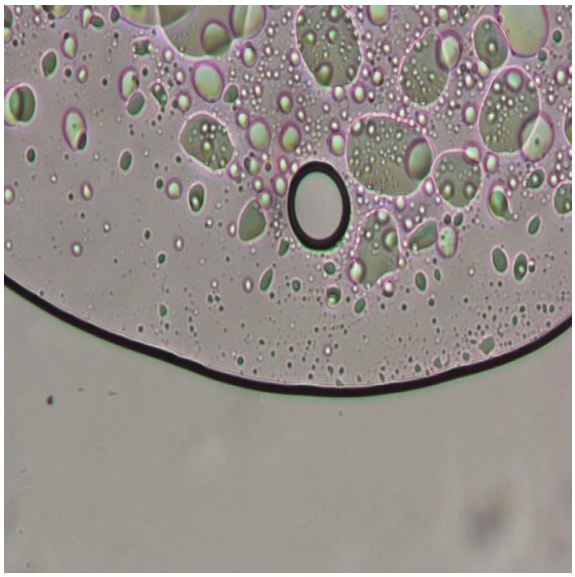


B After melting

Figure 3.4: HSM photos of the EFA raw material before and after melting.



A Before melting



B After melting

Figure 3.5: HSM photos of the physical mixture of the EFA raw material and 1.5% SLS before and after melting.

The images in Figure 3.4 illustrate the crystals of the EFA raw material as observed under a microscope. The crystals appeared rod shaped and very small, with darker spots representing

agglomerated clusters of crystals. When the melting point was reached, those clusters required more time to melt than the free-standing crystals. After melting was completed, small droplets of the amorphous EFA were left behind.

The appearance of the physical mixture of the EFA raw material and 1.5% SLS (Fig. 3.5) was very similar to that of the EFA raw material, with the only marked exception being that the crystals seemed smaller, most likely due to the mixing which had involved grinding. As in the EFA raw material, when the melting point of the physical mixture was reached, the free-standing crystals melted before the clusters.

3.2.1.4 X-ray powder diffraction (XRPD)

The XRPD method used is described in Section 2.7.4.

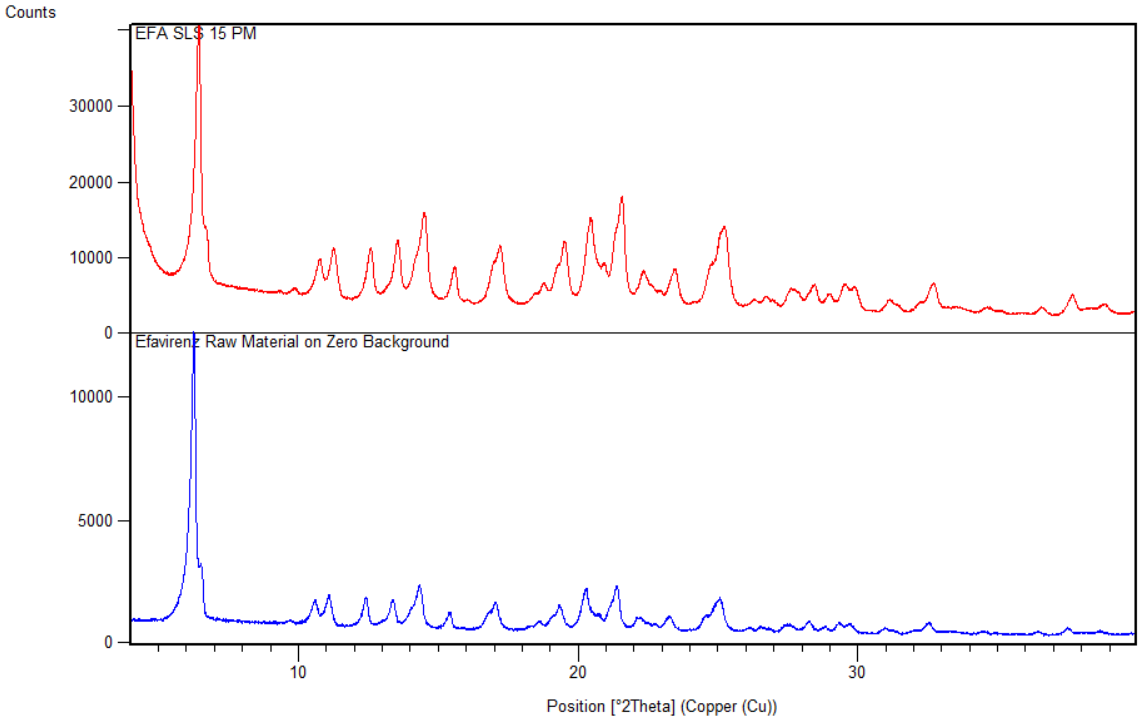


Figure 3.6: XRPD profile of the EFA raw material (bottom, blue) and a physical mixture of EFA and 1.5% SLS (top, red).

The definite peaks in the XRPD profiles of both the EFA raw material and the physical mixture containing EFA and 1.5% SLS (Fig. 3.6) indicated that they were crystalline in nature. Amorphous powders would have demonstrated a more meandering like profile.

3.2.1.5 Accelerated stability testing

HPLC was used for the assays during stability testing. STA was used to determine the melting points as well as any weight gain of the test samples, while XRPD analysis was used to determine the amorphous nature of the ASDs.

The accelerated stability studies were performed over a 3-month period at 40°C and 75% relative humidity (RH), as described in Section 2.7.6.

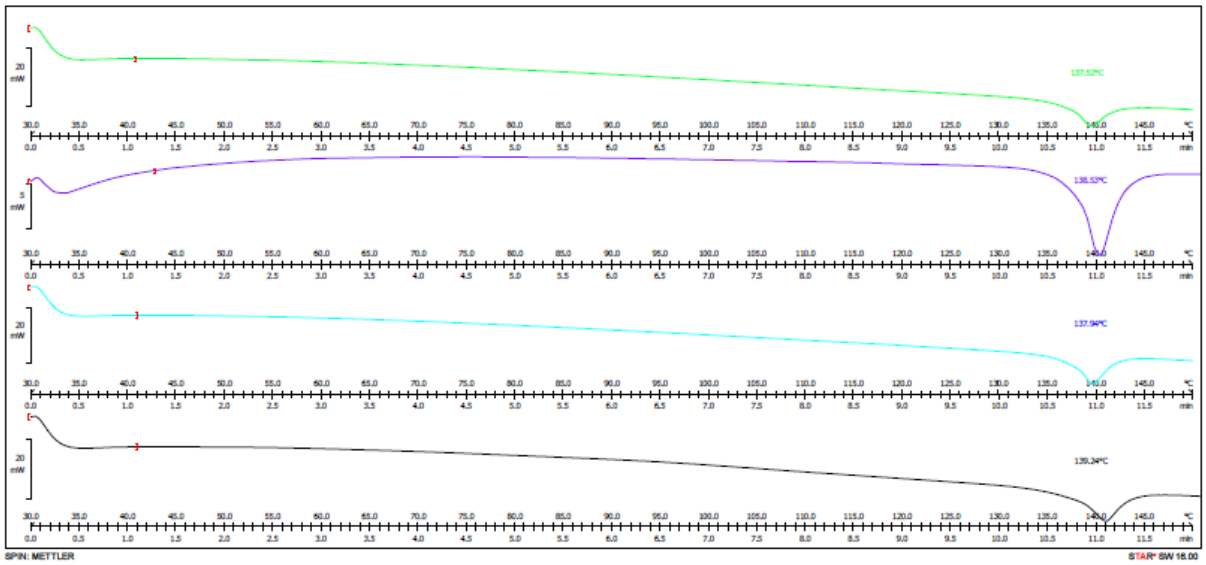


Figure 3.7: An overlay of the STA thermograms of a physical mixture of EFA and 1.5% SLS at initial (green), month 1 (purple), month 2 (blue) and month 3 (black) of stability testing.

Table 3.2: Moisture content of the EFA raw material over the duration of the stability test period as measured by means of STA (TG analysis)

Sample	Initial	Month 1	Month 2	Month 3
EFA raw material	0.5%	1.7%	1.8%	0.1%

The initial moisture content of the EFA raw material was determined as 0.5%. Analysis at months 1 and 2 showed that the moisture content had increased to 1.7% and 1.8%, respectively, after which it had dropped to almost 0% at month 3. According to the certificate of analysis of EFA, the limit for moisture in the raw material is 1%. The weight gains in months 1 and 2 could have been as a result of surface moisture, which had not altered the crystalline structure of the raw material.

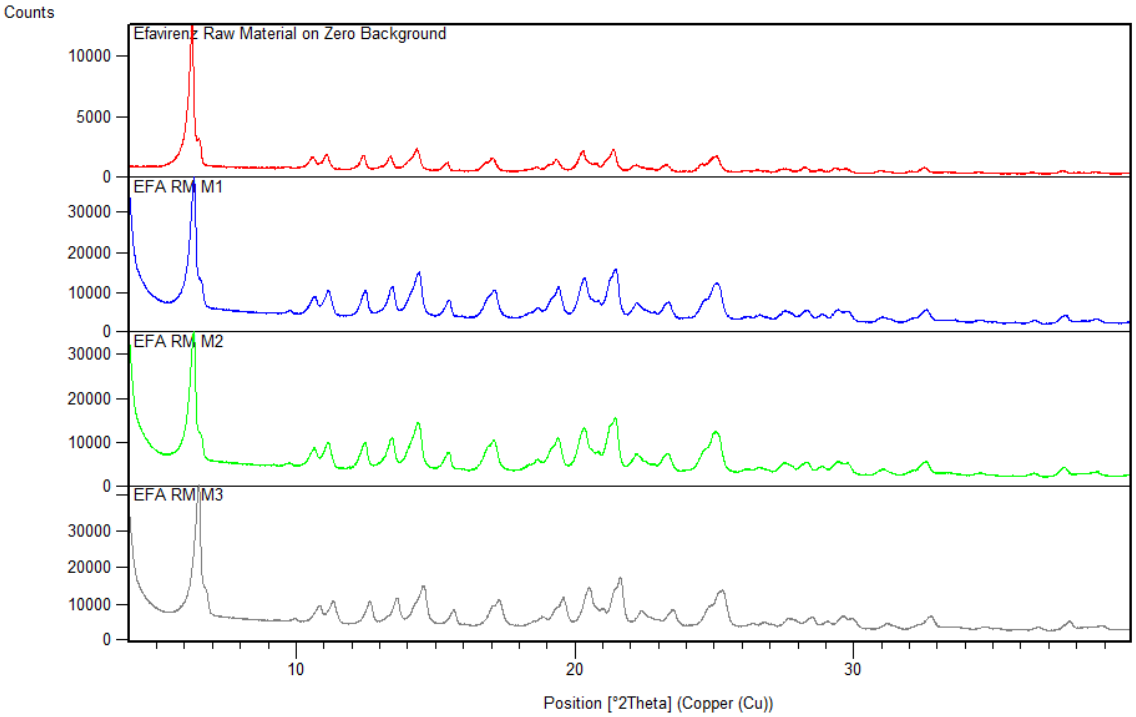


Figure 3.8: XRPD overlay of a physical mixture of EFA and 1.5% SLS at initial (red), month 1 (blue), month 2 (green) and month 3 (grey) of stability testing.

STA analysis of a physical mixture of EFA and 1.5% SLS indicated that the mixture had remained crystalline throughout the entire 3-month period of stability testing. No moisture had been absorbed and no hydrate had formed (Fig. 3.7).

XRPD profiles of a physical mixture of EFA and 1.5% SLS also confirmed that the mixture had stayed crystalline throughout the stability test period, as expected, since no new peaks had evolved, nor have any of the peaks shifted over time, as is evident from Figure 3.8.

Table 3.3: HPLC assay results of the EFA raw material over the duration of the stability test period

Sample	Initial	Month 1	Month 2	Month 3
EFA raw material	101.0%	101.5%	102.1%	44.1%

At months 1 and 2 of stability testing, EFA had shown no signs of degradation, whereas after 3 months, degradation had started to occur, with a total degradation of 55.9% being measured.

3.2.1.6 Powder dissolution studies

3.2.1.6.1 Validation of HPLC assay method

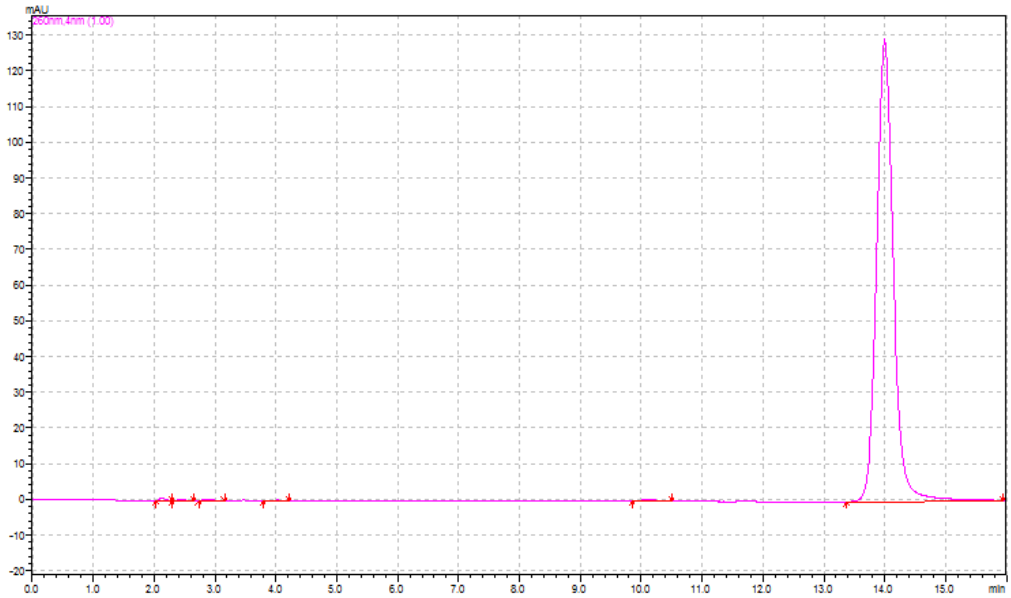


Figure 3.9: Chromatogram of EFA at 260 nm.

Figure 3.9 illustrates that the EFA peak renders at approximately 13 min. The area under the curve was used to measure the concentration of EFA present in the test samples.

3.2.1.6.2 Linearity

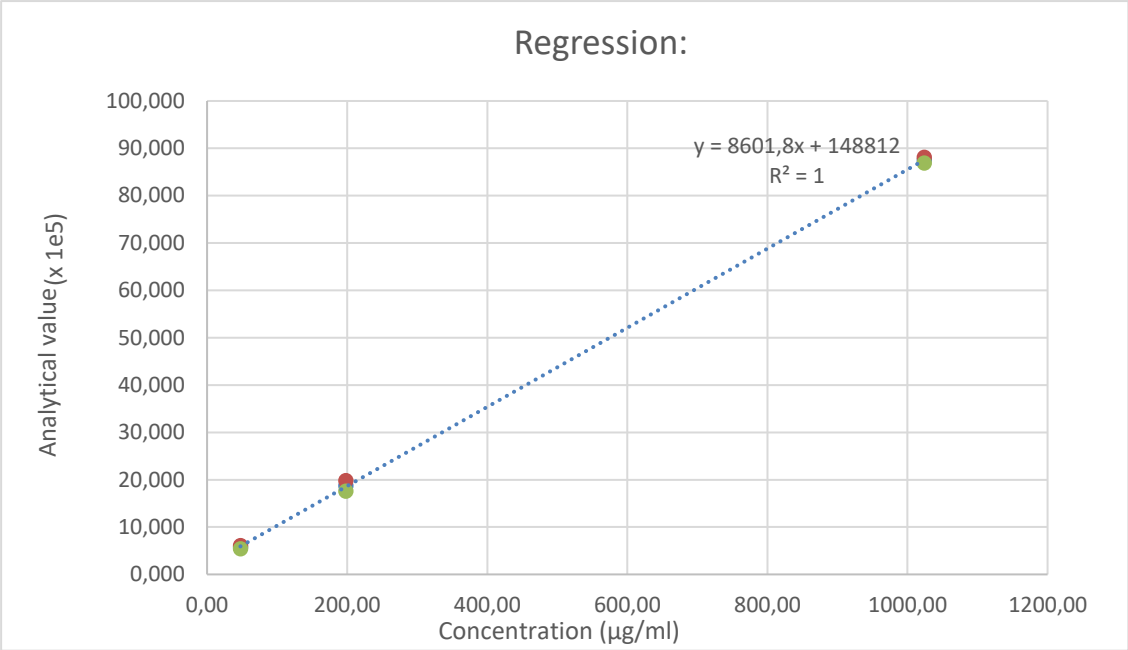


Figure 3.10: Linear regression curve of EFA.

While testing the validity of the HPLC method, a satisfactory R^2 value of 0.99998 was obtained.

The powder dissolution studies, as described in Section 2.7.7, were carried out on the EFA raw material and 1.5% SLS. SLS was added as a surfactant, since the wettability of EFA alone had proven problematic, as it had floated on the surface of the dissolution medium and had adhered to the stirrer rod.

The dissolution profile of EFA with 1.5% SLS is demonstrated in Figure 3.9, where the dissolution rate had started to plateau after 30 minutes, until a maximum of 3.31% of the initial amount of sample was dissolved at 180 minutes.

These extremely poor dissolution results confirmed that the powder dissolution of the very hydrophobic EFA raw material with SLS still remained a huge challenge.

The USP dissolution medium for efavirenz tablets is 1000 ml water with 2% SLS in the medium (USP, 2018). The ASD formulation that we had used, however, had incorporated the SLS in the ADS formulation and was it not part of the dissolution volume, which could have affected the wettability of the powder and hence led to the low dissolution results.

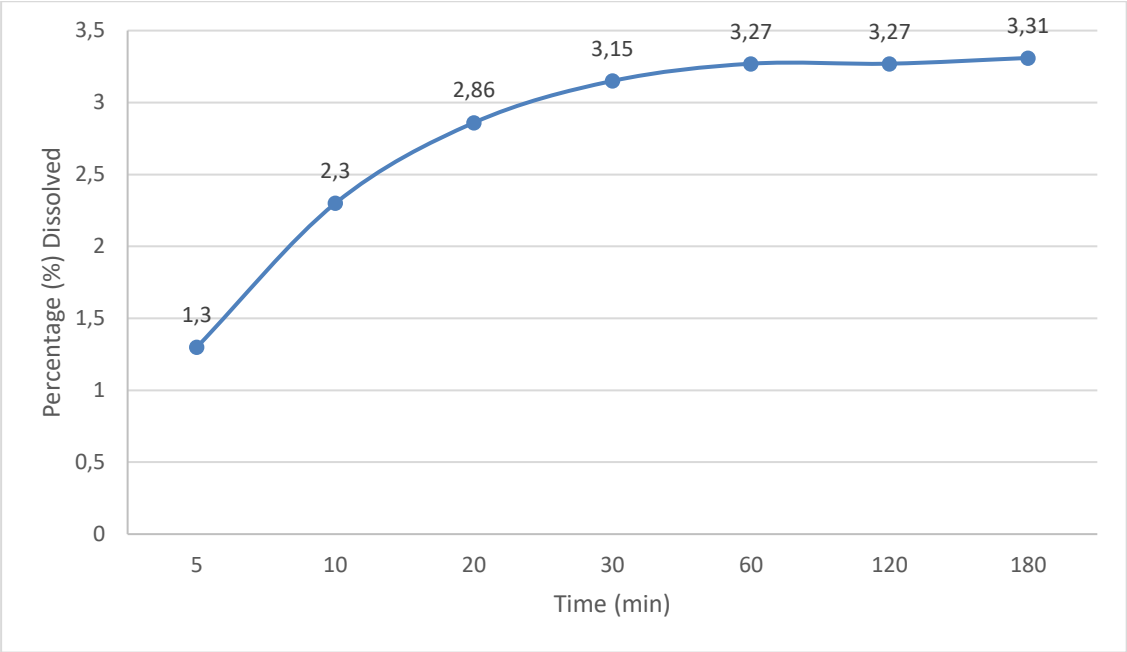


Figure 3.11: Percentage of the EFA raw material with 1.5% SLS that had dissolved in distilled water at specific time intervals over a 3-hour period.

3.2.1.6.3 EFA glass

Since Stieger *et al*. (2013) reported that EFA had formed an unstable glass and that it could be easily transformed into the crystalline form, the instability of the glass was a matter of concern when starting this project. The question remained, whether the combination of EFA and a polymer would form a stable ASD and whether it would remain stable over a period of time. According to Stieger *et al*. (2013), the EFA glass had transformed easily into the crystalline form, when agitating the glass.

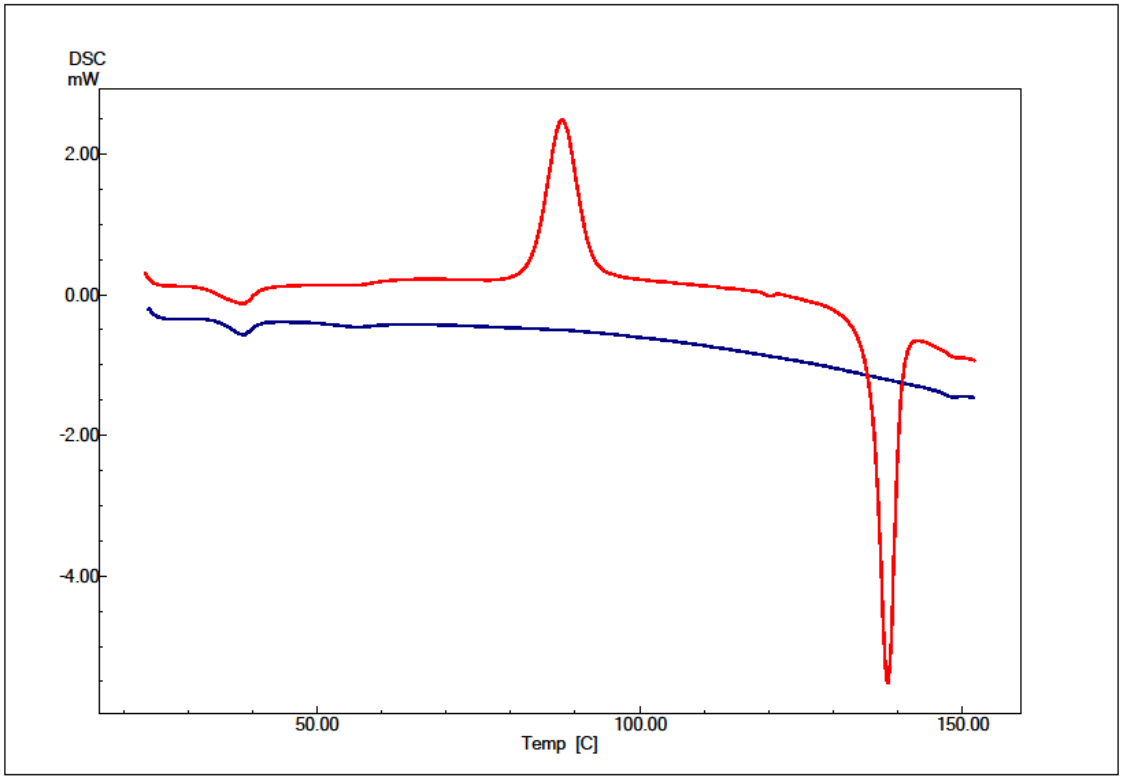


Figure 3.12: DSC thermogram overlay printed with permission from Stieger *et al*. (2013), illustrating the EFA glass (blue line) and the agitated glass (red line).

DSC analysis showed that only the agitated glass sample had recrystallised (between 80°C and 85°C), followed by melting of the crystallised product at 140°C. The non-agitated glass showed no crystallisation when heated up to the melting point (Fig. 3.12). It was expected that any physical disturbance would have quite a significant effect on the stability of the EFA glass. This was a matter of concern for the preparation of the ASD, since after solvent removal, the residue would require removal from the Petri dish by means of a spatula. Also, after removal from the Petri dish, the formed ASD would be ground in a mortar and pestle to obtain a powder suitable for dissolution and XRPD analyses.

3.3 Physico-chemical properties of the prepared ASDs

3.3.1 EFA/PVP 25

3.3.1.1 Thermal analysis – screening for miscibility of EFA/PVP 25

Miscibility refers to the ability of the API and polymer to form a homogeneous single phase when the two components are thoroughly mixed at molecular level. Normally, a single glass transition T_g indicates a miscible system. The absence of a T_g on a thermogram could be due to the inability, or lack of sensitivity of the thermal analysis instrument being used. Therefore, other analytical techniques should be used in conjunction with DSC, like XRPD, to confirm the amorphous nature of the ASD (Newman & Munson, 2012).

The screening for miscibility was executed by means of simultaneous thermal analysis (STA), according to the method described in Section 2.7.1. The EFA with PVP 25, PVP 30 and PVP VA 64, each in ratios of 3:1 and 1.5% SLS, were chosen, as highlighted in Table 3.1. Only those three proposed ASDs underwent further testing.

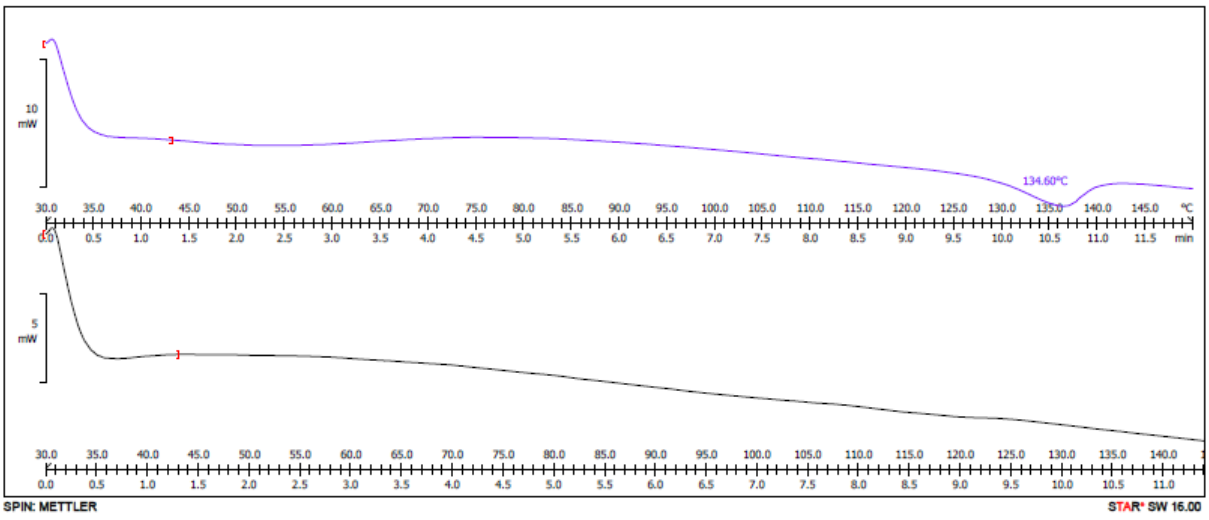


Figure 3.13: STA thermograms of an [EFA/PVP 25 (3:1) +1.5% SLS] physical mixture (top, purple), and a second run of the same sample (bottom, black).

Simultaneous thermal analysis of the [EFA/PVP 25 (3:1) +1.5% SLS] physical mixture indicated a melting point of 134.60°C, identical to that of the EFA raw material (no miscibility). After the initial run, the same sample was re-tested to investigate whether an ASD had formed. The lack of a melting point in Figure 3.13 (bottom, black) confirmed ASD formation. These results were indicative thereof that the two-component system was probably miscible.

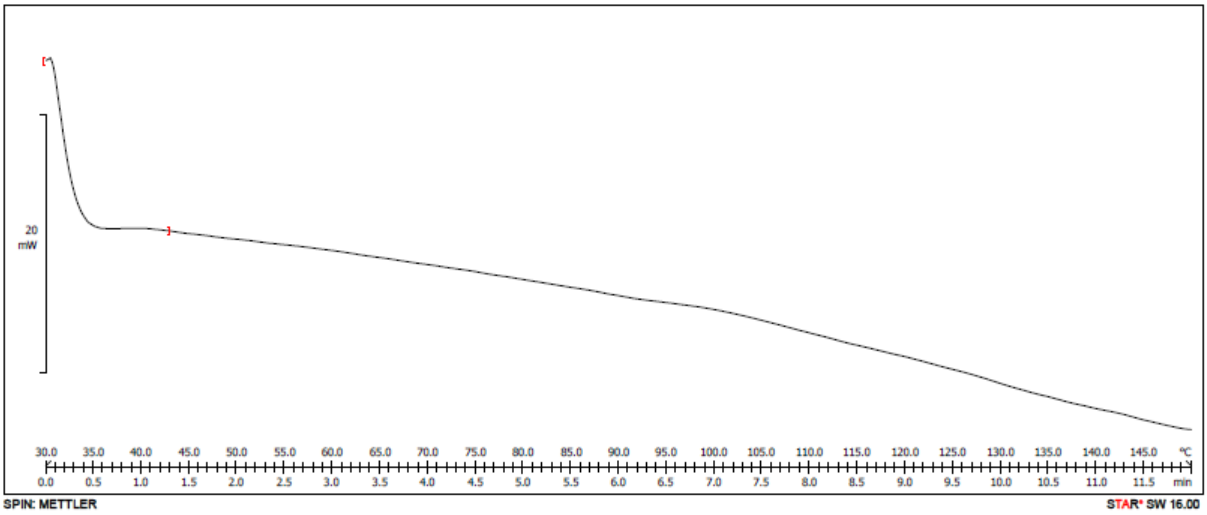
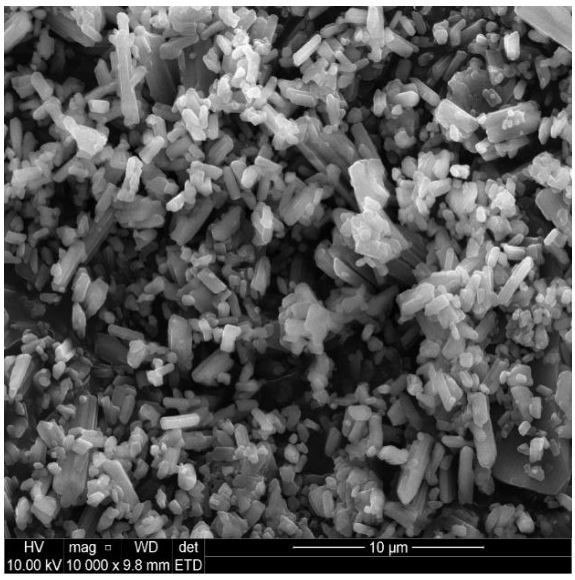


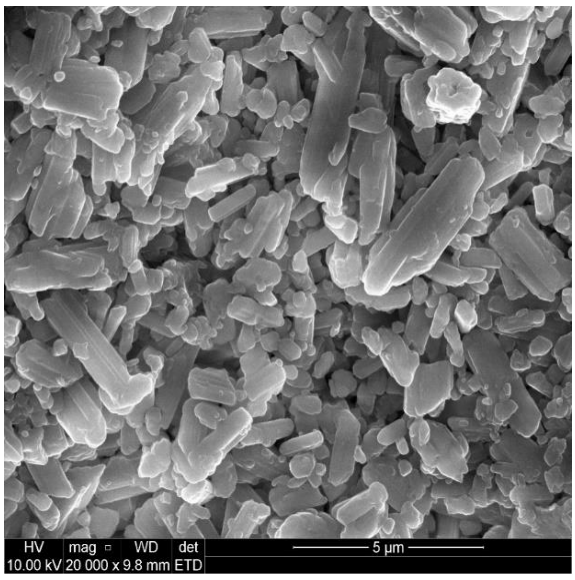
Figure 3.14: STA thermogram of [EFA/PVP 25 (3:1) + 1.5% SLS] ASD, created by rotary evaporation.

The simultaneous thermal analysis results of the ASD containing [EFA/PVP 25 (3:1) + 1.5% SLS] can be seen in Figure 3.14. Again, the absence of any melting point could mean possible ASD formation, but this required confirmation with XRPD analysis.

3.3.1.2 Scanning electron microscopy (SEM)

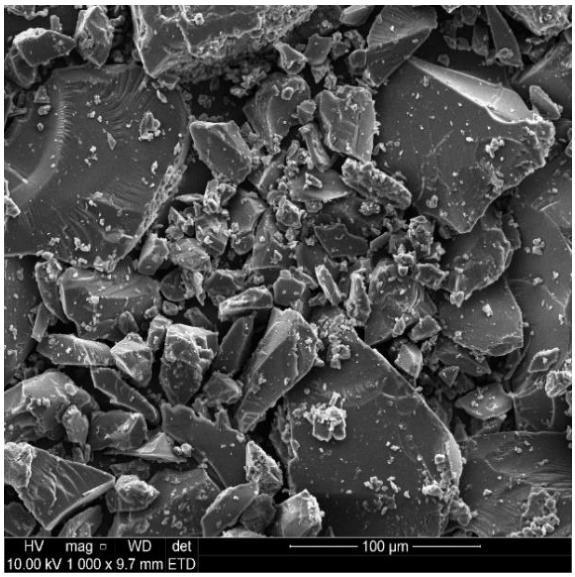


A 10 000x magnification

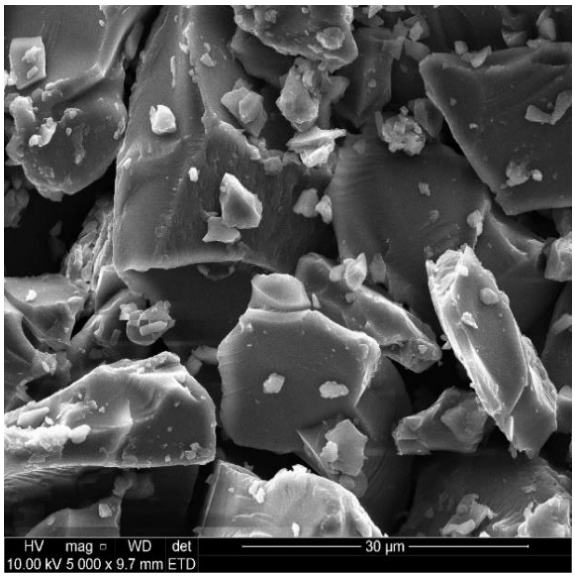


B 20 000x magnification

Figure 3.15: SEM photos of a physical mixture of [EFA/PVP 25 (3:1) and 1.5% SLS].



A 10 000x magnification



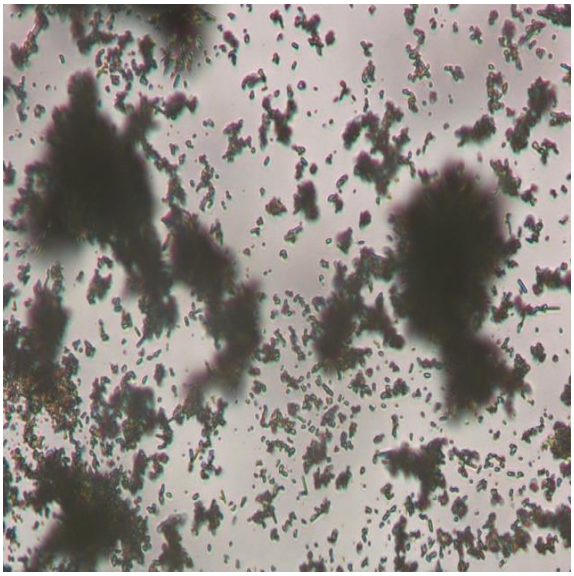
B 20 000x magnification

Figure 3.16: SEM photos of an ASD containing [EFA/PVP 25 (3:1) + 1.5% SLS].

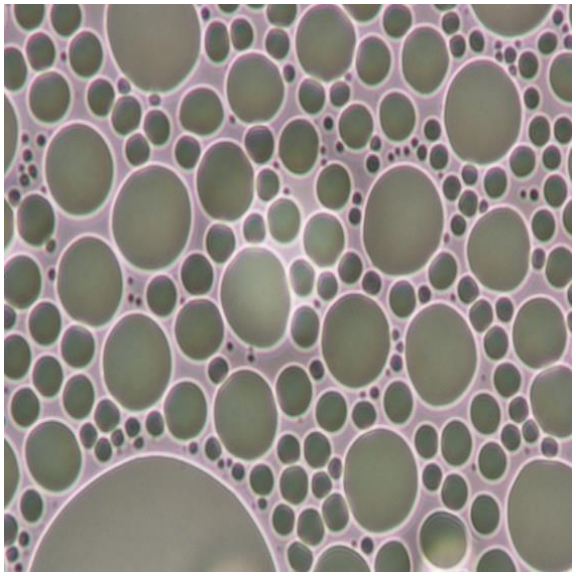
In the SEM photos taken of the physical mixture containing [EFA/PVP 25 (3:1) + 1.5% SLS] (Fig. 3.15), it is clear that the sample was crystalline, showing rod shaped crystals. These crystal rods were shorter than those of the EFA raw material (Fig. 3.2), due to the grinding when mixing the components, which reduced their lengths.

Comparison of the SEM photos of the ASD containing [EFA/PVP 25 (3:1) + 1.5% SLS] (Fig. 3.16) with those of the physical mixture (Fig. 3.15), revealed that the particle sizes of the ASD were larger and bulkier, and less uniform than those of the physical mixture. The particles of the ASD also differed from the physical mixture in appearance, as no definite shapes were observed, which could be described as broken shards, as opposed to the distinct, rod shaped particles of the physical mixture.

3.3.1.3 Hot-stage microscopy (HSM)



A Before melting



B After melting

Figure 3.17: HSM photos of the physical mixture of [EFA/PVP 25 (1:3) + 1.5% SLS].

The physical mixture of [EFA/PVP 25 (3:1) + 1.5% SLS] (Fig. 3.17) was more comparable to the physical mixture of EFA and SLS (Fig. 3.5), than to the EFA raw material (Fig. 3.4), as the sizes of the crystals were similar, because of the grinding to mix the components. Agglomerated clusters of crystals could also be observed, which required longer time to melt completely, after the melting point had been reached.

3.3.1.4 X-ray powder diffraction (XRPD)

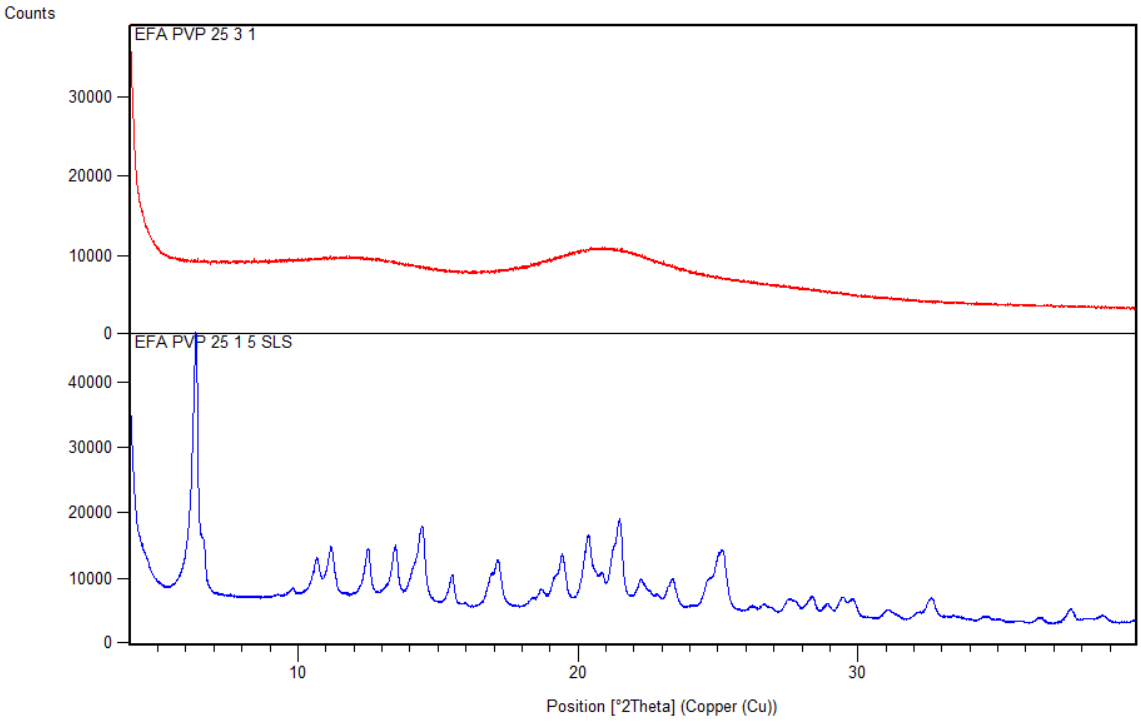


Figure 3.18: XRPD profile of an ASD containing [EFA/PVP 25 (1:3) + 1.5% SLS] (top, red) and a physical mixture of [EFA/PVP 25 (1:3) + 1.5% SLS] (bottom, blue).

The definite peaks in the XRPD profile of the physical mixture of [EFAPVP 25 (3:1) +1.5% SLS] (Figure 3.18) (bottom, blue) were indicative thereof that the sample was crystalline.

Analysis of the ASD containing [EFA/PVP 25 (3:1) + 1.5% SLS], created by rotary evaporation, indicated that it was amorphous, as could be observed from the lack of peaks in Figure 3.18 (top, red). Despite the grinding in a mortar and pestle during sample preparation, no transformation had occurred in the amorphous EFA. The polymer had inhibited any crystallisation and the product remained amorphous.

3.3.1.5 Stability testing

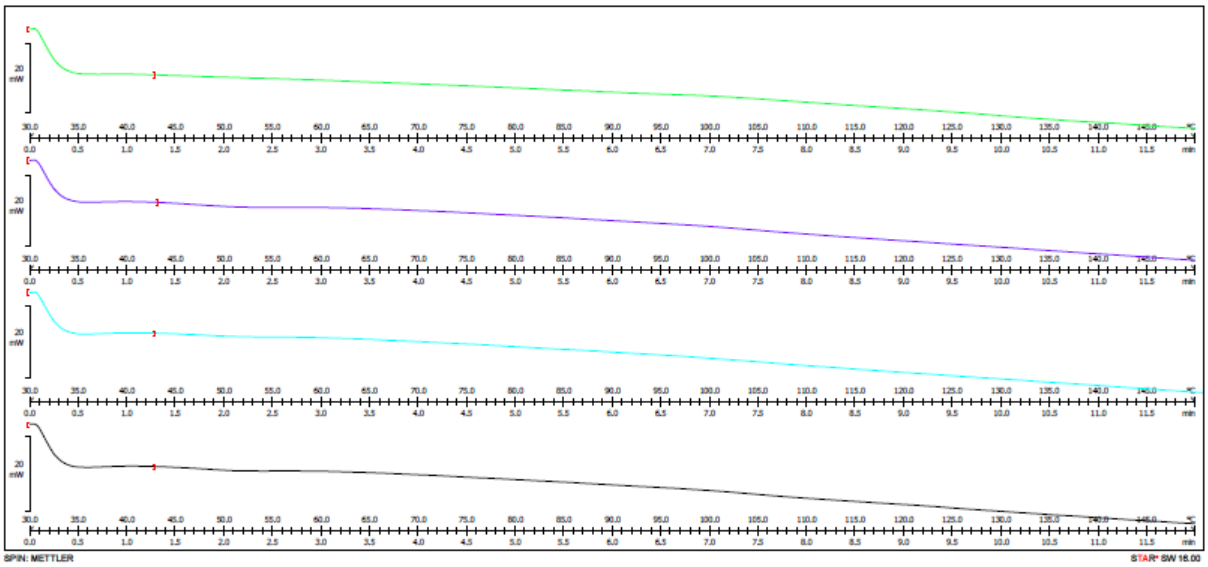


Figure 3.19: An overlay of the STA thermograms of an ASD containing [EFA/PVP 25 (1:3) + 1.5% SLS] at initial (green), month 1 (purple), month 2 (blue) and month 3 (black) of stability testing.

Table 3.4: Moisture content of EFA/PVP 25 over the duration of the stability test period as measured by means of STA (TG analysis)

Sample	Initial	Month 1	Month 2	Month 3
[EFA/PVP 25 (3:1) +1.5% SLS]	2.2%	1.5%	1.8%	2.0%

The initial moisture content of the ASD containing EFA/PVP 25 was 2.2%, which then dropped to 1.5% after 1 month of stability testing, where after the moisture content increased to 1.8% after 2 months and finally to 2% at month 3.

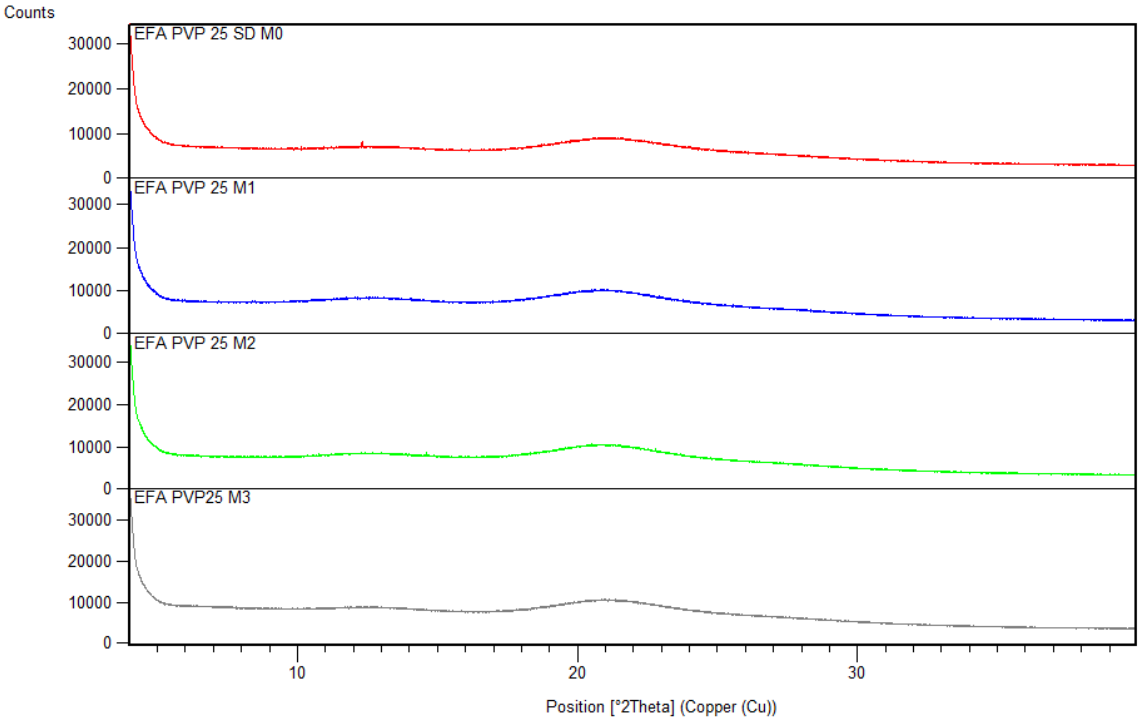


Figure 3.20: XRPD profile of an ASD containing [EFA/PVP 25 (3:1) + 1.5% SLS] at initial (red), month 1 (blue), month 2 (green) and month 3 (grey) of stability testing.

Simultaneous thermal analysis of the ASD containing [EFA/PVP 25 (3:1) + 1.5% SLS] presented with desirable results, as the ASD had remained in the amorphous form for the entire 3-month period of stability testing, as can be seen from the lack of melting points in Figure 3.18.

The XRPD profiles of the ASD containing [EFA/PVP 25 (3:1) + 1.5% SLS] over the 3 months of testing also presented with desirable results, as it confirmed that the ASD had stayed in the amorphous form for the entire 3-month period of stability testing, as can be seen from the lack of any significant peaks in Figure 3.20.

Table 3.5: HPLC assay results of EFA/PVP 25 over the duration of the stability test period

Sample	Initial	Month 1	Month 2	Month 3
[EFA/PVP 25 (3:1) +1.5% SLS]	100.3%	102.1%	79.2%	33.3%

After month 1 of stability testing, no degradation had taken place. After 2 months, degradation started taking place with a decrease in the API concentration of 20.8%, which was a lot more than the 2.05% decrease being measured in the EFA raw material sample (Table 3.3). After 3 months, a total degradation of 66.7% was measured, compared to the 55.9% of the EFA raw material. This ASD showed the lowest degree of degradation after 3 months of stability testing, compared

to the ASD containing EFA/PVP 30 that had a total degradation of 79.4% (Table 3.7), and the ASD containing EFA/PVP VA 64 with a total degradation of 78.6% (Table 3.9).

3.3.1.6 Powder dissolution studies

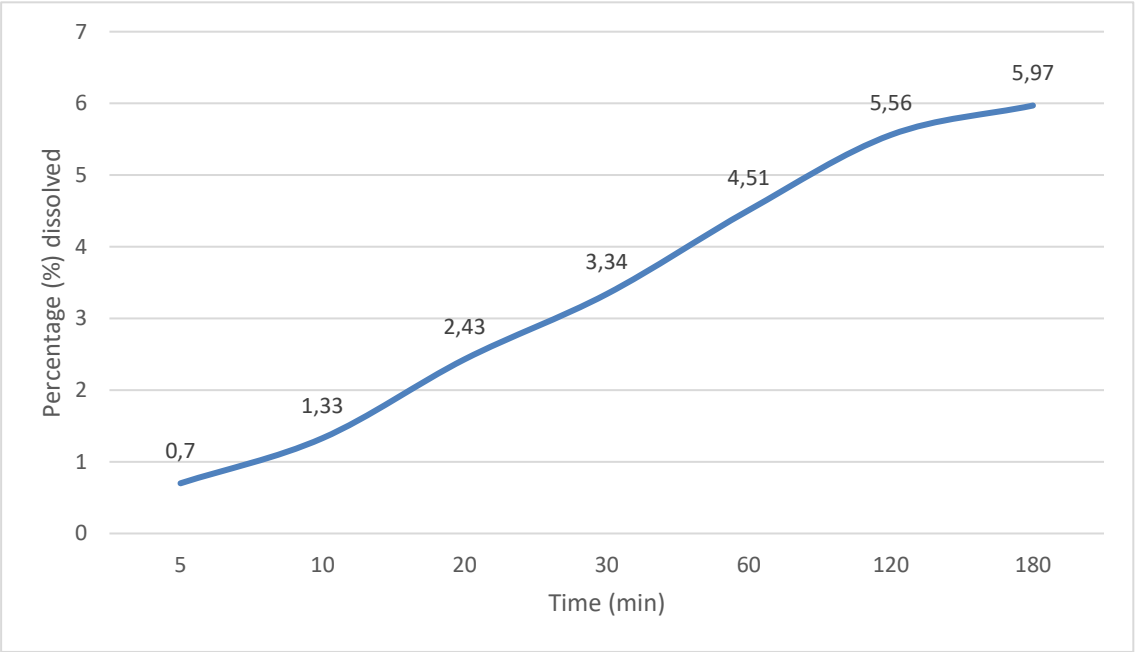


Figure 3.21: Dissolution profile of the ASD containing [EFA/PVP 25 (3:1) + 1.5% SLS].

Dissolution studies were carried out on the ASD, created by rotary evaporation, over a duration of 180 minutes. The dissolution rate for this ASD only started to plateau after 120 minutes, only reaching a maximum of 5.97% of the initial amount added at 180 minutes. The maximum dissolution of the ASD indicated a definite improvement over the EFA and 1.5% SLS physical mixture, with an improvement of 2.66% of the maximum dissolution obtained.

3.3.2 Efavirenz/PVP 30

3.3.2.1 Thermal analysis – screening for miscibility of EFA/PVP 30

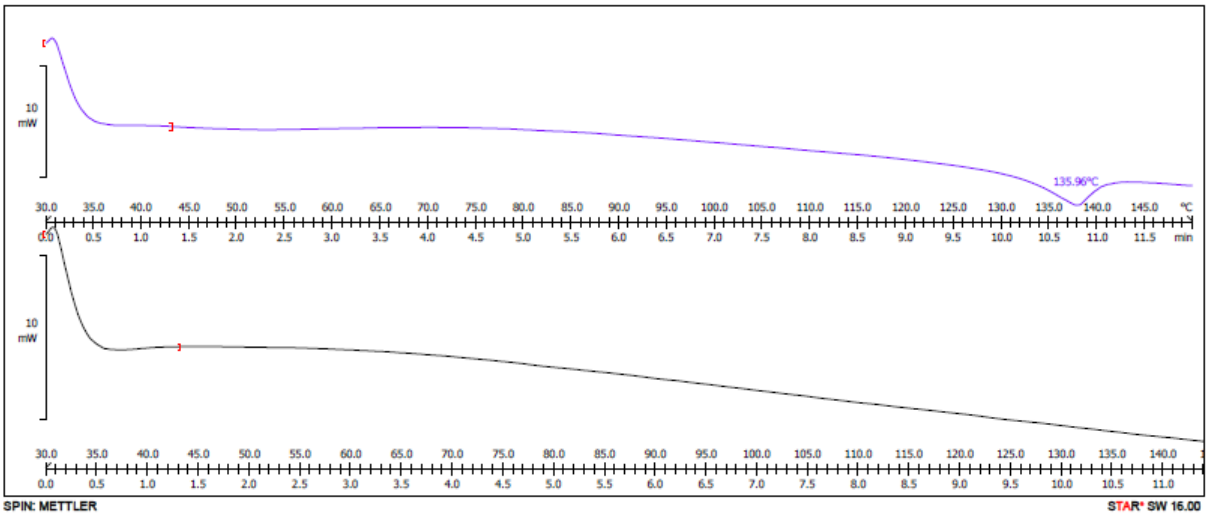


Figure 3.22: STA thermograms of an [EFA/PVP 30 (3:1) +1.5% SLS] physical mixture (top, purple), and a second run of the same sample (bottom, black).

Simultaneous thermal analysis of the [EFA/PVP 30 (3:1) +1.5% SLS] physical mixture (Fig. 3.22) indicated a melting point of 135.90°C. After the initial run, the same sample was re-analysed to investigate whether an ASD had been created after melting. The lack of a melting point in Figure 3.22 (bottom, black) was indicative thereof that an ASD had indeed formed. These favourable results qualified this sample for further testing.

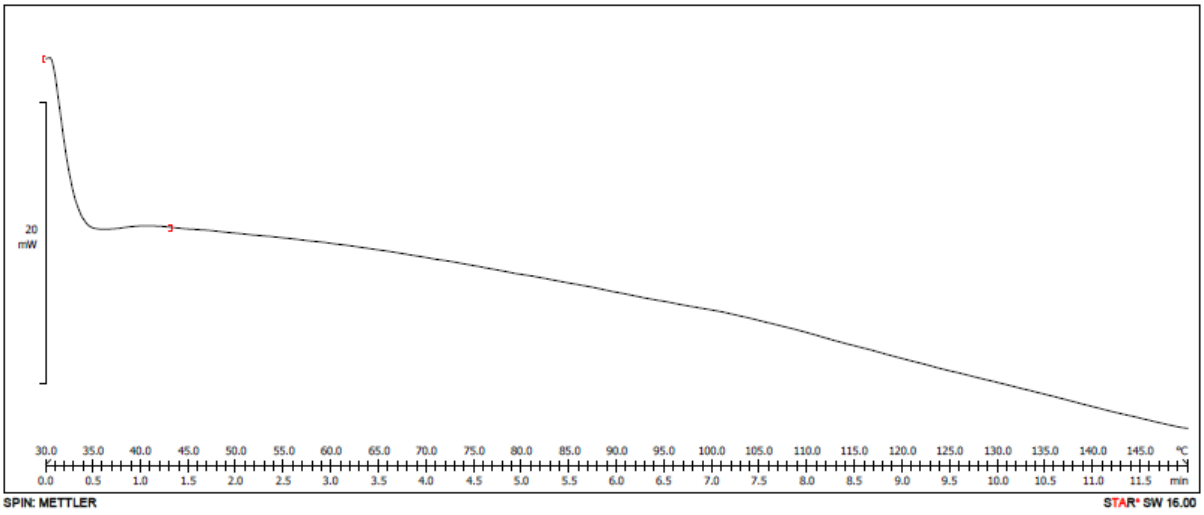
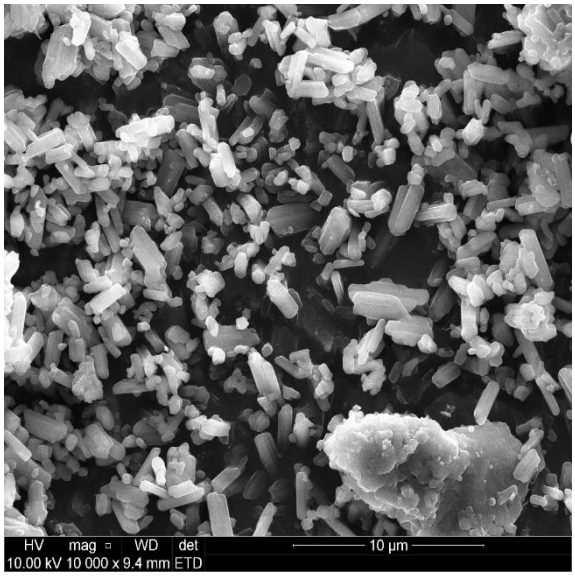


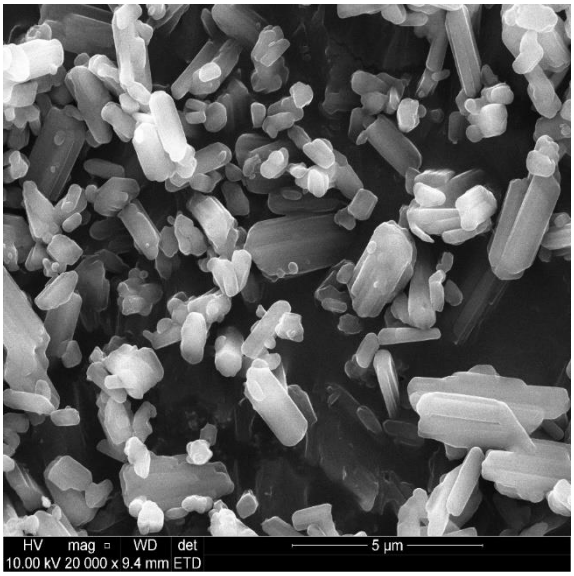
Figure 3.23: STA thermogram of the ASD containing [EFA/PVP 30 (3:1) + 1.5% SLS], created by rotary evaporation.

After initial testing, an ASD sample with [EFA/PVP 30 (3:1) + 1.5% SLS] was created by rotary evaporation and simultaneous thermal analysis was done on the resulting product to investigate whether an ASD had been created. Figure 3.23 clearly indicates that an ASD had been formed, due to the absence of a melting point, as well as the lack of any definite peaks.

3.3.2.2 Scanning electron microscopy (SEM)

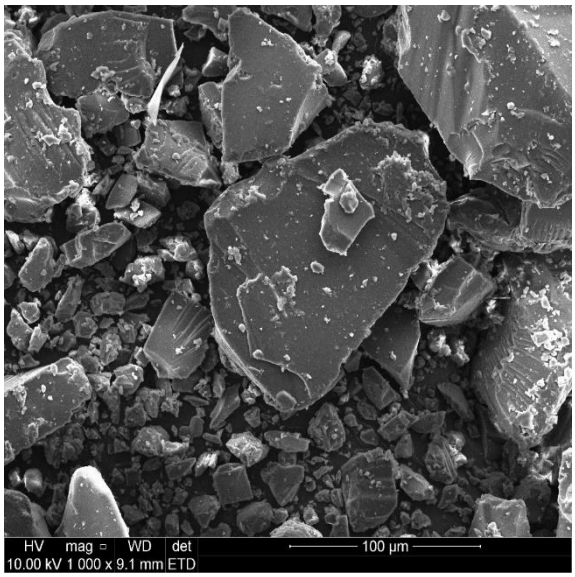


A 10 000x magnification

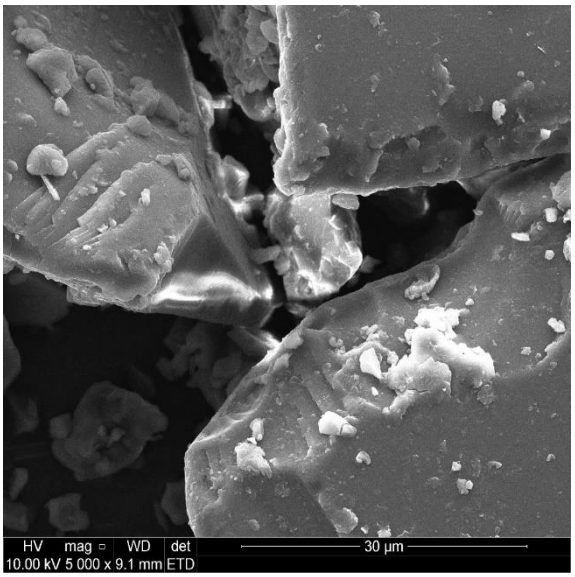


B 20 000x magnification

Figure 3.24: SEM photos of a physical mixture of [EFA/PVP 30 (3:1) + 1.5% SLS].



A 1 000x magnification



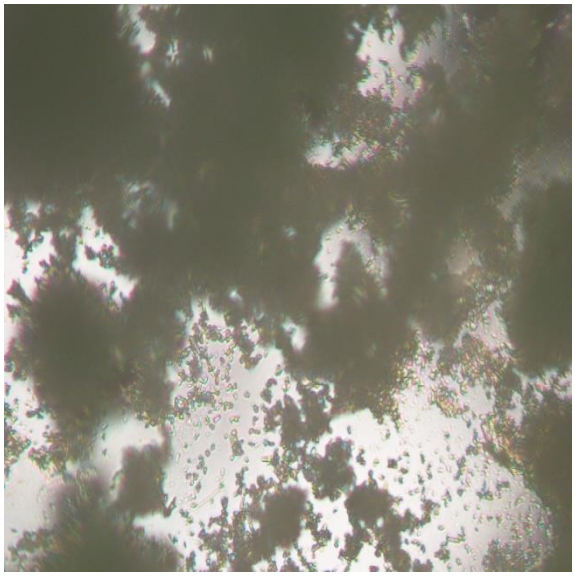
B 5 000x magnification

Figure 3.25: SEM photos of an ASD containing [EFA/PVP 30 (3:1) + 1.5% SLS].

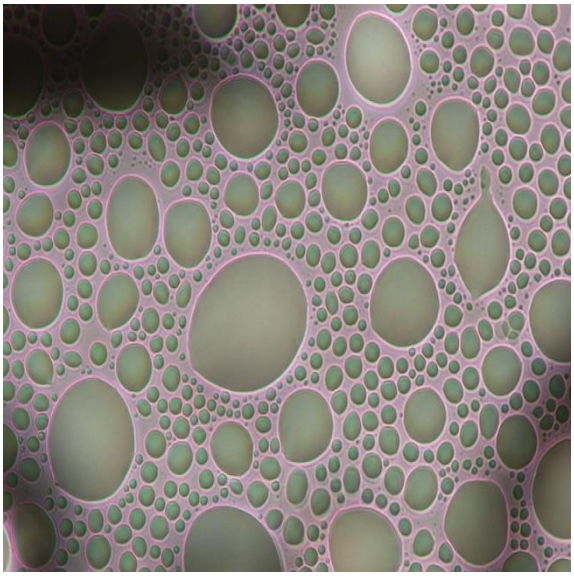
In the SEM photos taken of the physical mixture of [EFA/PVP 30 (3:1) + 1.5% SLS] (Fig. 3.24), distinct rod-shaped crystals can be seen. These crystals were smaller than those of the EFA raw material (Fig. 3.2), as the components were mixed by grinding, which reduced the length of the crystals.

From a comparison of the SEM photos of the ASD containing [EFA/PVP 30 (3:1) + 1.5% SLS] (Fig. 3.25) with those of the physical mixture (Fig. 3.24), it is clear that the appearance and sizes of particles differed. The particles of the ASD were larger and less uniform than those of the physical mixture. The shapes of the particles also differed largely, as no distinct and consistent shapes were present in the ASD, as in the physical mixture but the particles could rather be described as shards, as opposed to the rod-shaped particles of the physical mixture.

3.3.2.3 Hot-stage microscopy (HSM)



A Before melting



B After melting

Figure 3.26: HSM photos of the physical mixture of [EFA/PVP 30 (3:1) + 1.5% SLS].

Figure 3.26 displays the physical mixture of [EFA/PVP 30 (3:1) + 1.5% SLS] before melting. Larger agglomerated clusters could be seen than in the EFA raw material sample (Fig. 3.4), which most likely represented the larger PVP 30 crystals to which the EFA crystals clung. Those agglomerates required more time to melt, after the melting point had been reached. After having reached the melting point, small droplets of amorphous material formed (Fig. 3.26).

3.3.2.4 X-ray powder diffraction (XRPD)

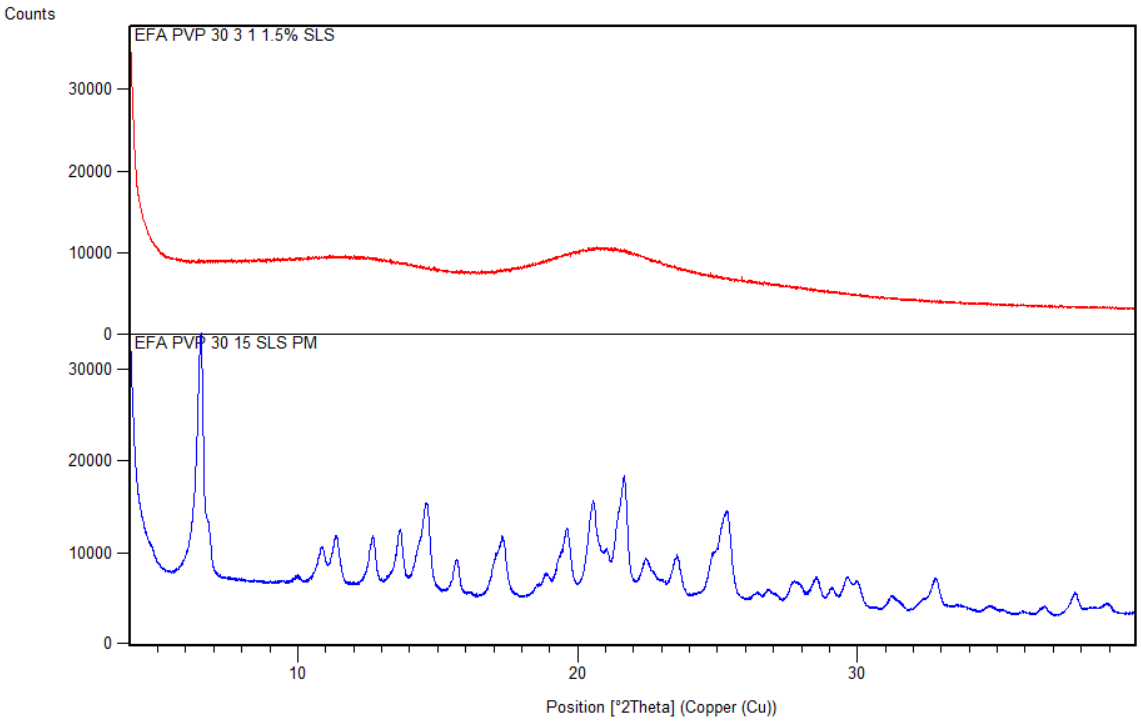


Figure 3.27: XRPD profile of an ASD containing [EFA/PVP 30 (3:1) + 1.5% SLS] (top, red) and a physical mixture of [EFA/PVP 30 (3:1) + 1.5% SLS] (bottom, blue).

The XRPD profile of the [EFA/PVP 30 (3:1) + 1.5% SLS] physical mixture indicated that it was crystalline, as was evident from the peaks that had formed in Figure 3.27 (bottom, blue).

The ASD containing [EFA/PVP 30 (3:1) + 1.5% SLS], created by rotary evaporation, was then re-analysed. The subsequent results indicated that it was indeed amorphous, as could be observed from the lack of any significant peaks in Figure 3.27 (top, red). These results were once again desirable.

3.3.2.5 Stability testing

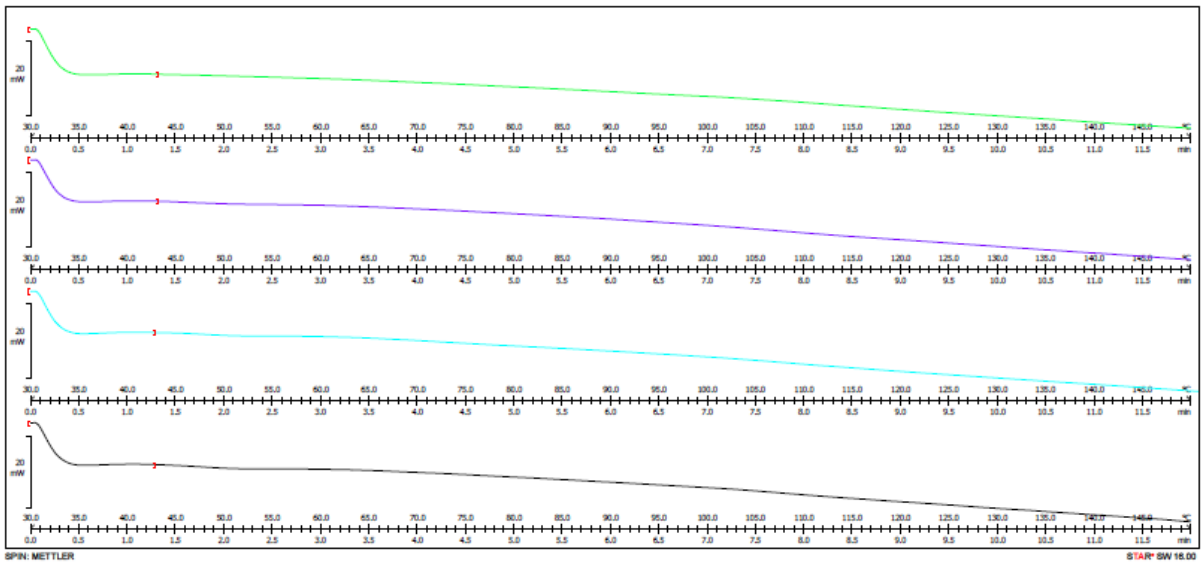


Figure 3.28: An overlay of the STA thermograms of an ASD containing [EFA/PVP 30 + 1.5% SLS] at initial (green), month 1 (purple), month 2 (blue) and month 3 (black) of stability testing.

Table 3.6: Moisture content of EFA/PVP 30 over the duration of the stability test period as measured by means of STA (TG analysis)

Sample	Initial	Month 1	Month 2	Month 3
[EFA/PVP 30 (3:1) +1.5% SLS]	2.3%	1.7%	1.9%	1.5%

The initial moisture content of the ASD containing EFA/PVP 30 was 2.3%, where after it decreased to 1.7% and 1.9% after 1 and 2 months, respectively, after which it decreased to 1.5% at month 3.

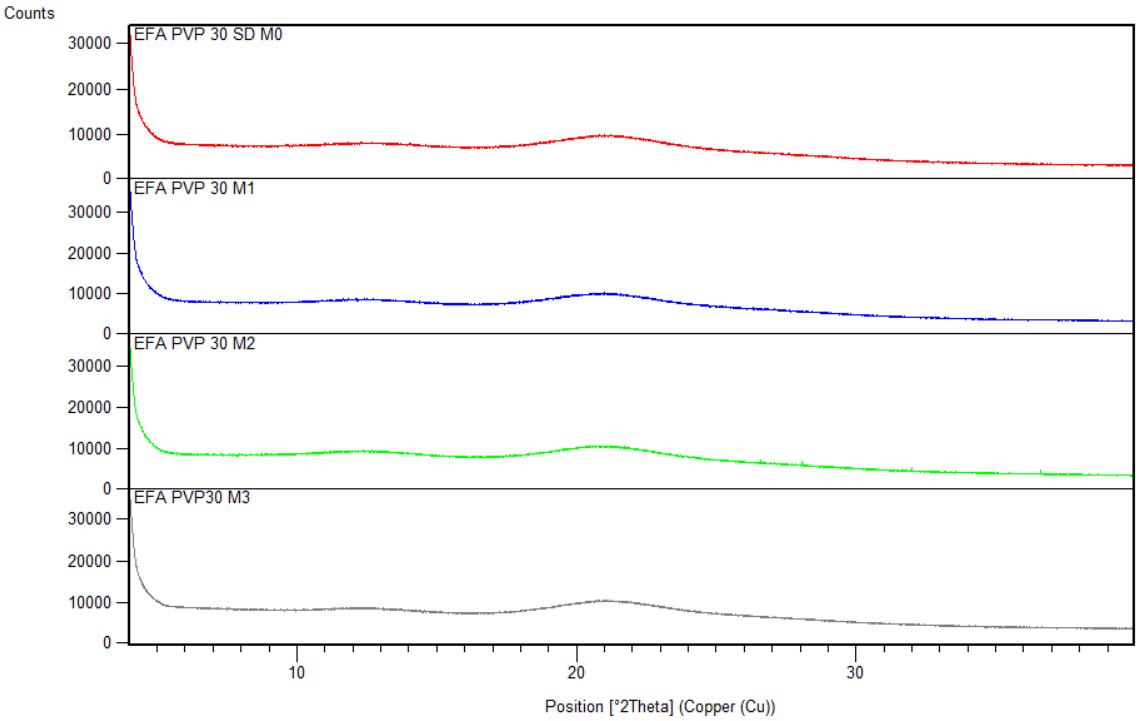


Figure 3.29: XRPD profile of an ASD containing [EFA/PVP 30 (3:1) + 1.5% SLS] at initial (red), month 1 (blue), month 2 (green) and month 3 (grey) of stability testing.

Simultaneous thermal analysis of the ASD containing [EFA/PVP 30 (3:1) + 1.5% SLS] indicated that the ASD had remained stable in an amorphous state throughout the entire 3-month stability testing period. This could be observed from the lack of any definite melting points, as illustrated by Figure 3.28.

The XRPD profiles of the ASD containing [EFA/PVP 30 (3:1) + 1.5% SLS] confirmed that it had remained stable in an amorphous state for the entire 3-month stability testing period. This could be observed from the lack of any discernible peaks in Figure 3.29.

Table 3.7: HPLC assay results of EFA/PVP 30 over the duration of the stability test period

Sample	Initial	Month 1	Month 2	Month 3
[EFA/PVP 30 (3:1) +1.5% SLS]	101.2%	77.3%	78.9%	20.6%

After months 1 and 2 of stability testing, the ASD containing EFA/PVP 30 showed degradation of approximately 22%. After 3 months, a total degradation of 79.4% had occurred, compared to the EFA raw material that had degraded with 55.9% (Table 3.3), and the ASD containing EFA/PVP 25 which had shown a 66.7% degradation (Table 3.5).

3.3.2.6 Powder dissolution studies

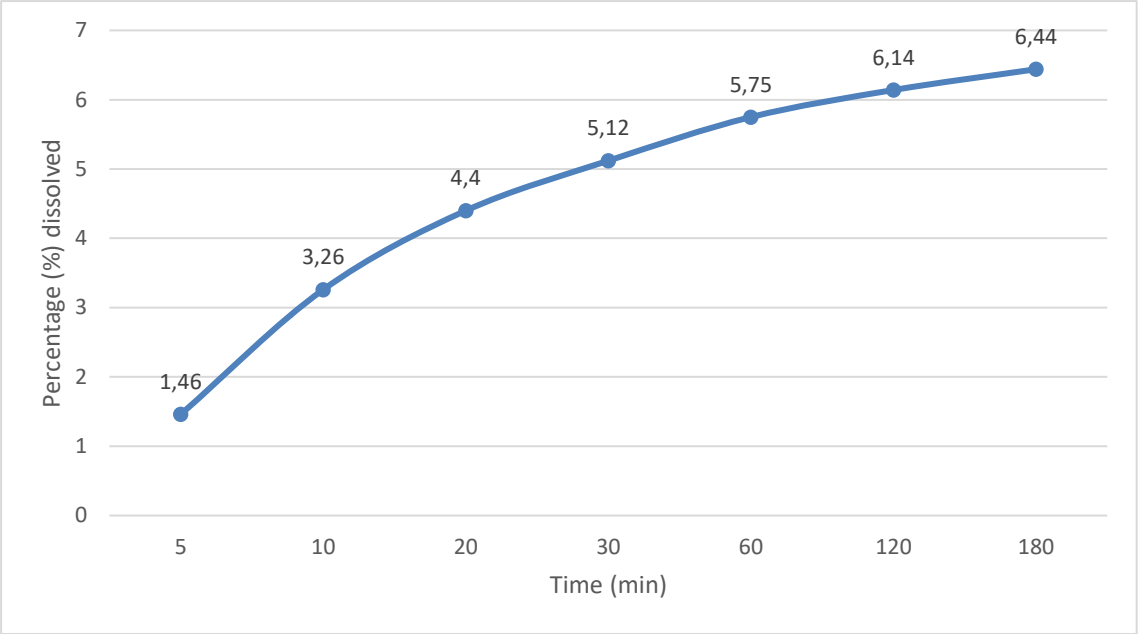


Figure 3.30: Dissolution profile of the ASD containing [EFA/PVP 30 (3:1) + 1.5% SLS].

Dissolution studies were done on the ASD containing [EFA/PVP 30 (3:1) + 1.5% SLS], created by rotary evaporation, over a duration of 180 minutes. The percentage of ASD having dissolved over time was more consistent for this ASD, compared to the ASD containing PVP 25, as can be observed in Figure 3.21. Although no definite plateau can be observed, the maximum dissolution at 180 minutes showed an improvement over both the crystalline physical mixture of EFA and 1.5% SLS, with an improvement of 3.31%, as well as the ASD containing PVP 25, with an improvement of 0.47%.

An increase in the test period would also likely result in a higher percentage of dissolved API, as no definite plateau had yet been reached.

3.3.3 Efavirenz/PVP VA 64

3.3.3.1 Simultaneous thermal analysis (STA) (TGA/DSC)

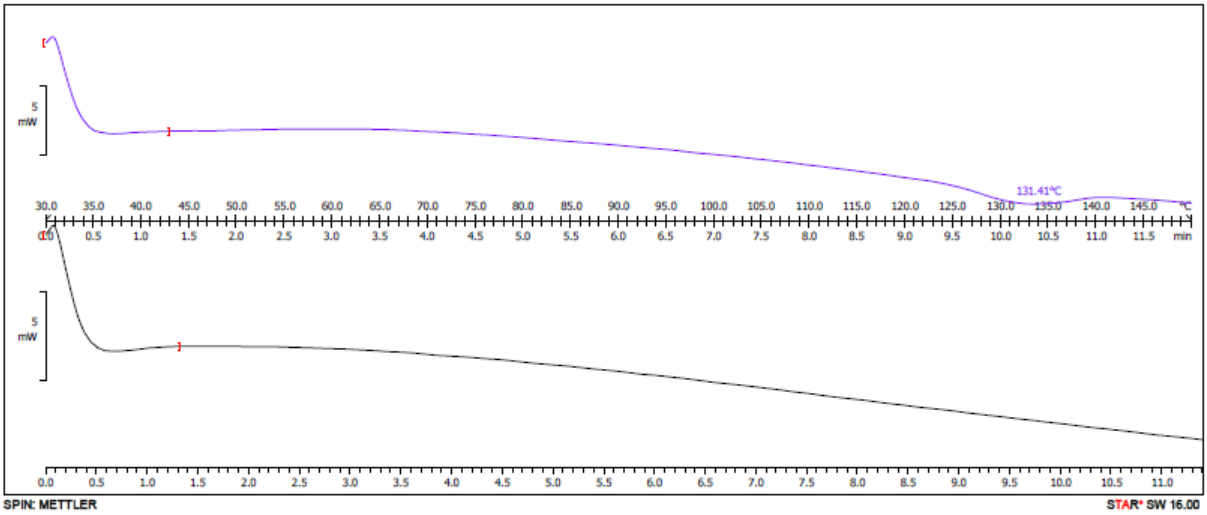


Figure 3.31: STA thermograms of an [EFA/PVP VA 64 (3:1) +1.5% SLS] physical mixture (top, purple), and a second run of the same sample (bottom, black).

Simultaneous thermal analysis of a physical mixture of [EFA/PVP VA 64 (3:1) +1.5% SLS] indicated a melting point of 131.41°C. After the initial run, the same sample was re-analysed to investigate whether an ASD had been created. In Figure 3.31 (bottom, black), the absence of a melting point, as well as the absence of definite peaks were indicative thereof that an ASD had indeed formed.

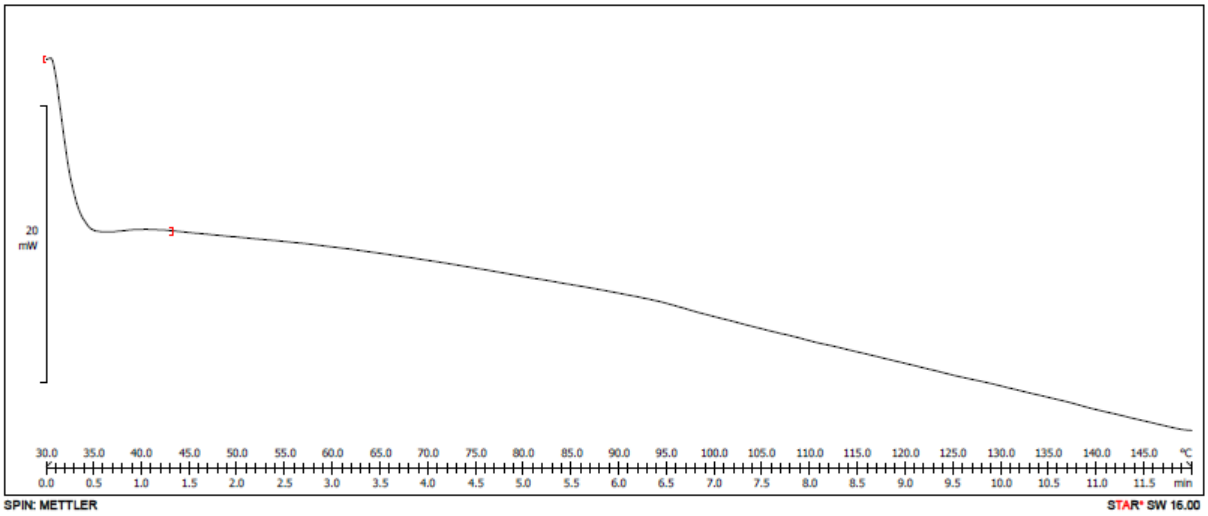
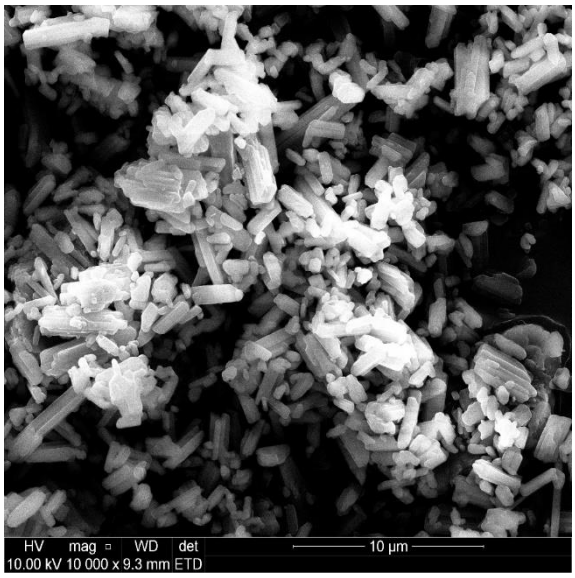


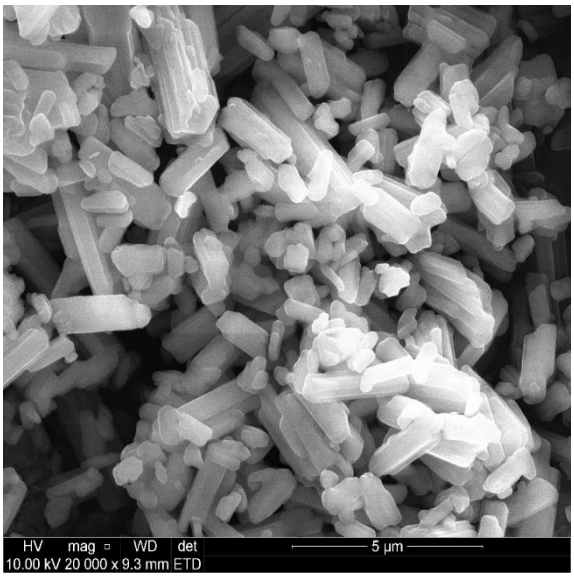
Figure 3.32: STA thermogram of the ASD containing [EFA/PVP VA 64 (3:1) + 1.5% SLS], prepared by rotary evaporation.

After initial testing, an ASD was created containing [EFA/PVP VA 64 (3:1) + 1.5% SLS]. Simultaneous thermal analysis was then carried out to investigate whether an ASD had indeed been created. Figure 3.32 confirmed that an ASD had been created, as can be seen from the lack of a melting point, as well as the lack of any definite peaks.

3.3.3.2 Scanning electron microscopy (SEM)

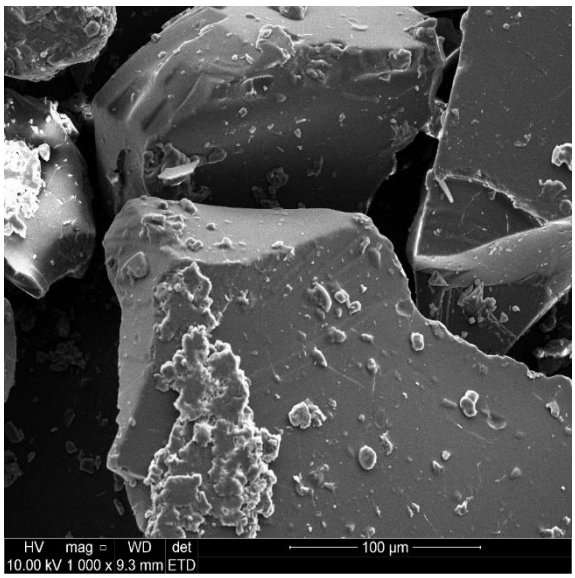


A 10 000x magnification

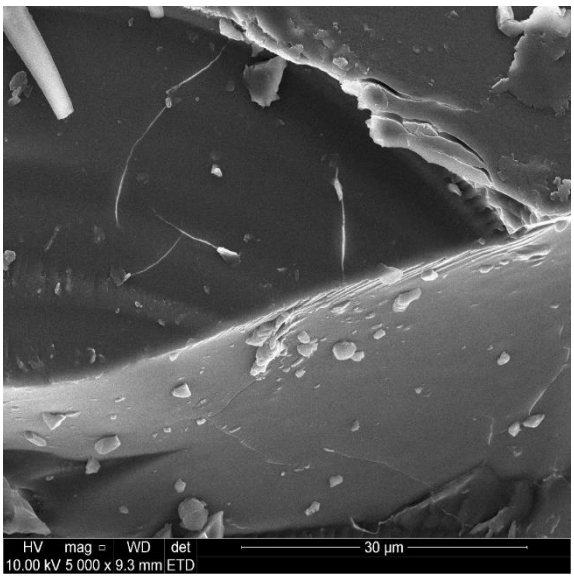


B 20 000x magnification

Figure 3.33: SEM photos of a physical mixture of [EFA/PVP VA 64 (3:1) + 1.5% SLS].



A 1 000x magnification



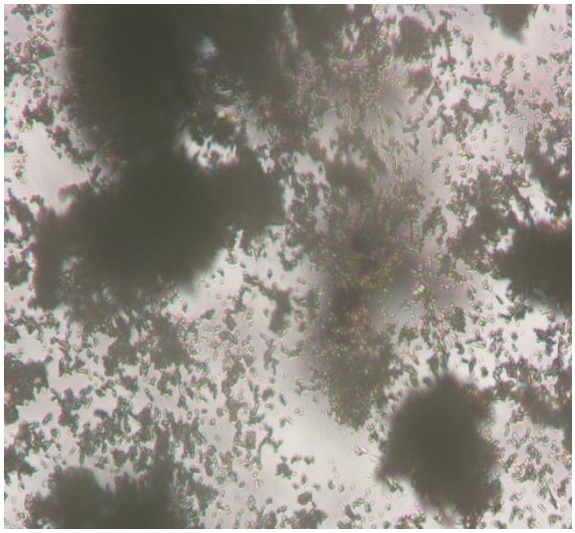
B 5 000x magnification

Figure 3.34: SEM photos of an ASD containing [EFA/PVP VA 64 (3:1) + 1.5% SLS].

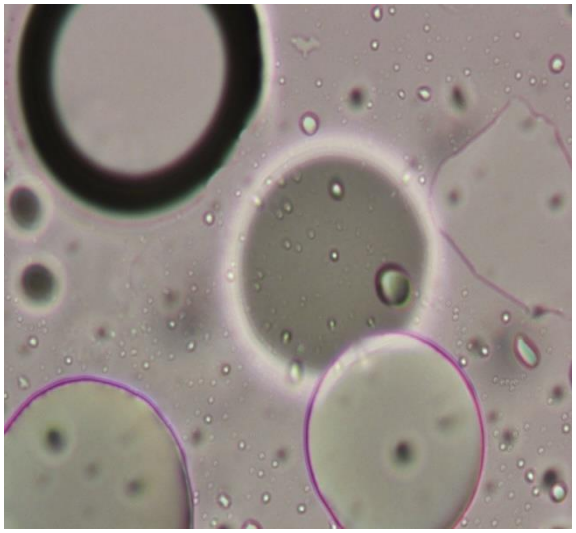
In the SEM photos taken of the physical mixture of [EFA/PVP VA 64 (3:1) + 1.5% SLS] (Fig. 3.33) distinct rod-shaped crystals can be seen. These crystals were shorter than those of the EFA raw material (Fig. 3.3), as the components were mixed by grinding during sample preparation, which had reduced the length of the crystals.

From a comparison of the SEM photos of the ASD containing [EFA/PVP VA 64 (3:1) + 1.5% SLS] (Fig. 3.34), with those of the physical mixture (Fig. 3.33), it is clear that the appearance and sizes of the particles differed. The particles of the ASD were larger and less uniform than those of the physical mixture. The shapes of the particles also differed largely, since no distinct and consistent shapes were present in the ASD, as in the physical mixture, and could the particles rather be described as shards, as opposed to the rod-shaped particles of the physical mixture.

3.3.3.3 Hot-stage microscopy (HSM)



A Before melting



B After melting

Figure 3.35: HSM photos of the physical mixture of [EFA/PVP VA 64 (3:1) + 1.5% SLS].

In the physical mixture of the [EFA/PVP VA 64 (3:1) + 1.5% SLS] sample (Fig. 3.35), once again, larger agglomerated clusters than those of the EFA raw material (Fig. 3.4) were observed, which most likely represented the larger PVP VA 64 crystals to which the EFA crystals clung. Those agglomerated clusters required more time to melt, compared to the free standing EFA crystals, after having reached the melting point.

3.3.3.4 X-ray powder diffraction (XRPD)

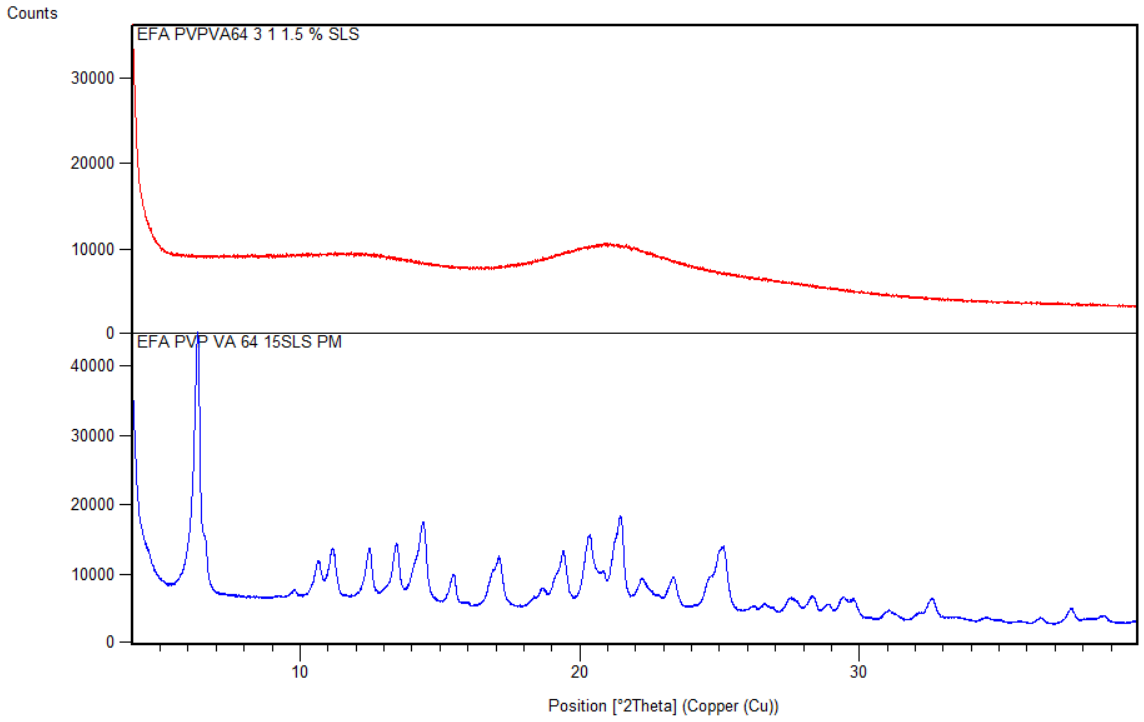


Figure 3.36: XRPD profile of an ASD containing [EFA/PVP VA 64 (3:1) + 1.5% SLS] (top, red) and a physical mixture of [EFA/PVP VA 64 (3:1) + 1.5% SLS] (bottom, blue).

The XRPD profile of the [EFA/PVP VA 64 (3:1) + SLS 1.5%] physical mixture indicated that it was crystalline, as could be observed from the peaks having formed in Figure 3.36 (bottom, blue).

The ASD containing the [EFA/PVP VA 64 (3:1) + 1.5% SLS], created by rotary evaporation, was then analysed, which indicated that it was indeed amorphous, as can be observed from the lack of significant peaks in Figure 3.36 (top, red). These results obtained were once again desirable.

3.3.3.5 Stability testing

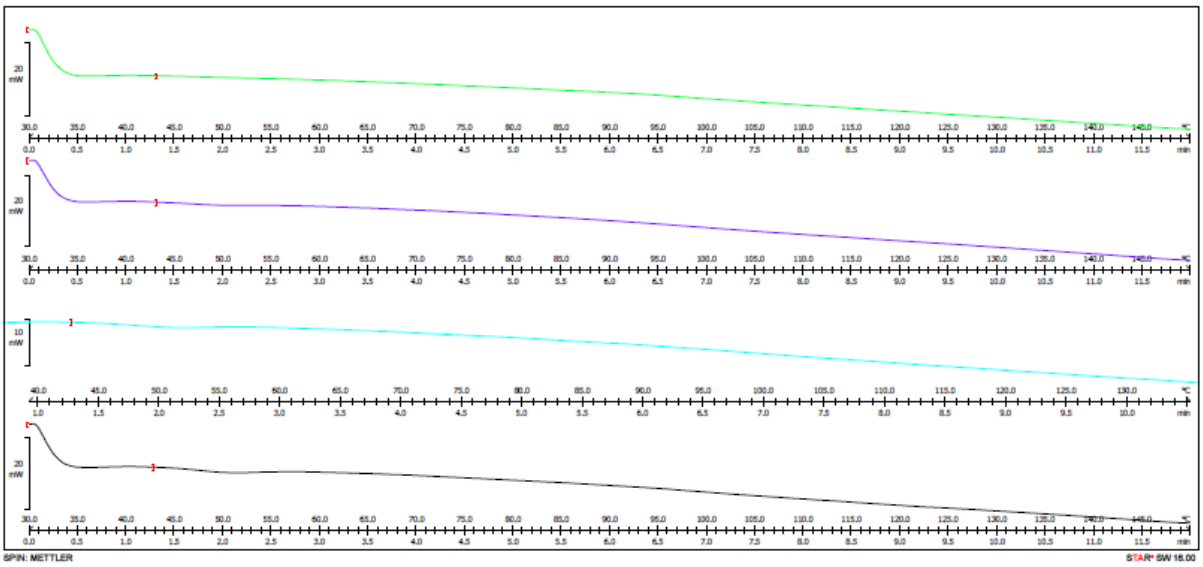


Figure 3.37: An overlay of the STA thermograms of an ASD containing [EFA/PVP VA 64 + 1.5% SLS] at initial (green), month 1 (purple), month 2 (blue) and month 3 (black) of stability testing.

Table 3.8: Moisture content of EFA/PVP 64 over the duration of the stability test period as measured by means of STA (TG analysis)

Sample	Initial	Month 1	Month 2	Month 3
[EFA/PVP VA 64 (3:1) +1.5% SLS]	1.5%	1.1%	1.3%	1.1%

The initial moisture content of the ASD containing EFA/PVP VA 64 was 1.5% and after the first month of stability testing it decreased to 1.1%. Thereafter it again increased to 1.3% at month 2, but finally decreased to 1.1% at month 3.

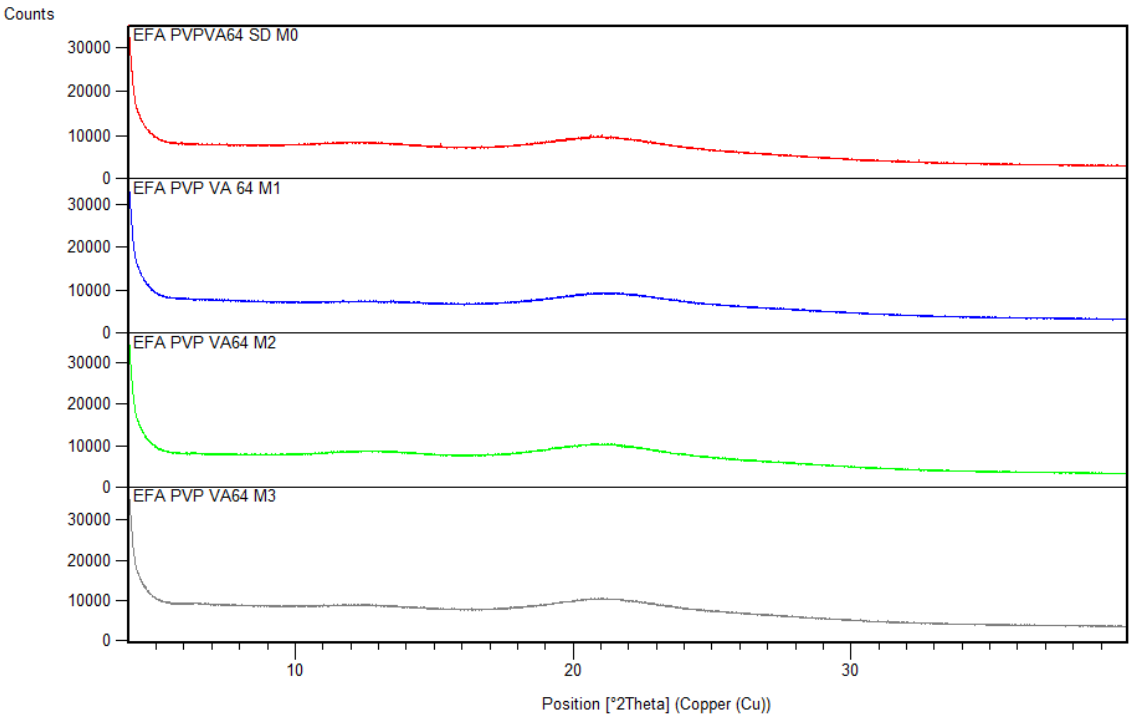


Figure 3.38: XRPD profile of an ASD containing [EFA/PVP VA 64 (3:1) + 1.5% SLS] at initial (red), month 1 (blue), month 2 (green) and month 3 (grey) of stability testing.

Simultaneous thermal analysis of the ASD containing [EFA/PVP VA 64 (3:1) + 1.5% SLS] indicated that the ASD had remained stable in an amorphous state throughout the entire 3-month stability testing period. This could be observed from the lack of definite melting points in Figure 3.37.

XRPD profiles of the ASD containing [EFA/PVP VA 64 (3:1) + 1.5% SLS] confirmed that it had remained stable in an amorphous state for the entire 3-month stability testing period. This could be observed from the lack of discernible peaks in Figure 3.38.

Table 3.9: HPLC assay results of EFA/PVP VA 64 over the duration of the stability test period

Sample	Initial	Month 1	Month 2	Month 3
[EFA/PVP VA 64 (3:1) +1.5% SLS]	101.6%	77.5%	78.4%	21.4%

At months 1 and 2 of stability testing, the ASD containing EFA/PVP VA 64 showed degradation of more than 22%. After 3 months, a total degradation of 78.6% had occurred, compared to the EFA raw material that had shown a total degradation of 55.9% (Table 3.3).

3.3.3.6 Powder dissolution studies

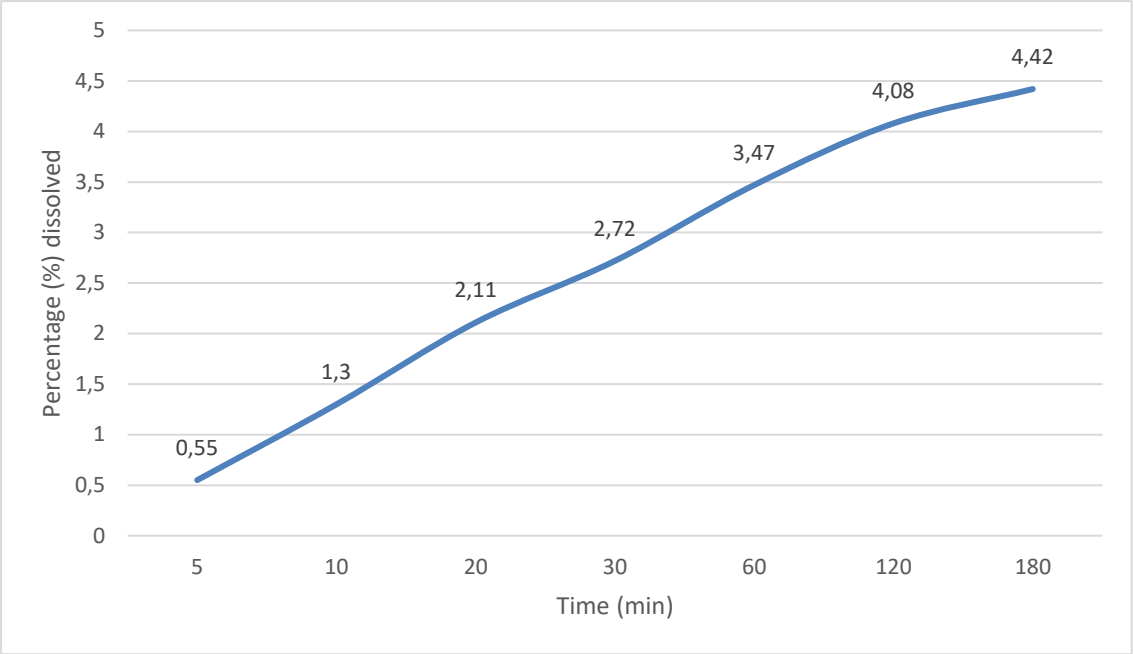


Figure 3.39: Dissolution profile of the ASD containing [EFA/PVP VA 64 (3:1) + 1.5% SLS].

Dissolution studies were done on the ASD containing [EFA/PVP VA 64 (3:1) + 1.5% SLS] over a duration of 180 minutes. Although Figure 3.39 shows no definite plateau, an improvement of the maximum percentage of the initial amount of API being dissolved was 4.42%, compared to the physical mixture containing EFA and 1.5% SLS, having shown an improvement of 1.11%.

An increase in the duration of the dissolution test would also likely result in an increase in the maximum percentage of the API that would dissolve, since no plateau had yet been reached.

3.4 Conclusion

Poorly soluble efavirenz (EFA), known for being highly unstable in pure amorphous form, was prepared in different amorphous solid dispersions (ASDs), by using different polymers in varying ratios. Physically stable ASDs were prepared with PVP 25, PVP 30 and PVP VA 64.

The prepared ASD formulations seemed stable, although their theoretical glass transition temperatures (T_g) were determined at below 80ºC, which reportedly is ideal for a stable ASD.

Thermal analyses and powder X-ray diffractometry had proven the amorphous nature of the relevant ASDs. After three months of accelerated stability studies at 40ºC and 75% RH, no recrystallisation had occurred. Surprisingly, chemical degradation was observed for the efavirenz raw material and for most of the prepared ASDs after 2 months of stability studies. The efavirenz raw material, however, only showed degradation after month 3 (55.9%), lesser than the values

being determined for the three ASDs. After 3 months of stability testing, the chemical degradation of efavirenz was measured as being higher than 65% in all three the prepared ASDs. Maurin *et al.* (2002) reported that the degradation of efavirenz followed first order kinetics and that the pH of maximum stability had been measured at 4. They had, however, determined this in a hydrolysis experiment, which differs from stability testing. The moisture in the 75% relative humidity conditions could have played a catalytic role in the degradation being observed during this study. The DSC thermograms and XRPD analyses, however, showed no extra peaks, nor possible degradation products. This degradation phenomenon required further investigation, which would include an HPLC method specific for stability and degradation products. No stability testing on efavirenz powder and without packaging materials was found in the available literature, which made the results worth investigating in another study.

The ASD with the best dissolution results and highest apparent solubility was the one containing [EFA/PVP 30 (1:3) + 1.5% SLS]. A 100% improvement in apparent solubility was obtained, compared to that of the crystalline efavirenz raw material and the 1.5% SLS physical mixture (Fig. 3.40). Submerging of the [EFA/PVP 30 (1:3) + 1.5% SLS] powder in water for 3 hours had no measurable effect on stability and did not lead to recrystallisation.

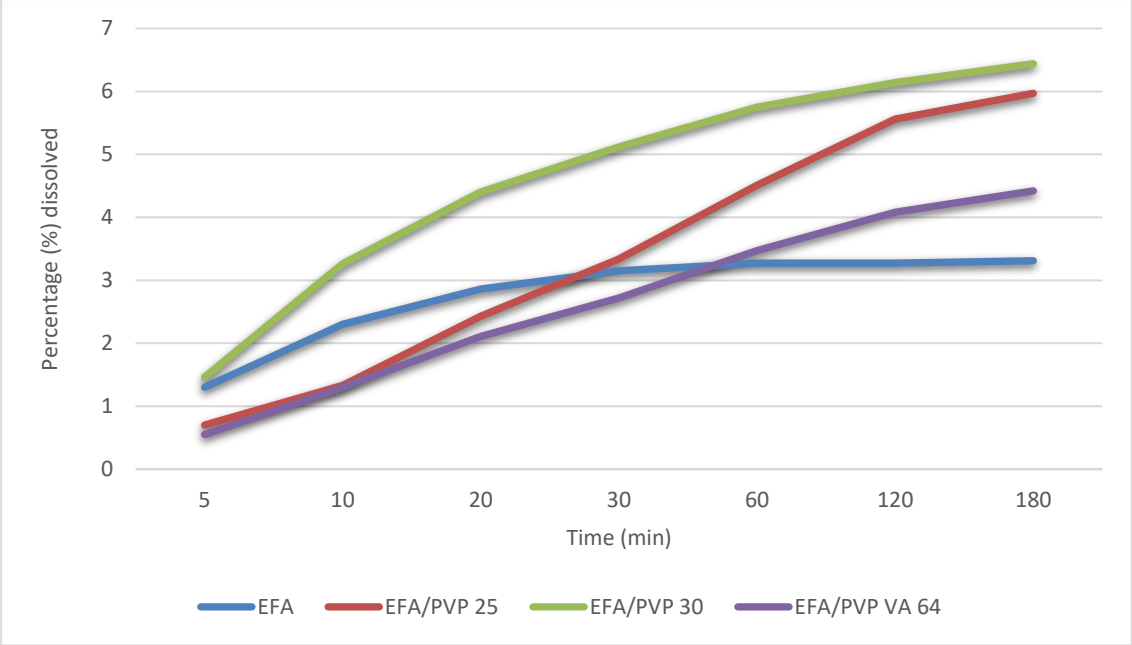


Figure 3.40: Overlay of dissolution profiles of efavirenz and efavirenz ASDs.

As mentioned earlier, the ASD formulation that was used in this study, incorporated the SLS in the ADS formulation and was not part of the dissolution volume, which could have affected the wettability of the powder and led to lower dissolution values. The optimal efavirenz ASD still needs more experimenting, to at least try and improve the dissolution results, since it was still below 10%. On hindsight, although the ratio of a 3:1 (EFA/polymer) seemed like a physically

stable ASD, the poor solubility of efavirenz was not markedly improved. On the positive side, it was found that a small percentage of the polymer had stabilised the EFA ASD. However, to improve the solubility, the polymer ratio should be increased.

The chemical degradation of both the efavirenz raw material and the prepared ASDs was disappointing and would need further investigation.

The modified ‘Screening of polymers for amorphous drug stabilisation’ (SPADS) method yielded an efavirenz ASD that was more soluble than the crystalline form and much more stable (physical stability, no recrystallisation) than the pure amorphous form.

References

Chu, K.A. & Yalkowsky, S.H. 2009. An interesting relationship between drug absorption and melting point. *International journal of pharmaceutics*, 373:24-40.

Maurin, M.B., Rowe, S.M., Blom, K. & Pierce, M.E. 2002. Kinetics and mechanism of hydrolysis of efavirenz. *Pharmaceutical research*, 19(4):517-521.

Narayan, P., Porter, W.W. III, Brackhagen, M. & Tucker, C. 2015. Polymers and surfactants. (*In* Newman, A. *ed*. Pharmaceutical amorphous solid dispersions. Hoboken: John Wiley & Sons Inc. p. 42-84).

Newman, A. & Munson, E. 2012. Characterising miscibility in amorphous solid dispersions. American pharmaceutical review, May 9. [Web:] www.americanpharmaceuticalreview.com/Featured-Articles/112448-Characterizing-Miscibility-in-Amorphous-Solid-Dispersions/ [Date of access: 2018-08-12].

Stieger, N., Aucamp, M. & Liebenberg, W. 2013. Relative stability of efavirenz glass: agitated *vs*. non-agitated. Poster presented at the Annual Meeting of the American Association of Pharmaceutical Scientists, November 10-24, San Antonio, USA. [Web:] http://www.aapspharmaceutica.com. [Date of access: 2018-07-12].

United States Food and Drug Administration. 2017a. Inactive ingredient approved drug products: Hypromellose acetate succinate. [Web:] https://www.accessdata.fda.gov/scripts/cder/iig/getiigWEB.cfm [Date of access: 2017-05-22].

United States Food and Drug Administration. 2017b. Inactive ingredient approved drug products: Copovidone K90. [Web:] https://www.accessdata.fda.gov/scripts/cder/iig/getiigWEB.cfm [Date of access: 2017-05-22].

United States Food and Drug Administration. 2017c. Inactive ingredient approved drug products: Polyethylene glycol 8000. [Web:] https://www.accessdata.fda.gov/scripts/cder/iig/getiigWEB.cfm [Date of access: 2017-05-22].

United States Food and Drug Administration. 2017d. Inactive ingredient approved drug products: Polysorbate 80. [Web:] https://www.accessdata.fda.gov/scripts/cder/iig/getiigWEB.cfm [Date of access: 2017-05-22].

United States Food and Drug Administration. 2017e. Inactive ingredient approved drug products: Sodium lauryl sulfate. [Web:] https://www.accessdata.fda.gov/scripts/cder/iig/getiigWEB.cfm [Date of access: 2017-05-22].

United States Food and Drug Administration. 2017f. Inactive ingredient approved drug products: Lecithin. [Web:] https://www.accessdata.fda.gov/scripts/cder/iig/getiigWEB.cfm [Date of access: 2017-05-22].

United States Food and Drug Administration. 2017g. Inactive ingredient approved drug products: Lauroyl polyoxylglycerides. [Web:] https://www.accessdata.fda.gov/scripts/cder/iig/getiigWEB.cfm [Date of access: 2017-05-22].

USP see United States Pharmacopoeia.

United States Pharmacopoeia. 2018. [Web:] https://online.uspnf.com/uspnf/document/GUID-C986119A-FC7B-4E57-A098-F0BC6982B475_1_en-US

Chapter 4

Preparation of Praziquantel Amorphous Solid Dispersions

4.1 Primary screening to identify suitable praziquantel polymers

As stated in Section 3.1, a combined glass transition temperature (T_g) of 80°C or higher would be ideal for ensuring the stability of any prepared amorphous solid dispersion (ASD). The calculated theoretical T_g values for each ASD consisting of praziquantel and a polymer are summarised in Table 4.1. Formula 3.1 was also used to calculate these theoretical T_g values.

Although initial testing had indicated that viable praziquantel ASDs could be prepared in combination with each of the polymers, HPMC, HPMCAS, PVP 25, PVP 30 and PVP VA 64 in a ratio of 3:1 (API:polymer), only the praziquantel:HPMCAS ASD turned out as being stable and miscible.

The acronym of **PZQ** is used for **praziquantel** from hereafter.

4.2 Physico-chemical properties of praziquantel (PZQ)

4.2.1 Thermal analysis

4.2.1.1 Simultaneous thermal analysis (STA) of the PZQ raw material

STA analysis was performed according to the method as described in Section 2.7.1.

Table 4.1: Theoretical T_g values obtained for PZQ (T_g = 38°C) and polymer combinations (blue shaded sample represents the one that went through to the final test round)

Praziquantel and Polymer	Ratio	Theoretical T_g (°C)
PZQ:HPMC	1:1	76.5
	1:2	89.33
	1:3	95.75
	1:4	99.6
	2:1	63.67
PZQ:HPMCAS	1:1	81.5
	1:2	96
	1:3	103.25
	1:4	107.6
	2:1	67
PZQ:PVP 25	1:1	95
	1:2	114
	1:3	123.5
	1:4	129.2
	2:1	76
PZQ:PVP 30	1:1	93.5
	1:2	112
	1:3	121.25
	1:4	126.8
	2:1	75
PZQ:PVP VA 64	1:1	69.5
	1:2	80
	1:3	85.25
	1:4	88.4
	2:1	59

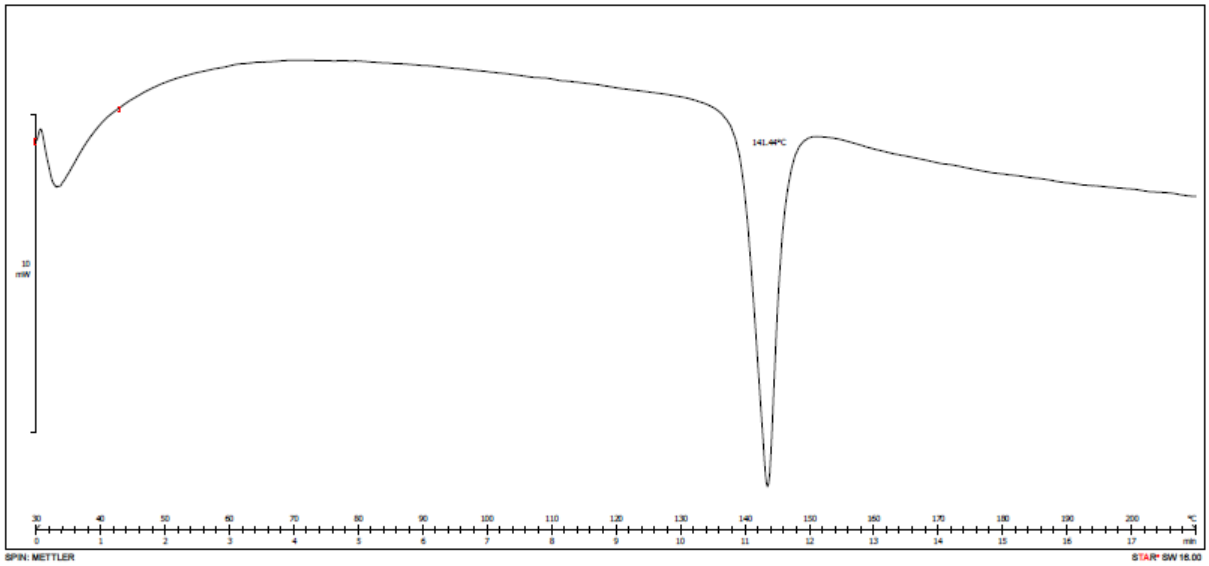
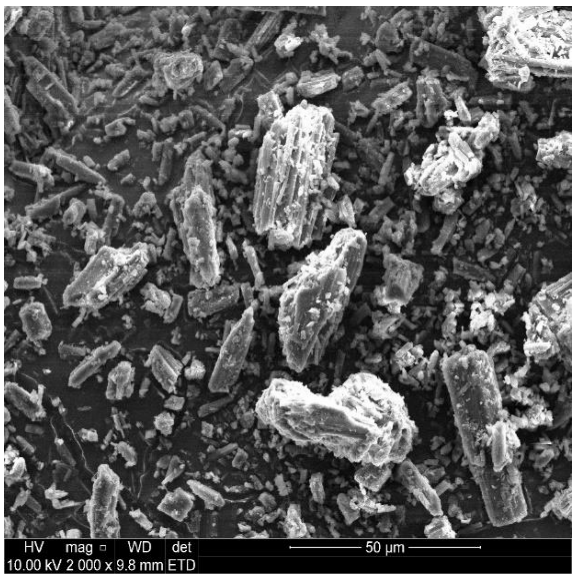


Figure 4.1: Simultaneous thermal analysis (STA) thermogram of the PZQ raw material with a melting point of 141.44°C.

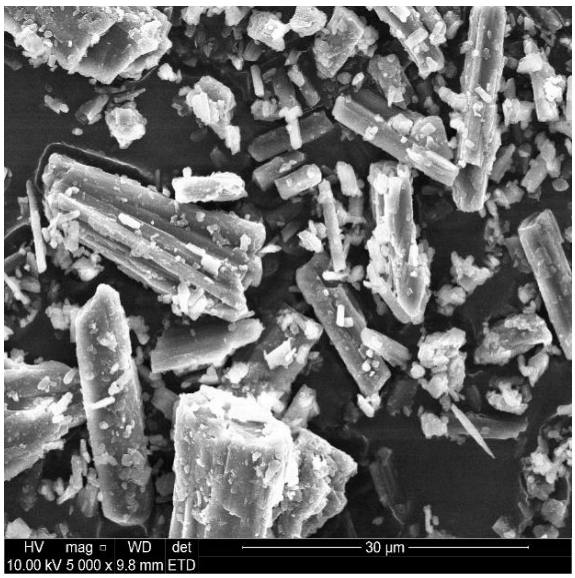
STA of the PZQ raw material indicated a melting point of 141.44°C (Fig. 4.1), which confirmed that it was crystalline.

4.2.1.2 Scanning electron microscopy (SEM)

The scanning electron microscopy images were recorded according to the method being described in Section 2.7.3.



A 2 000x magnification



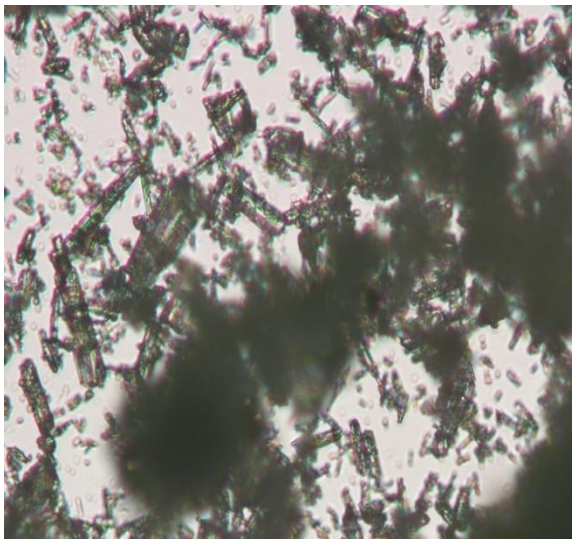
B 5 000x magnification

Figure 4.2: SEM photos of the PZQ raw material.

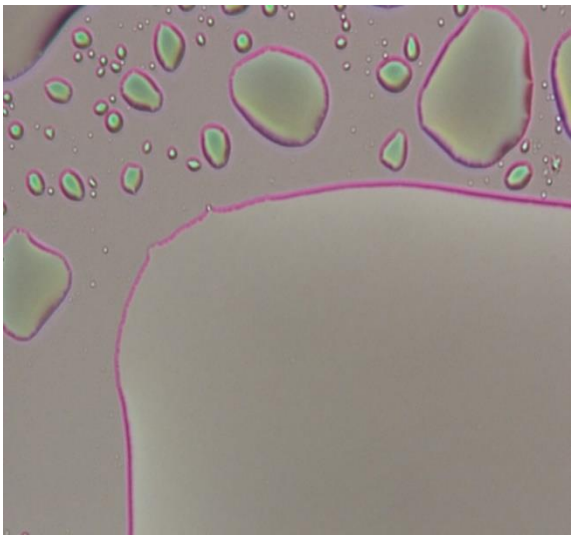
In the SEM photos taken of the PZQ raw material (Fig. 4.2), clear rod-shaped crystals of varying sizes were observed.

4.2.2 Hot-stage microscopy (HSM)

The HSM photos were taken according to the method as described in Section 2.7.2.



A Before melting



B After melting

Figure 4.3: HSM photos of the PQZ raw material before and after melting.

The HSM images of the PZQ raw material (Figure 4.3) also showed crystals that were not uniform in size. Agglomeration was not prevalent in this powder, most likely as a result of the larger crystals being present in these samples. After melting, the droplets that were left behind were indicative thereof that an amorphous state had been reached.

4.2.3 X-ray powder diffraction (XRPD)

XRPD analysis was performed according to the method as described in Section 2.7.4.

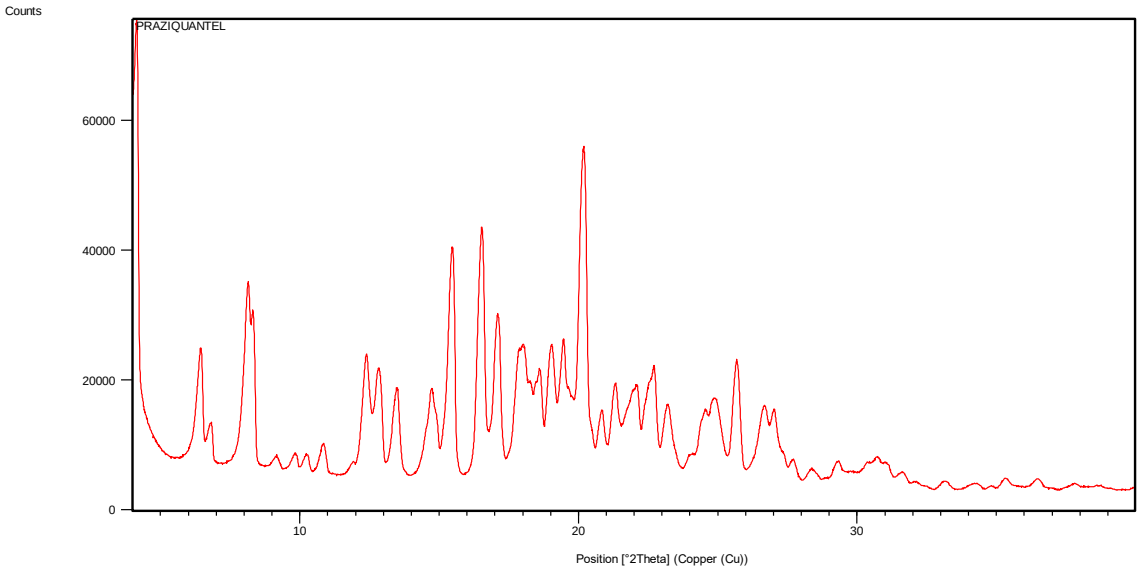


Figure 4.4: XRPD profile of the PZQ raw material.

The XRPD profile of the praziquantel raw material (Fig. 4.4) indicated that it was crystalline, as expected, as could be observed from the definite peaks.

4.2.4 Powder dissolution studies

4.2.4.1 Validation of the HPLC method

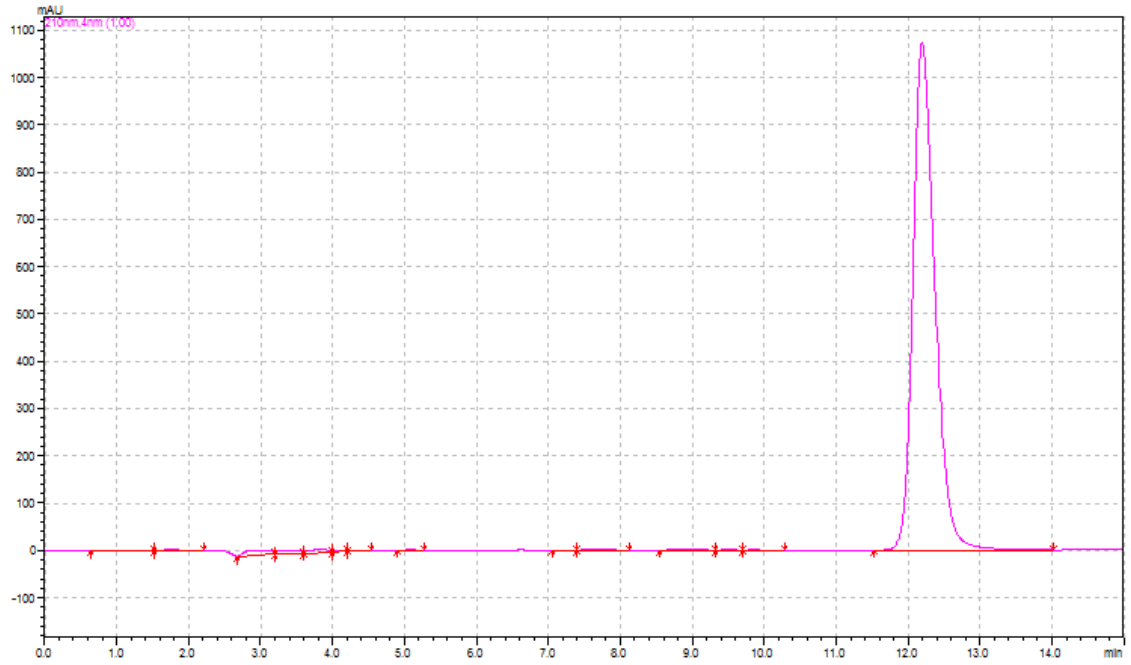


Figure 4.5: HPLC chromatogram of the PZQ raw material.

Figure 4.5 clearly demonstrates the defined PZQ peak at approximately 12.5 min. The area under the curve was used to measure the concentration of PZQ present in the test samples.

4.2.4.2 Linearity of the method used

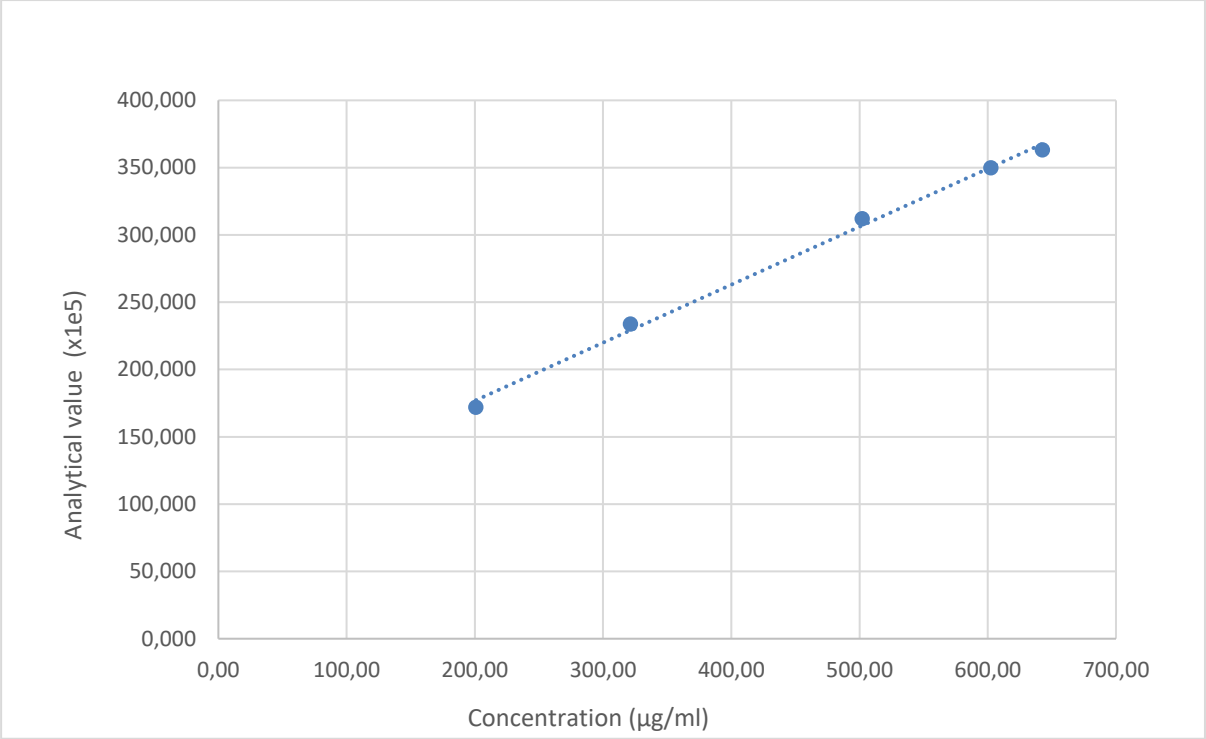


Figure 4.6: Linear regression curve of the PZQ raw material.

While testing the validity of the HPLC method, a satisfactory R^2 value of 0.9965 was obtained.

The powder dissolution studies were carried out as described in Section 2.7.7.

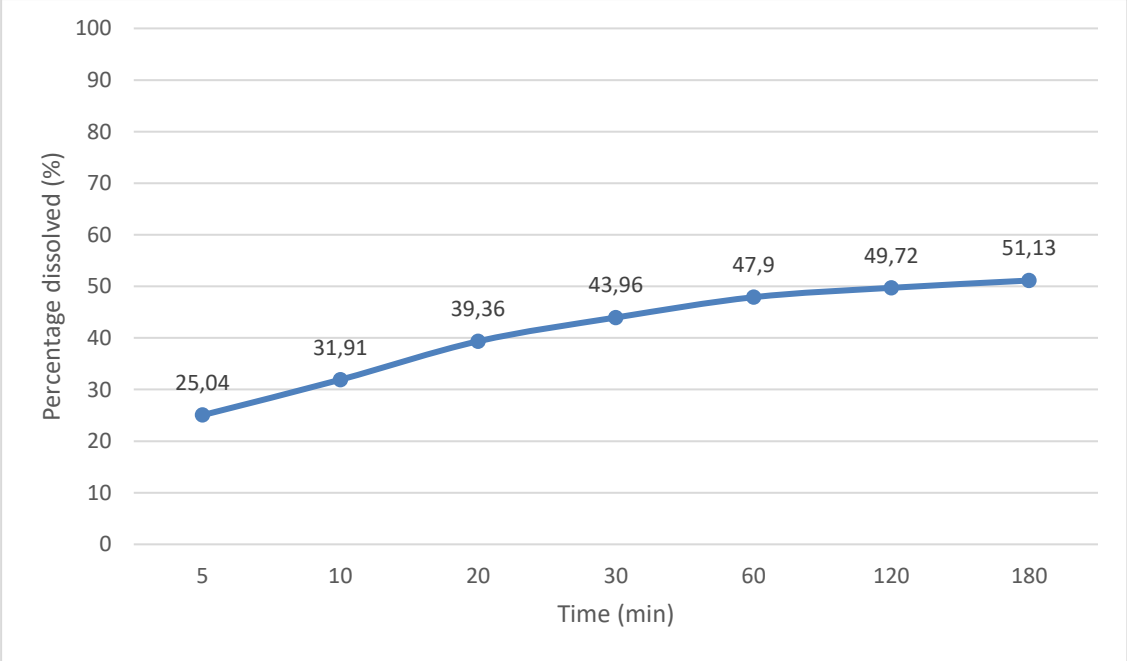


Figure 4.7: Percentage of the PZQ raw material that had dissolved in distilled water at specific time intervals over a 3-hour period.

The dissolution profile of the PZQ raw material is illustrated in Figure 4.7. The dissolution rate had started to plateau at 120 minutes and the maximum percentage of dissolved PZQ was recorded at 51.13% at 180 minutes.

An increase in the duration of the dissolution experiment might have resulted in a higher maximum percentage of dissolved raw material, as it continued to rise up to the 180-minute end mark.

4.3 Unsuccessful praziquantel/polymer ASD candidates

Preliminary testing had delivered promising results, indicative thereof that it would be possible to prepare suitable praziquantel ASDs in combination with each of the polymers, HPMC, HPMCAS, PVP 25, PVP 30 and PVP VA 64 in a ratio of 1:3 (API:polymer). While trying to create ASDs through rotary evaporation, all of the mixtures were crystalline, instead of amorphous, and were no further test results therefore generated, other than simultaneous thermal analyses on the physical mixtures.

The only ASD that had formed was the PZQ/HPMCAS (1:3) combination, but the resulting product was rubbery and elastic, which made it impossible to grind into a powder for further testing.

4.3.1 Simultaneous thermal analysis (STA) (TGA/DSC)

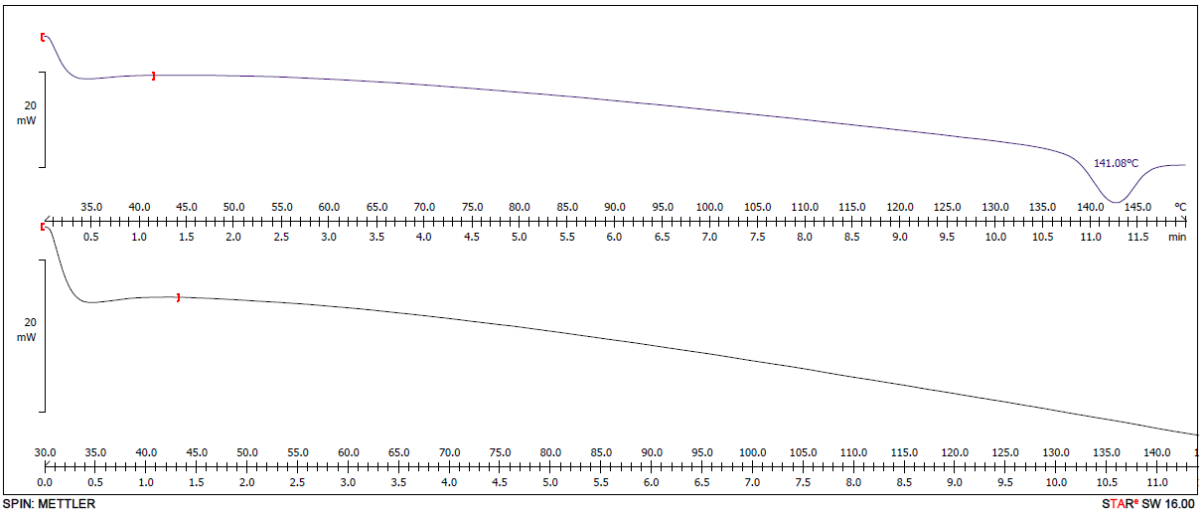


Figure 4.8: STA thermograms of the PZQ/HPMC (1:3) physical mixture (top, purple), and a second run of the same sample (bottom, black).

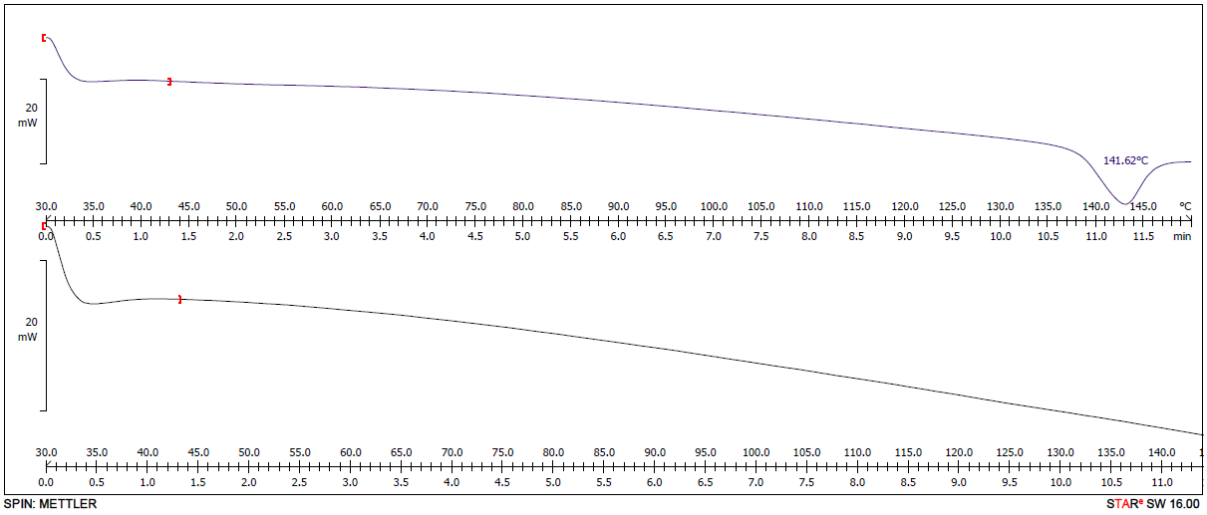


Figure 4.9: STA thermograms of the PZQ/PVP 25 (1:3) physical mixture (top, purple), and a second run of the same sample (bottom, black).

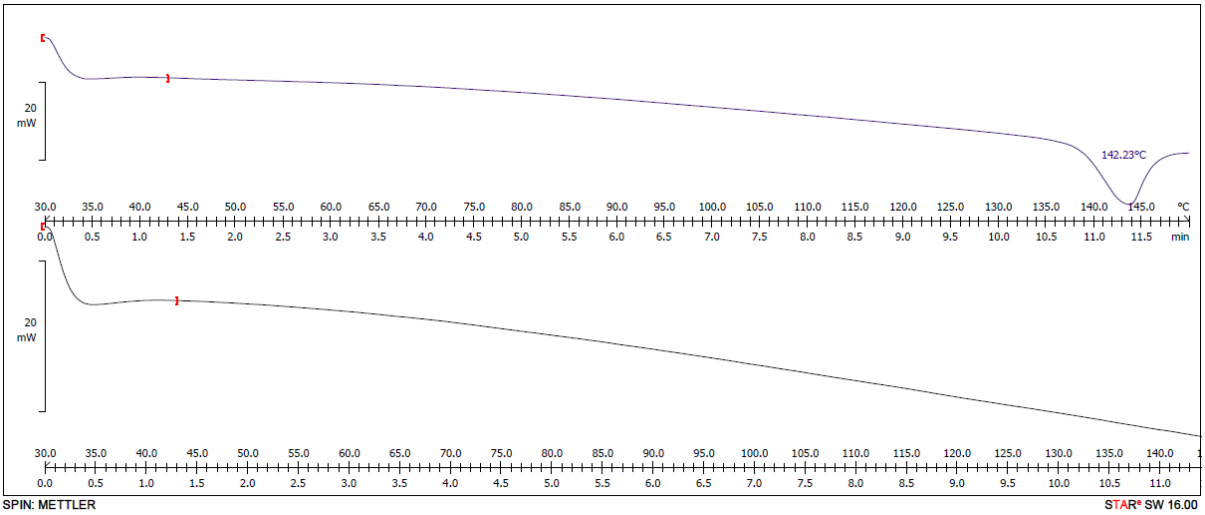


Figure 4.10: STA thermograms of the PZQ/PVP 30 (1:3) physical mixture (top, purple), and a second run of the same sample (bottom, black).

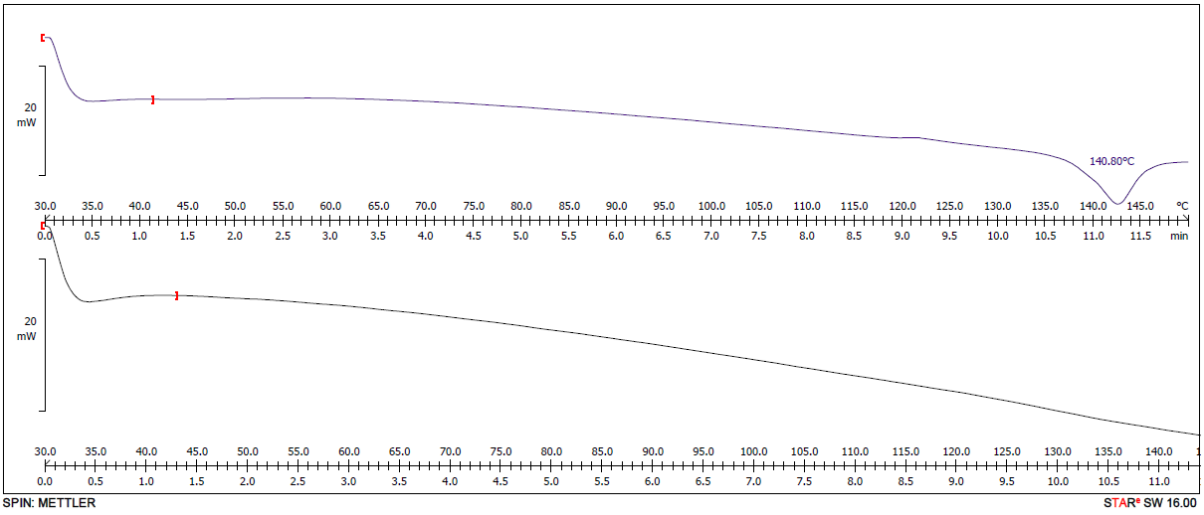


Figure 4.11: STA thermograms of the PZQ/PVP VA 64 (1:3) physical mixture (top, purple), and a second run of the same sample (bottom, black).

Figures 4.8 - 4.11 demonstrate that, while performing simultaneous thermal analyses, promising results had been achieved by having first run the thermal analysis on each of the physical mixtures (top, purple), which delivered consistent melting points, ranging from 140.80°C to 142.23°C. The second thermal analysis run on the same samples each delivered an ASD, evident from the lack of a melting point. These results suggested that a manufacturing method, like heat extrusion, would be the better choice for producing ASDs, rather than rotary evaporation.

4.4 ASD containing praziquantel/HPMCAS

4.4.1 Simultaneous thermal analysis (STA) (TGA/DSC)

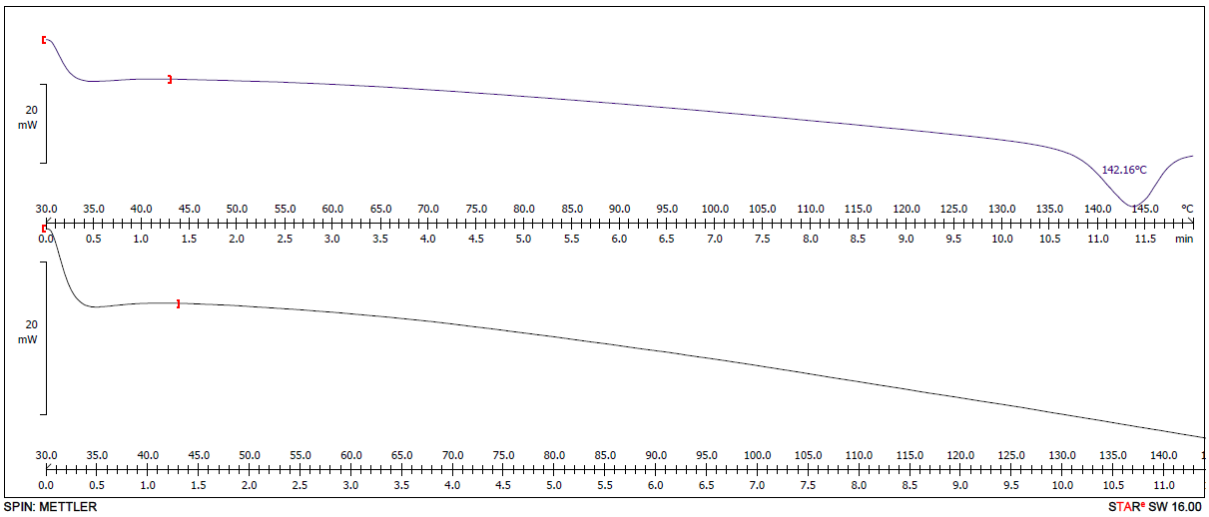
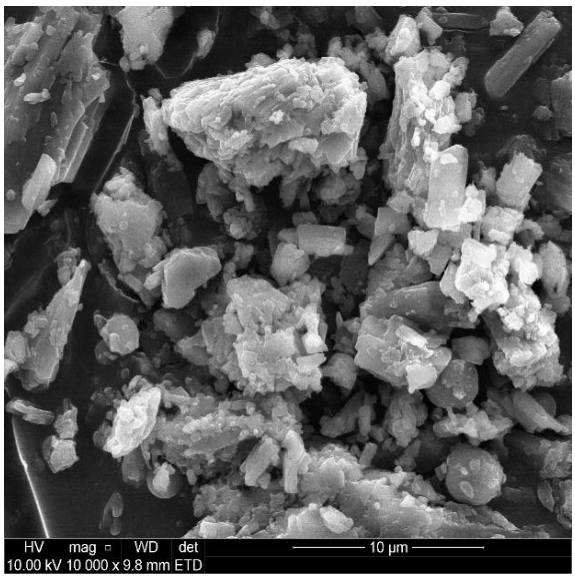


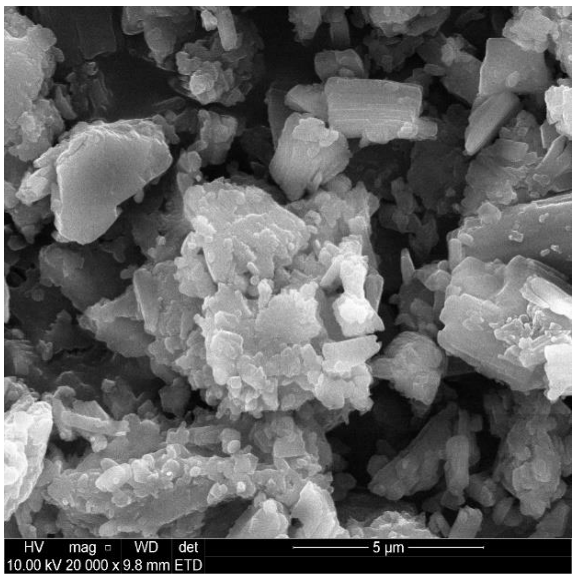
Figure 4.12: STA thermograms of the PZQ/HPMCAS (1:3) physical mixture (top, purple), and a second run of the same sample (bottom, black).

Simultaneous thermal analysis (Fig. 4.12) of the PZQ/HPMCAS (1:3) physical mixture (top, purple) had a melting point of 142.16°C, whereafter the same sample was re-analysed (bottom, black), resulting in a thermogram with no melting point, indicative thereof that an ASD had formed.

4.4.2 Scanning electron microscopy (SEM)



A 10 000x magnification



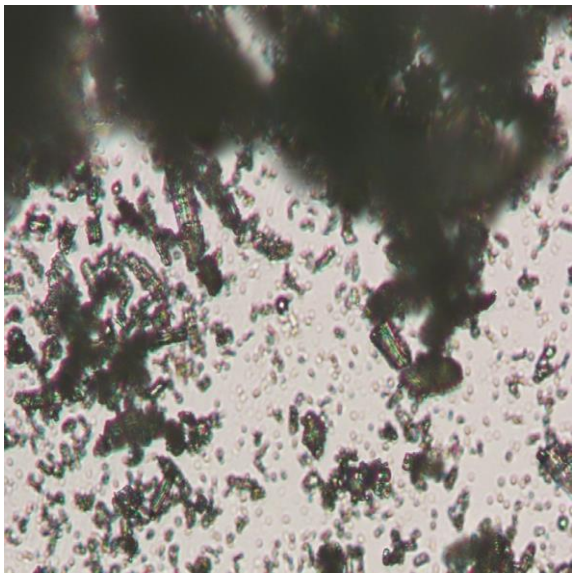
B 20 000x magnification

Figure 4.13: SEM photos of a physical mixture of PZQ and HPMCAS (1:3).

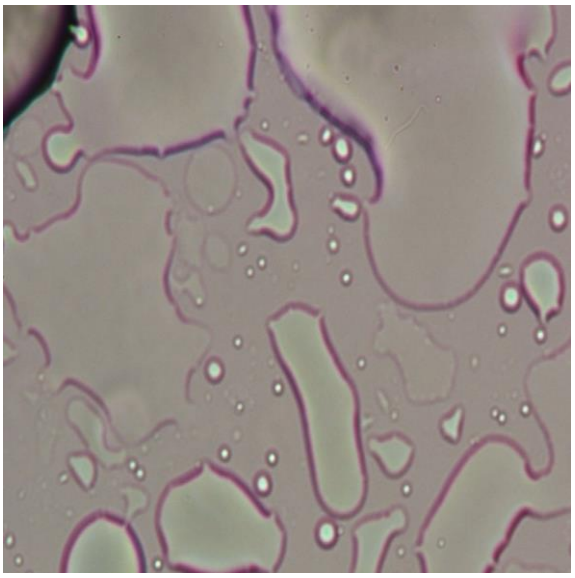
The SEM photos taken of the physical mixture of PZQ and HPMCAS (1:3) (Fig. 4.13) showed no definite crystal shape, nor size, which could have indicated that the physical mixture was probably inclined to become amorphous through grinding.

SEM photos were not taken of the ASD being prepared through rotary evaporation, since the resulting product could not be ground into smaller particles for comparison to the physical mixture.

4.4.3 Hot-stage microscopy (HSM)



A Before melting



B After melting

Figure 4.14: Images of the physical mixture of PZQ/HPMCAS (1:3) as observed under the microscope.

HSM photos of the physical mixture of PZQ/HPMCAS (1:3) (Fig. 4.14) were similar to those of the PZQ raw material (Fig. 4.3), in the sense that the particle sizes were inconsistent, while agglomeration was not prevalent. Figure 4.14 indicates that an amorphous state was reached after the melting point had been reached, as could be observed from the glass like nature of the melt.

4.4.4 X-ray powder diffraction (XRPD)

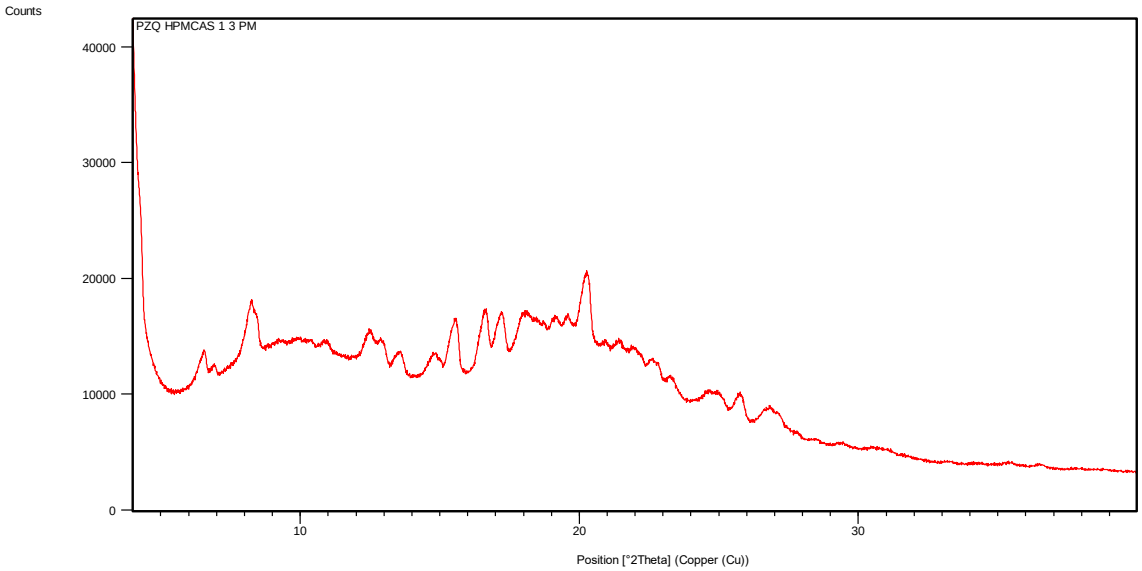


Figure 4.15: XRPD profile of the PZQ/HPMCAS (1:3) physical mixture.

The XRPD profile, as depicted in Figure 4.15, had a section with peaks (crystalline component), followed by a smoother section (amorphous component), which was indicative thereof that the composition of the PZQ/HPMCAS (1:3) physical mixture was crystalline with an amorphous component (Fig. 4.4). Since grinding in a mortar had been partly successful in forming a type of amorphous product, ball milling could be explored as a suitable alternative method of manufacturing, as it could lead to an ASD (a total amorphous product).

XRPD analysis could not be performed on the ASD that had been prepared through rotary evaporation, as the rubbery like and elastic product could not be ground into a powder.

4.4.5 Stability testing

Stability testing was not carried out, as the prepared ASD could not be ground into a powder form.

4.4.6 Dissolution studies

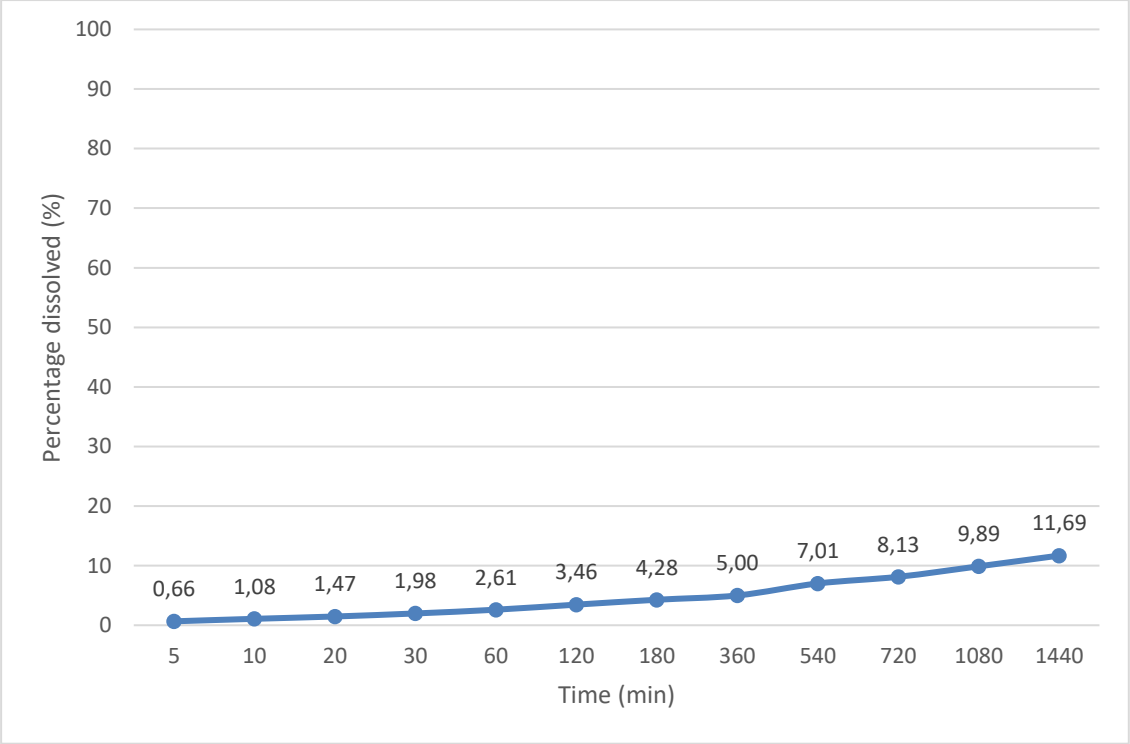


Figure 4.16: The percentage of PZQ from the ASD containing PZQ/HPMCAS (1:3) having dissolved in distilled water at specific time intervals over a 24-hour period.

The dissolution of the ASD containing PZQ/HPMCAS (1:3) in distilled water, showed a maximum percentage of dissolved PZQ of 11.69% after 24 hours. The results were disappointing, since the raw material had achieved dissolution rates higher than 50% over the same duration of time in water.

The same dissolution was subsequently repeated in a buffered solution, with the results illustrated in Figure 4.17. HPMCAS is used in the pharmaceutical field for gastro-resistant coatings, and it reportedly achieves its highest solubility at pH 6.8 (Anon., 2018). The acetyl and succinyl groups present in HPMCAS make it gastro resistant (Anon., 2018).

Dissolution of the PZQ/HPMCAS (1:3) ASD was carried out over a 24-hour period in a buffered solution at pH 6.8, since HPMCAS is generally used for modified release at this pH. Figure 4.17 demonstrates that dissolution had started to reach a plateau at around 360 minutes and the API was almost completely dissolved (99.39%) at 1440 minutes. These results represented a significant improvement in dissolution rates, compared to those obtained in the water medium.

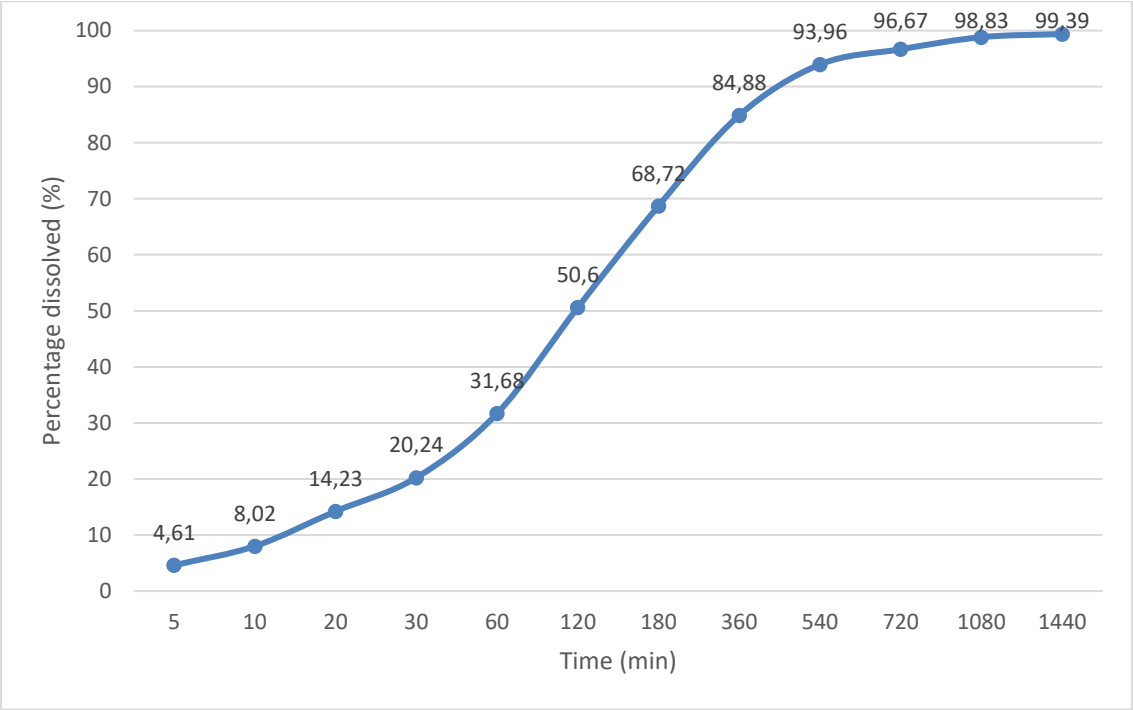


Figure 4.17: The percentage of PZQ from the ASD containing PZQ/HPMCAS (1:3) having dissolved in a buffer solution (pH 6.8) at specific time intervals over a 24-hour period.

4.5 Conclusion

The rotary evaporation preparation method used in this study to attempt the formation of suitable amorphous solid dispersions (ASDs) with the API, praziquantel (PZQ), in combination with different polymers each, had been problematic. Although rotary evaporation is frequently used in laboratory scale productions of ASDs, it was unsuitable for use with the different praziquantel/polymer combinations during this study. The preliminary screening results indicated that the different ASDs had formed with thermal heating, which suggested that a method that would only involve heat, could be more successful. The PZQ and polymer combinations delivered a crystalline end product through rotary evaporation. The manufacturing process for an ASD consisting of PZQ should be further investigated, while other laboratory scale methods, such as hot melt extrusion, should also be explored. The latter is a popular manufacturing method being employed in the industry, because no solvents are involved in the production process.

Only one of the prepared ASDs (PZQ/HPMCAS (1:3)) seemed to be amorphous. Its physical appearance, as well as elastic and rubber like properties unfortunately made further testing difficult, if not impossible. The results from XRPD analysis of this PZQ/HPMCAS combination, after mixing in a mortar with pestle, resulted in an amorphous component together with a crystal component. The ball milling technique could be further explored as an alternative manufacturing method for producing this specific ASD.

The dissolution profile of the ASD containing PZQ/HPMCAS (1:3) in pH 6.8 showed promising dissolution properties, despite the end product not being a feasible powder. Unfortunately, no other physico-chemical properties of this ASD could be tested, because of the rubber like end product that prevented powder sample preparation.

References

Anon. 2018. [Web:] https://www.seppic.com/aqoat [Date of access: 2018-08-12].

Chapter 5

Conclusion

Most active pharmaceutical ingredients (APIs) are produced as solids in the form of crystalline powders. To be able to deliver consistent quality and effectiveness, a better understanding of the solid-state properties of these powders is required. Such properties include polymorphic form, stability, solubility, dissolution rate, thermal behaviour, pharmacokinetics and surface activity. In the case of poorly soluble APIs, poor bioavailability is expected, which can be overcome by altering the solid-state properties of the said API. This can be achieved by means of changing the polymorphic form, or by creating an inclusion compound, such as a hydrate, a solvate, an amorphous solid dispersion (ASD), a clathrate, or a salt of the drug. Amorphous solid dispersions were the primary focus of this study. An ASD can be created through various methods, including addition of an anti-solvent, hot melt, spray drying, hot melt extrusion, solvent evaporation, or freeze drying. The primary preparation method that was used in this study was solvent evaporation by using a rotary evaporator. The glass transition temperature (T_g) is important when attempting to create a stable ASD and is 50°C generally added to the glass transition temperature of the API to ensure a stable final ASD product.

In this study, the APIs being investigated were efavirenz (EFA) and praziquantel (PZQ). Efavirenz is a non-nucleoside transcriptase inhibitor, used in combination therapy for HIV/AIDS. It has a poor solubility, but high membrane permeability, which makes it an ideal candidate for creating an ASD. It is a fine white powder with a solubility of 0.093 µg/ml in water at 25°C and has a melting point of about 138.53°C. Contrary, praziquantel is an anti-helminthic agent and is the drug of choice for the treatment of schistosomiasis (bilharzia). It is also a fine white powder with a solubility of 400 µg/ml in water at an unspecified temperature, while it has a melting point of about 141.44°C.

Various polymers, each in combination with either of the two APIs, were used to form various binary systems (ASDs), in attempts to increase the physical stability and hopefully the solubility of the APIs. The polymers used were hydroxypropyl methylcellulose (HPMC), hydroxypropyl methylcellulose acetate succinate (HPMCAS), polyvinylpyrrolidone (PVP) 25, PVP 30 and the PVP VA 64 copolymer. HPMC is used for various applications in pharmaceutical manufacturing, for example as a binder in preventing precipitation, for maintaining super saturation and as a hydrophilic matrix in extended release tablet forms. HPMCAS is a mixture of acetic and mono-succinic acid esters of HPMC and is widely used in the creation of ASDs. PVP is mainly used as a binder or disintegrant in tablets and is the most common polymer being used in pharmaceutical manufacturing. Vinylpyrrolidone-vinyl acetate copolymer (PVP VA 64) is used in granulation, as a dry binder in tabletting, as well as a solubilizer in hot melt extrusion processes.

Sodium lauryl sulphate (SLS) was also added as a surfactant in the ASDs that were created with efavirenz, due to wettability having been problematic. The addition of SLS increased wettability of the API, which aided in the dissolution studies. The maximum oral potency of SLS is 96 mg, which was not exceeded by only using small amounts (1.5% per dose).

The aims of this study therefore were to improve the solubilities and dissolution rates of both efavirenz and praziquantel, as well as to produce stable ASDs. A modified 'Screening of polymers for amorphous drug stabilisation' (SPADS) method was used for the screening of the ASDs. SPADS is a labour efficient way of screening for stabilisation, using polymers.

The characterisation methods used were simultaneous thermal analysis (STA), hot-stage microscopy (HSM), scanning electron microscopy (SEM), X-ray powder diffraction, high performance liquid chromatography (HPLC), stability testing and powder dissolution studies.

The prepared efavirenz ASDs in combination with each of the different polymers had T_g values below 80°C. Although theoretically this was not the ideal T_g for stability, even with the lower T_g values, the ASDs had remained physically stable up to the 3 months of stability testing at 40°C and 75% RH. In other words, the ASDs had remained amorphous and no crystallisation had occurred over the 3-month period. Although physically stable, HPLC assays revealed the occurrence of chemical degradation and the total degradation of the efavirenz raw material at month 3 was 55.9%, the ASD containing [EFA/PVP 25 (3:1) + 1.5% SLS] showed a total degradation of 66.7%, the ASD containing [EFA/PVP 30 (3:1) + 1.5% SLS] showed a total degradation of 79.4% and the ASD containing [EFA/PVP VA 64 (3:1) + 1.5% SLS] showed a total degradation of 78.6%. It was clear that the ASD containing PVP 25 as polymer, had experienced the least level of degradation and that it would be the ASD of choice for further alterations and testing.

The dissolution profiles of the efavirenz ASDs also indicated that the solubility had increased, compared to that of the raw material. After 3 hours of dissolution testing, the total percentage of dissolved efavirenz from the ASD containing [EFA/PVP 25 (3:1) + 1.5% SLS] was 5.97%, from the ASD containing [EFA/PVP 30 (3:1) + 1.5% SLS] it was 6.44% and from the ASD containing [EFA/PVP VA 64 (3:1) + 1.5% SLS] it was 4.42%. With an increase in the amount of dissolved efavirenz of almost double (6.44%), the ASD containing [EFA/PVP 30 (3:1) + 1.5% SLS] had performed the best, compared to efavirenz raw material, which had dissolved 3.31% after 3 hours. Since the solubility improvement was not very significant, future ASDs could be prepared with a higher percentage of the polymer and surfactant, as this could possibly assist in increasing the solubility properties of efavirenz.

Praziquantel ASD preparation had been problematic and was it only possible to prepare one in combination with HPMCAS at a ratio of 1:3 (API:polymer). This ASD, however, posed further challenges during attempts to test it, as it was rubbery and elastic, and hence impossible to grind

into a powder. As a result, no stability testing could be carried out, nor XRPD profiling, since the necessary fine powder could not be prepared. XRPD profiling of the physical mixture of praziquantel and HPMCAS indicated an inclination for possibly becoming amorphous during grinding.

Dissolution test results of the praziquantel ASD in water showed a decrease in the percentage of dissolved API even after 24 hours, with only 11.69% having dissolved, compared to the 51.13% of the raw material after only 3 hours. Dissolution was then carried out in a buffered solution (pH 6.8), because HPMCAS is used in modified release preparations where it dissolves at this pH. This test delivered satisfactory results, as a total of 99.39% of the praziquantel had dissolved after 24 hours, indicating that a possible extended release dosage form could be considered.

Alternative preparation methods, such as hot-melt extrusion, during which no solvents are engaged, should be investigated for the preparation of ASDs, containing praziquantel.

To summarise, ASDs containing efavirenz were found to be physically stable over the duration of the 3 months of accelerated stability testing. No recrystallisation was observed and these ASDs had remained amorphous. The solubility test results were, however, disappointing. The polymer ratio could be increased to try and overcome the poor solubility profile of the efavirenz ASDs. The preparation of ASDs containing praziquantel was quite challenging, if not impossible. Only the PZQ/HPMCAS combination had resulted in an ASD, which exhibited excellent dissolution results, although the final product's physical properties were undesirably elastic and rubber like, which prevented grinding into powder form. ASDs containing praziquantel would require further investigation regarding suitable manufacturing processes.

Annexure

Poster presented at CoBNeST event in October 2018.

Stable amorphous solid dispersions containing efavirenz as active ingredient

Alwyn van Aswegen[1]*, Nicole Stieger[1] and Wilna Liebenberg[1]

[1]Centre of Excellence for Pharmaceutical Sciences, Faculty of Health Sciences, North-West University, Potchefstroom, South Africa

Purpose: The aim of this study was to prepare a stable efavirenz amorphous solid dispersion (ASD)[1] by using an efficient modified screen polymers for amorphous drug stabilisation (SPADS)[2,3] method (Figure 1), thereby contributing towards testing of the method for suitability in the academic environment.

Methods: A SPADS method modified for the academic research environment[3] was used to find an optimal mixture and ratio of drug:polymer:surfactant whilst minimising costs and labour. The unsuccessful and/or less successful combinations in each step were abandoned and promising combinations went on to further testing until the ASD with the best physico-chemical properties was obtained.

The active pharmaceutical ingredient (API), polymer and surfactant were dissolved in 99.9% ethanol and evaporated using a rotary evaporator, followed by oven drying for 24 hours. The ASD was ground and physico-chemical tests were performed. The ASD was evaluated by means of thermal analysis, X-ray powder diffraction, dissolution testing and HPLC assay. Accelerated stability testing was also performed.

Results: Poorly soluble efavirenz[4], known to be highly unstable in pure amorphous form[5], was prepared in ASD form with different polymers and ratios. The stability of each was tested. Stable amorphous solid dispersions were successfully prepared with PVP-25, PVP-30 and PVP-VA64.

Thermal analysis and powder X-ray diffractometry proved the amorphous nature of the relevant ASDs. After 3 month accelerated stability studies at 40°C and 75% RH, no recrystallisation or degradation had occurred. The addition of SLS was required to improve wettability and dissolution profiles as efavirenz is extremely hydrophobic.

The ASD with the best dissolution results and highest apparent solubility was [efavirenz:PVP-30 (1:3) + 1.5%SLS]. A 100% improvement in apparent solubility was obtained compared to crystalline efavirenz raw material and 1.5 % SLS physical mixture. Submersing [efavirenz:PVP-30 (1:3) + 1.5%SLS] powder in water for three hours had no measurable impact on stability and did not lead to crystallisation.

Conclusion: The modified SPADS method yielded an efavirenz ASD that was more soluble than the crystalline form and much more stable than the pure amorphous form. The ASD remained chemically and physically stable for at least 3 months at 40°C and 75%H.

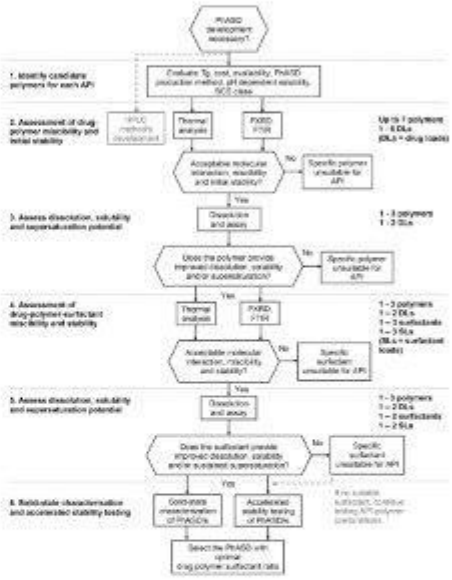


Figure 1: Modified SPADS (screen polymers for amorphous drug stabilisation) process[3].

References:

1. Zografi, G. & Newman, A. 2015. Introduction to amorphous solid dispersions. In Newman, A. Ed. Pharmaceutical amorphous solid dispersions. Wiley:NJ. p.1-41.
2. Narayan, P., Porter, W.W.III, Brackhagen, M. & Tucker, C. Introduction to amorphous solid dispersions. In Newman, A. Ed. Pharmaceutical amorphous solid dispersions. Wiley:NJ. p.72.
3. Stieger, N. & Liebenberg, W. 2017. Developing a modified SPADS process for academic research. Ongoing NRF/NWU research project. NRF grant #112078.
4. Moffat, A.C., Osselton, M.D. & Widdop, B. Eds. 2004. Clarke's Analysis of Drugs and Poisons. 3rd ed. Pharmaceutical Press, (2) 1935 p.
5. Stieger, N., Aucamp, M.E. and Liebenberg, W. 2013. Relative stability of efavirenz glass: Agitated vs. non-agitated. Poster presented at the 28th Annual Meeting of the American Association of Pharmaceutical Scientists, November 10-14, San Antonio, TX, USA.

Acknowledgements: This work is based on the research supported in part by the National Research Foundation of South Africa (Grant Number: 112078), and North-West University.